Clinical Health Journal
VOLUME 21, JULY/AUGUST, 2025
ISSN: 2636 - 7017

The relation between corneal optical quality and clinical ocular surface manifestations in Chinese female with Sjogren's syndrome dry eye

Persistence of hepatitis C virus in peripheral blood mononuclear cells of patients who Artificial intelligence in in-vitro fertilization (IVF): A new era of precision and personalization in fertility treatments achieved sustained virological response following treatment with direct-acting antivirals is associated with a distinct pre-existing immune exhaustion status

CT texture features of lung adenocarcinoma with HER2 mutation

Artificial intelligence in in-vitro fertilization (IVF): A new era of precision and personalization in fertility treatments

Just 1 Capsule

to gain freedom from

ACUTE PAIN

Dosage:
One capsule thrice a day

INDICATION

- Migraine Headache
- Dental Pain
- Period Pain
- Back Pain

Shalina
www.shalina.com

Shalina Healthcare Nigeria Ltd.
19 Fatai Atere Road, Matori, Mushin, Lagos State, Nigeria
Contact No: +234 - 8107539929
nigeria@shalina.com

Recommended by:
The Pharmaceutical Society of Nigeria (PSN)

Uncontrolled Type 2 Diabetes

NIDD

(Glibenclamide 5 mg)

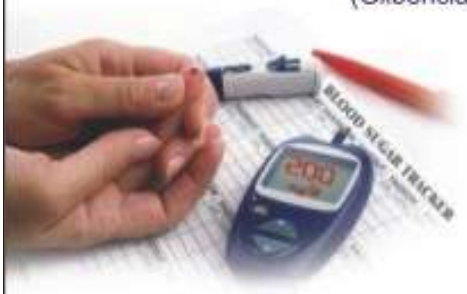

- Induces rapid insulin secretion
- Increases B cell sensitivity to glucose
- Can delay need for insulin
- Provides better patient compliance

The ideal Sulfonylurea for Glycemic control

DIBINORM

Metformin 500 mg

First line choice for Obese DIABETICS

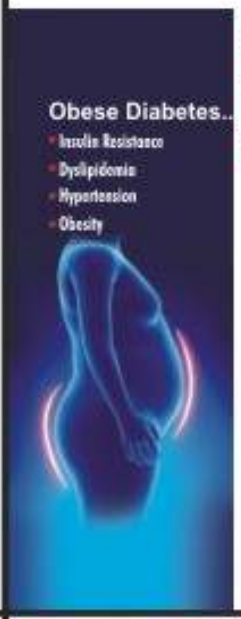

- Delays the progression of type 2 diabetes
- Effectively reduces plasma glucose level
- Reduces triglyceride and LDL-UKPDS
- Reduces diabetic complications and total mortality
- Offers enhanced compliance and safety profile

Metformin Beyond Diabetes

For comprehensive management of Type 2 Diabetes

Glimefil

Glibenclamide 5mg + Metformin 500mg Tablets

Enhances insulin secretion and saves B-cell

- Standard therapy for precise blood sugar control
- Delays the progression of Type 2 Diabetes
- Ensures 24 hr. Glycemic control
- Once daily advantage

GLUCOSE ↑↑↑

Triggers Micro & Macro Vascular Complications

GLYTROL

Gliclazide 80 mg

Excellent glycemic control

- Restores the First Phase Insulin secretion
- Increases B-cell sensitivity to glucose

Benefits beyond glycemic control

- Potent sulfonylurea with a low rate of secondary failure
- Better choice in long-term sulfonylurea therapy
- Prevents oxidative stress-induced B-cell damage

REFER TO THE PRODUCT INSERT FOR MORE INFORMATION

Manufactured by:
Unique Pharmaceuticals Limited
11, Fatai Atere Way, Matori, Mushin, Lagos.
Tel: 0809 742 1000 E-mail: mail@uniquepharm.com

...where only the best is good enough

ASTYFER®

AMINO ACIDS, IRON & VITAMIN B COMPLEX Liquid and capsule

INDICATIONS

For anaemic patients in the following conditions

- Anaemia in surgical patients following surgery.
- Anaemia due to nutritional deficiencies.
- Pregnancy and lactation.
- Anaemia due to heavy bleeding during menstruation.

DOSAGE

ADULTS
Capsule: 1 capsule twice a day
Liquid: 10ml twice a day
CHILDREN
Liquid: 5ml twice a day
PRESENTATION
Capsule: two blisters of 15 capsules each per pack Liquid: 200ml

NEW PACK

The Superior Blood Builder

FIDSON

...We value life

CORPORATE HEAD OFFICE:
268, Ikorodu Road, Obanikoro, Lagos, Nigeria.
Tel: +234 (0) 807 700 8888, email:info@fidson.com
Website: www.fidson.com

FIDSON

..we value life

FLUTEX®

FLUOXETINE CAPSULE USP 20mg.

- Minimal Discontinuation Symptoms
- Excellent Safety and Tolerability Profile
- High Efficacy in co-morbid conditions

...BRING BACK THE BEAUTY OF LIFE

FIDSON
Fidson Healthcare Plc
...We value life

CORPORATE HEAD OFFICE:
268, Ikorodu Road, Obanikoro, Lagos. Nigeria. Tel: +234 (0) 807 700 8888
Email: info@fidson.com, Website: www.fidson.com

FROST & SULLIVAN 2014 BEST PRACTICES AWARD
NIGERIAN PHARMACEUTICAL GROWTH EXCELLENCE LEADERSHIP AWARD

Ceflonac®-SP

Aceclofenac / Paracetamol / Serratiopeptidase Tablets

ACECLOFENAC

- Better safety profile than conventional NSAIDs due to it's preferential cox-2 blockade

SERRATIOPEPTIDASE

- Anti inflammatory, antiedemic and fibrinolytic activity
- Reduces swelling and improves microcirculation

PARACETAMOL

- Analgesic and antipyretic effect
- Rapidly and completely absorbed from the GI tract

Geneith PHARMACEUTICALS LIMITED
...offering quality healthcare

Integrity
Commitment
Innovation

Website: www.geneithpharm.com @geneithpharm +2348129008556

Rectal suppositories for aches, pains & feverish conditions.

Insert the Relief

Manufactured & Marketed by:

Daily-Need Industries Ltd

Quality | Integrity | Transparency

Email: info@dailyneedgroup.com | www.dailyneedgroup.com

ABOUT CLINICAL HEALTH JOURNAL

Clinical Health Journal aims at reaching your target audiences by promoting, sharing and distributing quality scientific and medical peer-reviewed contents source from credible and leading journals across the world thereby advancing scientific research benefits to the global scientific community.

With our multiple channels filtering strategy, we deliver authoritative and timely contents that are of immediate interest to the practicing physicians, drive quality traffic and meet publishers expectation. These include review articles, case reports, short communications, original scientific studies that have direct clinical significant and position papers on healthcare issues. The journal carry news on conferences, workshops and products. We cover extensively all areas of medicine. The journal publishes 6 issues per year.

ISSN
2636 - 7017
Frequency
Bi-monthly
Subject
All subjects in medicine
Readership
Medical doctors, Medical students, Pharmacists, Nurses and healthcare professionals

Volume in 2023
19
Published print since
August 2006
Online Full Text Availability
2023
Journal Type
Open Access
Journal Website
https://clinicalhealthjournal.com

Published By
Genmax Communications Nigeria Limited
(Clinical Health Journal)
No. 1 Bariyu Street, Isolo, Lagos, Nigeria.
clinicalhealthjournal1@gmail.com
bridget.clinicalhealthjournal@gmail.com

TABLE OF CONTENTS

zolon
Healthcare Limited
(A member of the Emzor Group)

INTELLIGENT zolon Healthcare Limited (A member of the Emzor Group) SOLUTIONS

Biophin injection

Ceftriaxone sodium BP 1g

Edic Building, 13, Town Planning Way, Ilupeju, Lagos, Nigeria. Tel: +234 (0) 700 225 5965, 0700 CALL ZOLON

Zolon Healthcare Limited Zolon Healthcare Limited Zolon Healthcare Limited Zolon Healthcare

www.zolonhealthcare.com

INTELLIGENT SOLUTIONS

aventra proVision

HALT ALLERGY

CLEARS RED EYES | RELIEVES ITCHY EYES | STOPS WATERY EYES

+234 807 700 8888 info@fidson.com
268, Ikorodu Road, Obanikoro, Lagos, Nigeria. www.fidson.com
aventraprovision.com

SCAN ME

The relation between corneal optical quality and clinical ocular surface manifestations in Chinese female with Sjogren's syndrome dry eye

Jingyu Zhang, Qian Deng, Maierhaba Maitiyaer, Li Wang, Amy Michelle Huang, Yue Liang, Qiudan Huang, ShuiLian Yu & Zhiping Liu

Abstract

Objective

To evaluate the relation between corneal optical quality and ocular surface manifestations in Chinese female patients with Sjogren's syndrome dry eye (SSDE).

Methods

Cross-sectional study of female SSDE patients. Demographic information and ophthalmological and rheumatological indicators were collected. Ocular Surface Disease Index (OSDI) and Chinese Dry Eye Questionnaire (CDEQ), best-corrected visual acuity (BCVA), first and mean noninvasive tear break-up time (FNIBUT and MNIBUT), Schirmer I testing, Oxford Staining Score (OSS), meibomian gland loss (MGL), and optical quality were evaluated using generalized estimating equation (GEE) models. Multinomial logistics regression models and multiple linear regression models were employed to assess the correlations between dry eye indicators and corneal optical quality.

Results

27 SSDE patients (47 eyes), 9 Non-Sjögren's Syndrome dry eye patients (NSSDE, 14 eyes), and 23 normal controls (NC, 44 eyes) were included. More severe dry eye signs and poorer results of corneal optical qualities were found in Chinese female SSDE patients (all $p < 0.05$). More severe dry eye signs (CDEQ score, FNIBUT, MNIBUT, OSS, Schirmer I test, lipid layer distribution, and MGL) and poorer results of corneal optical qualities (angle a) were found in SSDE patients (all $p < 0.05$). In addition, there was a significant difference in astigmatism (posterior corneal surface astigmatism, and the types of astigmatism on the anterior and posterior surface of the cornea) between the groups (all $p < 0.05$).

Conclusions

Chinese females with DE, and particularly those with concurrent SS, demonstrated poorer ocular surface and corneal optical quality measures than those without DE.

Introduction

Dry eye (DE) disease is a common, chronic, inflammatory condition. According to previous studies, women are more susceptible to DE compared to men, and the prevalence increases with age [1]. Dry eye (DE) is a common, chronic, inflammatory condition that affects the ocular surface and tear film, leading to discomfort, visual impairment, and reduced quality of life [2]. This disease can trigger changes in the ocular surface and tear film [3,4], which in turn can increase ocular discomfort, fatigue, and visual impairment that can interfere with a patient's daily activities, such as reading, driving, and electronics use, to varying degrees [1]. DE disease can cause corneal damage, such as by inducing inflammation, protein and lipid deposition, corneal edema, and corneal neovascularization. This adversely affects corneal refraction and the optical pathway to the retina, and in severe cases, it can even lead to blindness [5]. Currently, abnormal visual function is included in the definition and diagnostic criteria of DE disease by Asia Dry Eye Society [6].

Certain systemic diseases, such as Sjogren's syndrome (SS), are considered to be a risk factor for DE disease [7]. This systemic autoimmune disease involves the exocrine glands and is primarily associated with immune cell dysregulation [8,9]. The disease has an insidious onset and diverse clinical manifestations, with up to 98% of patients presenting with dryness of various organ systems [10]. Many patients present with dry mouth and eyes due to decreased function of the salivary and lacrimal glands [11]. SS, an autoimmune disease, is a significant risk factor for DE, often presenting with severe ocular surface manifestations due to decreased tear production and increased tear film instability [11]. Tear film instability and ocular surface inflammation can lead to a vicious cycle that complicates the treatment of DE

disease [12,13]. If this disease is not treated in a timely manner, the patient's symptoms may worsen, become more difficult to treat, and may lead to permanent ocular damage.

Previous studies have explored the impact of DE on corneal optical quality [14], but the relationship remains incompletely understood, particularly in Chinese female patients with SSDE. This study aims to fill this gap by evaluating the correlation between corneal optical quality and clinical ocular surface manifestations in Chinese female patients with SSDE. This research aims to elucidate the relationship between corneal optical quality and clinical ocular surface manifestations in Chinese females with Sjogren's syndrome dry eye (SSDE), and to identify potential indicators for early intervention to preserve visual quality.

Methods

Study design and participants

This cross-sectional case–control study was performed according to the principles of the Declaration of Helsinki and was approved by the Ethics Committee of the Second Hospital of Guangzhou Medical University (2019-hs-12).

We recruited 27 SSDE patients (47 eyes), 9 Non-Sjögren's Syndrome dry eye patients (NSSDE, 14 eyes), and 23 normal controls (NC, 44 eyes) from July 2021 to December 2023. Flowchart of participant screening was shown in Fig. 1. The diagnosis and classification of SS patients were identified by a rheumatologist (YSL) in accordance with the 2016 American College of Rheumatology/European League Against Rheumatism classification criteria for primary Sjogren's syndrome [15]. The inclusion criteria included the following: (1) aged 20–60 years; (2) intraocular pressure (IOP) < 21 mmHg; (3) no other systemic or ocular diseases. Exclusion criteria included the following: ocular anatomical abnormalities (eyelid entropion, eyelid scarring, etc.); history of glaucoma; contact lenses wearers; intraocular surgery within the last 12 months; recent eye infection; and pregnant or lactating women. The sample size for the Non-Sjögren's Syndrome dry eye (NSSDE) group was limited due to the specific inclusion criteria and the relative rarity of this subgroup among the overall dry eye population. While NSSDE patients are encountered in clinical practice, recruiting a larger sample size within the study timeframe was challenging. Future studies may focus on expanding this cohort to provide more robust data.

Patients were included based on the presence of clinically significant dry eye symptoms and signs in at least one eye. While dry eye disease (DED) often affects both eyes, particularly in patients with Sjogren's syndrome, the severity and manifestations can vary between eyes. Therefore, both eyes were included if they met the inclusion criteria, while only one eye was included if the other did not meet the criteria or if the patient had unilateral disease.

All the participants received a standardized ophthalmological examination consisting of best corrected visual acuity (BCVA), IOP, and slit-lamp examination at the time of enrollment.

Dry eye questionnaire collection

Participants were instructed to fill out the Ocular Surface Disease Index (OSDI) and Chinese Dry Eye Questionnaire, which required them to describe the impact of their current symptoms on their daily lives. The OSDI ranged from 0–100, while the Chinese Dry Eye Questionnaire ranged from 0–48. An OSDI score of less than 20 is

Fig. 1

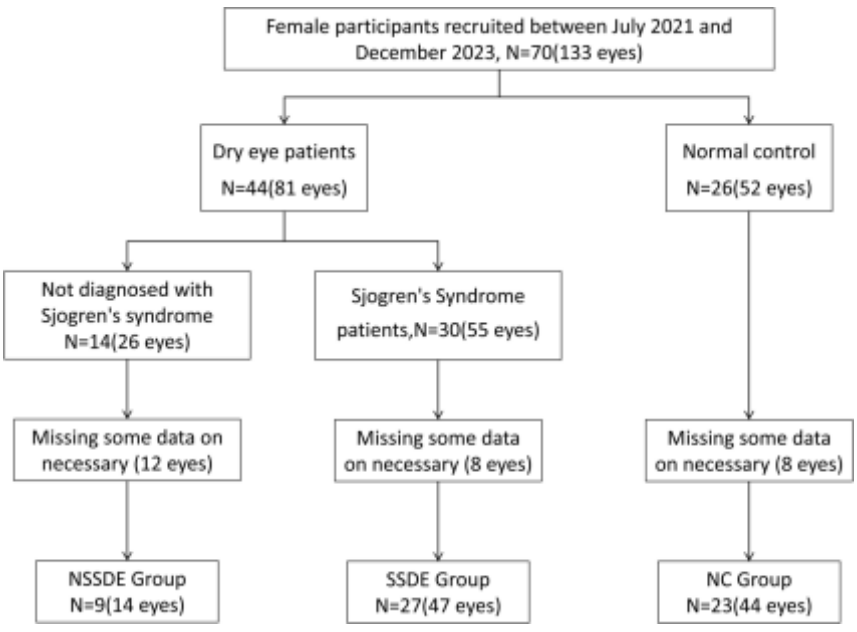

Flowchart of study participants. SSDE, Sjogren's syndrome dry eye. NSS, Non-Sjögren's Syndrome dry eye. Some patients who were missing data on several essential indicators (e.g., best-corrected visual acuity, ocular surface staining, etc.) were excluded

considered normal or mild dry eye; 20–45 is considered moderate; and more than 45 is considered severe dry eye [16]. An CDEQ score of more than 7 is considered as symptomatic DE [17].

Ocular surface measures

We examined tear meniscus height (TMH), staining of the ocular surface, first and mean noninvasive tear break-up time (FNIBUT and MNIBUT), lipid layer condition, bulbar conjunctival hyperemia (BCH), and the condition of meibomian gland loss (MGL). The above subjects were measured and evaluated using a Keratograph 5 M (Oculus, Wetzlar, Germany), which has a high level of discrimination and diagnostic accuracy [18]. The staining map obtained by Oculus was scored in conjunction according to the Oxford Staining Score(OSS) to assess the damage to the ocular surface [19]. In addition, the best corrected visual acuity (BCVA) and intraocular pressure (IOP) of all patients were tested before the ocular surface examination. Best-corrected visual acuity (BCVA) was measured and converted to LogMAR for analysis. Original measurements were taken using a standard ETDR chart. The conversion formula is:logMAR = log10 (?1/visual acuity value)".

Examinations were conducted in a controlled environment with a temperature of 22-25 ? and humidity of 40–60%. Participants were acclimated to the room for at least 15 min before testing. Ocular surface tests were performed in the following order: tear meniscus height (TMH), first and mean noninvasive tear break-up time (FNIBUT and MNIBUT), meibomian gland loss (MGL), ocular surface staining, and Schirmer I test. This sequence minimizes the impact of eyelid manipulation and fluorescein instillation on subsequent measurements. Lipid layer distribution was assessed using the Keratograph 5 M (Oculus, Wetzlar, Germany) and graded based on the presence and uniformity of the lipid layer. Meibomian gland loss was evaluated using the meiboscore system validated by Reiko Arita [20].

Based on previous study, fluorescein staining with the yellow filter has the advantage of simultaneous observation of both corneal and conjunctival damage in patients with dry eye without the need for additional vital staining [21]. Corneal staining was assessed 2–3 min after fluorescein instillation to ensure stable conditions. The Schirmer I test was performed with the eyes closed to standardize tear production measurement. Fluorescein strips (Oculus, Wetzlar, Germany) and Schirmer test strips (Tianjin Jingming New Technology Develop-ment Co., Ltd., Tianjin, China) were used.

The Schirmer I test without anesthesia was used to measure tear production. A dry Schirmer test strip was inserted over the outer one-third of the lower eyelid margin and the distance that the tears traveled along the test strip at 5 min was recorded as the Schirmer I score.

Corneal optical quality measures

The Pentacam (Oculus, Wetzlar, Germany) was used to assess corneal morphology, including astigmatism on the anterior and posterior surfaces. The iTrace wavefront aberrometer (Tracey Technologies, Houston, TX, USA) was used to directly measure corneal optical quality, including total corneal high-order aberrations (tHOAs), spherical aberrations (SAs), comas, modulation transfer function (MTF), and angles a and ?. These measurements provide a comprehensive evaluation of corneal optical quality.

Statistical analysis

The statistical power was calculated using PASS 15.0 software. Stata statistical software (V.17.0, Stata Corp, College Station, TX) was used for statistical analyses in this study, and $p < 0.05$ was considered a statistically significant difference. Means, standard errors, and weighted percentages were used for continuous variables, and frequency and weighted percentages were used for categorical variables. Generalized estimating equation (GEE) models were used to count for inter-correlation of eyes within study subjects. Eyes (left or right) were set as within-subject variables in the GEE models. The measurements were dependent variables, while age, and eye were set as covariates. Normality of distribution was verified using the Kolmogorov–Smirnov test. Given the small sample size of the NSSDE group, normality tests were performed on each dataset. For variables that did not follow a normal distribution, data were presented as median (interquartile range, Q1-Q3) to accurately reflect the central tendency and dispersion (Supplementary Table 1). Group comparisons for normally distributed continuous variables were performed using GEE. Kruskal–Wallis tests were utilized to analyze non-normally distributed data. Categorical data were compared using $?^2$ tests. Receiver operating characteristic (ROC) and area under the curve (AUC) were used to assess the predictive ability of statistically significant ocular surface indicators for DE disease. To explore the relationship between ocular surface indicators and corneal optical quality indicators and between-group differences, prior to conducting regression analysis, associations between dependent and independent variables were assessed using Kendall's tau-b correlation coefficient.

For multiple linear regression analysis, the dependent variable was continuous and normally distributed (e.g., corneal optical quality indicators). For multinomial logistic regression analysis, the dependent variable was categorical, following a binomial distribution (e.g., presence or absence of specific ocular surface manifestations).

Results

Clinical ocular surface manifestations and optical quality performance

Sample size calculation was performed based on the expected effect size. In our current study, a sample size of 30 eyes in the SSDE group, 10 eyes in the NSSDE group, and 30 eyes in the NC group achieved a statistical power of 93% in differentiating the Schirmer I test, OSS, FNIBUT, and MNIBUT measurements.

In this study, participants were recruited between July 2021 and December 2023 at the Second Affiliated Hospital of Guangzhou Medical University. 27 SSDE patients (47 eyes), 9 NSSDE patients (14 eyes), and 23 NC participants (44 eyes) met the inclusion and exclusion criteria. We performed further SS disease diagnosis and corneal optical quality assessment on these participants. After diagnosis by the same rheumatologist according to the 2016 American College of Rheumatology/European League Against Rheumatism classification criteria for primary Sjogren's syndrome, the above participants were enrolled in this study. Rheumatologic indicators of SSDE patients are shown in Table 1.

As shown in Table 2, compared to the NSSDE group and NC group, those with SSDE had decreased tear film breakup times (5.580 ± 0.529 s, $p < 0.001$; 9.186 ± 0.844 s, $p = 0.001$), and lower tear secretion (4.617 ± 0.579 mm/5 min, $p < 0.001$) over the same period of time. Uneven distribution of the lipid layer ($p = 0.003$) was observed in SSDE patients. Additionally, the upper MGL ($p < 0.001$) and lower MGL ($p = 0.001$) were worse in SSDE patients. The results of the participant questionnaire showed that the CDEQ scores of SSDE patients were higher than those of the NC group (11.143 ± 1.368, $p = 0.001$). BCVA was converted to logarithmic minimum angle of resolution(logMAR). There was a statistically significant difference in logMAR between the three groups of participants ($p = 0.001$), but this was perhaps due to the greater mean age of the SS group ($p < 0.001$). The ability of statistically different ocular surface indicators to discriminate SS can be reflected in Fig. 2. OSS, Schirmer I test, CDEQ, FNIBUT and MNIBUT all exhibit robust discriminatory capacity with AUCs of 0.962, 0.953, 0.861, 0,799 and 0.769, respectively.

Table 1 Demographics, ocular characteristics, and rheumatologic indicators of included participants

Characteristics	SSDE(*n* = 27)	NSSDE(*n* = 9)	NC(*n* = 23)	*P*
Age, mean ± SE(years)	48.26 ± 1.88	39.78 ± 4.42	27.74 ± 1.55	*0.001**
OSDI, mean ± SE	17.023 ± 4.449	3.085 ± 1.085	5.173 ± 1.849	0.057
CDEQ, mean ± SE	11.143 ± 1.368	-	4.250 ± 1.016	0.001
Duration, mean ± SE(years)	2.616 ± 0.775	2.600 ± 1.076	-	0.992
ESSDAI, mean ± SE	7.680 ± 1.532	8.143 ± 3.262	-	0.891
IgM, mean ± SE (Reference Range: 0.4–2.3 g/L)	1.136 ± 0.108	1.107 ± 0.330	-	0.913
IgA, mean ± SE (Reference Range: 0.7-4 g/L)	3.390 ± 0.363	2.723 ± 0.549	-	0.379
IgG, mean ± SE (Reference Range: 7-16 g/L)	16.304 ± 1.502	17.226 ± 3.351	-	0.784
GLB, mean ± SE (Reference Range: 20-40 g/L)	33.296 ± 1.824	33.314 ± 3.887	-	0.996
ESR, mean ± SE (Reference Range: < 20 mm/h)	35.870 ± 7.686	38.429 ± 13.652	-	0.873
CRP, mean ± SE (Reference Range: < 8 mg/L)	8.514 ± 5.001	7.591 ± 6.204	-	0.926
RF, mean ± SE (Reference Range: < 20U/L)	17.217 ± 3.611	35.242 ± 21.592	-	0.178

Abbreviations: SSDE Sjögren's Syndrome dry eye, *NSS* Non-Sjögren's Syndrome dry eye, *NC* normal controls, *n* number of participants, *OSDI* ocular surface disease index, *CDEQ* Chinese dry eye questionnaire, *ESSDAI* EULAR Sjögren's syndrome disease activity index. *IgM* Immunoglobulin M, *IgA* Immunoglobulin A, *IgG* Immunoglobulin G, *GLB* Globulin, *ESR* electron spin resonance, *CRP* C-reactive protein, *RF* Rheumatoid factor Bold *p*-value represents < 0.05.* *indicates that the data is the result of a Kruskal–Wallis tests*

The results of the analysis of the indicators related to corneal optical quality are presented in Table 3. Angle a ($p = 0.001$), posterior corneal surface astigmatism ($p = 0.001$), and the types of astigmatism on the anterior ($p = 0.0211$) surface of the cornea were significantly different between the groups.

The P-values in Tables 1, 2 and 3 represented the statistical significance of differences between the three groups (SSDE, NSSDE, and normal controls) for each variable. These values indicated whether there were significant differences in ocular surface manifestations and corneal optical quality indicators among the groups.

Correlation of ocular surface manifestations and visual performance

Correlation analyses were performed

Table 2 Ocular surface manifestations among three groups

Characteristics	SS (*n* = 47 Eyes, 44.76%)	NSS (*n* = 14 Eyes, 13.33%)	NC (*n* = 44 Eyes,41.90%)	*P*
BCVA(LogMAR), mean ± SE	0.022 ± 0.022	- 0.037 ± 0.012	- 0.082 ± 0.011	0.001
IOP, mean ± SE(mmHg)	14.489 ± 0.536	14.241 ± 0.905	14.687 ± 0.397	0.907*
TMH, mean ± SE(mm)	0.187 ± 0.010	0.205 ± 0.022	0.255 ± 0.026	0.078
Schirmer I test, mean ± SE(mm/5 min)	4.617 ± 0.579	5.357 ± 1.117	21.455 ± 1.224	< 0.001
OSS, mean ± SE	7.833 ± 0.729	0.250 ± 0.163	1.265 ± 0.261	0.001*
FNIBUT, mean ± SE(s)	5.580 ± 0.529	10.455 ± 2.234	12.620 ± 1.028	< 0.001
MNIBUT, mean ± SE(s)	9.186 ± 0.844	12.457 ± 2.089	16.036 ± 0.890	0.001*
BCH, mean ± SE	1.000 ± 0.065	0.900 ± 0.133	0.780 ± 0.043	0.088*
Lipid layer color, NO. (%)				0.060
Colorful	36(80.00)	9(64.29)	42(95.45)	
Uncolorful	9(20.00)	5(35.71)	2(4.55)	
Lipid layer distribution, NO. (%)				0.003
Even	25(55.56)	13(92.86)	40(90.91)	
Uneven	20(44.44)	1(7.14)	4(9.09)	
Upper MGL, NO. (%)				< 0.001
Normal	3(6.38)	4(28.57)	19(47.50)	
Deficiency < 1/3	23(48.94)	6(42.86)	18(45.00	
1/3 < Deficiency < 2/3	14(29.79)	3(21.43)	1(2.50)	
Deficiency > 2/3	7(14.89)	1(7.14)	2(5.00)	
Lower MGL, NO. (%)				0.001
Normal	7(14.89)	7(50.00)	30(71.43)	
Deficiency < 1/3	24(51.06)	5(35.71)	8(19.05)	
1/3 < Deficiency < 2/3	11(23.40)	2(14.29)	1(2.38)	
Deficiency > 2/3	5(10.64)	0(0.00)	3(7.14)	

Abbreviations: SS Sjögren's Syndrome, *NSS* Non-Sjögren's Syndrome dry eye, *NC* Normal control, *n* number of eyes, *BCVA* best-corrected visual acuity, *LogMAR* logarithmic minimum angle of resolution, *IOP* intraocular pressure, *OSDI* ocular surface disease index, *CDEQ* Chinese dry eye questionnaire, *TMH* tear meniscus height, *OSS* Oxford Staining Score, *FNIBUT* first noninvasive tear break-up time, *MNIBUT* mean noninvasive tear break-up time, *BCH* bulbal conjunctival hyperemia, *MGL* meibomian gland loss

Bold *p*-value represents < 0.05. ** indicates that the data is the result of a Kruskal–Wallis tests*

Fig. 2

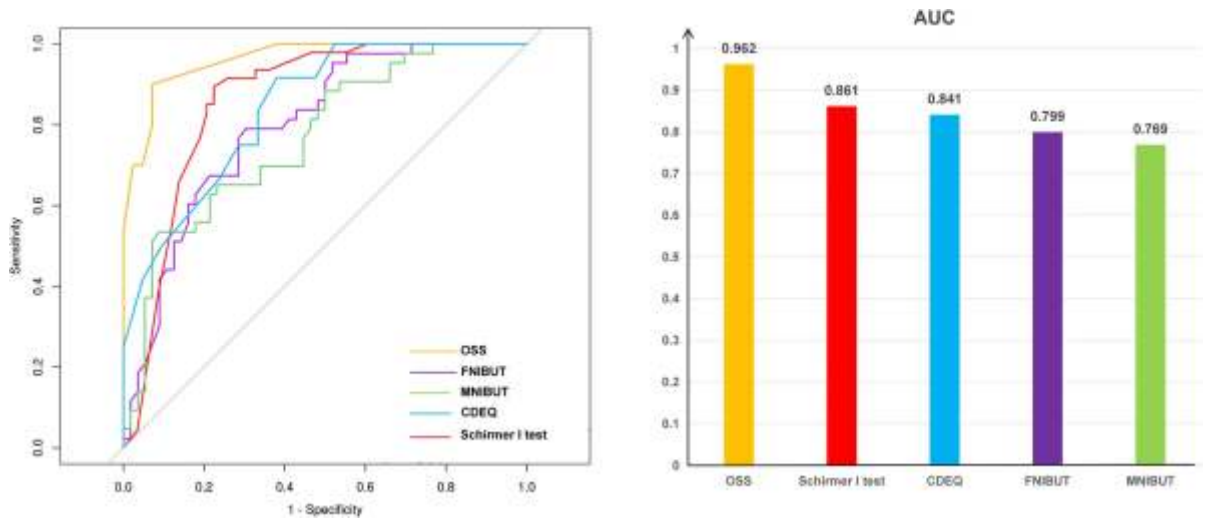

Receiver Operating Characteristic (ROC) and area under the curve (AUC) of statistically significant indicators to diagnose SS. OSS, Oxford Staining Score; CDEQ, Chinese Dry Eye Questionnaire; FNIBUT and MNIBUT, first and mean noninvasive tear break-up time

Table 3 Visual performance related indicators of included participants in three groups

Characteristics	SS(47 eyes)	NSS(14eyes)	NC(44 eyes)	*P*
tHOAs, mean ± SE	0.240 ± 0.064	0.165 ± 0.018	0.494 ± 0.064	0.807*
Coma, mean ± SE	0.107 ± 0.023	0.086 ± 0.015	0.260 ± 0.064	0.280*
Spherical Aberration, mean ± SE	0.036 ± 0.023	0.026 ± 0.010	- 0.018 ± - 0.064	0.469*
Trefoil, mean ± SE	0.132 ± 0.036	0.080 ± 0.129	0.263 ± 0.064	0.799*
Angle α, mean ± SE	0.365 ± 0.019	0.384 ± 0.020	0.237 ± 0.064	0.001*
Angle κ, mean ± SE	0.361 ± 0.023	0.258 ± 0.034	0.250 ± 0.064	0.820*
MTF, mean ± SE	0.564 ± 0.019	0.593 ± 0.344	0.544 ± 0.064	0.533*
Corneal astigmatism				
Anterior surface of the cornea, mean ± SE	0.806 ± 0.078	1.471 ± 0.268	0.857 ± 0.065	0.099
Posterior surface of the cornea, mean ± SE	0.257 ± 0.020	0.486 ± 0.051	0.330 ± 0.027	0.001
Types of astigmatism on the anterior surface of the cornea, NO. (%)				0.021
Regular astigmatism	32(68.09)	13(92.86)	38(86.36)	
Irregular astigmatism	8(17.02)	1(7.14)	0(0.00)	
Oblique axis astigmatism	7(14.89)	0(0.00)	6(13.64)	
Types of astigmatism on the posterior surface of the cornea, NO. (%)				0.329
Regular astigmatism	45(95.74)	13(92.86)	44(100.00)	
Irregular astigmatism	1(2.13)	1(7.14)	0(0.00)	
Oblique axis astigmatism	1(2.13)	0(0.00)	0(0.00)	

Abbreviations: SS Sjögren's Syndrome, *NSS* Non-Sjögren's Syndrome dry eye, *NC* Normal control, *n* number of eyes, *tHOAs* total corneal high-order aberrations, *MTF* modulation transfer function
Bold *P*-value represents < 0.05. ** indicates that the data is the result of a Kruskal–Wallis tests*

Table 4 Correlation analysis between Statistically significant optical quality characteristics and dry eye

Characteristics	Tau-b	*P*
Angle α	0.324	< 0.001
PCSA	- 0.156	0.062
ACSAT	0.178	0.055

Abbreviations: DE dry eye, *PCSA* Posterior corneal surface astigmatism, *ACSAT* anterior corneal surface astigmatism type, *Tau-b* Kendall's tau-b rank correlation coefficient
Bold *p*-value represents < 0.05

to assess the relationship between ocular surface manifestations and corneal optical quality indicators. Significant correlations identified in this step were further explored using multiple linear regression and multinomial logistic regression analyses to quantify the effect size and adjust for potential confounders (Table 4). Results confirmed a statistically robust association between Angle a and dry eye (DE) (Tau-b = 0.324, p < 0.001), while other parameters showed no significant correlations. We used multinomial linear regression analysis to investigate the relation ship between DE and Angle a. All ocular surface indicators demonstrating statistically significant differences were incorporated as confounding factors in the regression model construction to control for potential bias.

The groups of patients were not age-matched, so age and BCVA were treated as confounders in model 1. In Model 2, OSS, FNIBUT, MNIBUT, Schirmer I test, lipid layer distribution, and upper and lower MGL were also considered as confounders. The ß-values of these models and their 95% confidence intervals, as well as the p-values, are presented in Table 5. The results showed that DE had a correlation with angle a, and this correlation was more pronounced in patients with angle a = 0.3 (ß = 0.062, 95% CI: 0.016,0.108; P = 0.01) than in patients with angle a > 0.3 (ß = 0.048, 95% CI: 0.034,0.941; P = 0.035). This linear correlation still remained in Model I, but was no longer statistically significant in Model 2.

Discussion

DE is now a major social and personal economic burden in some developed countries [22]. According to epidemiologic surveys, it is more prevalent in Asia than in Europe and North America [23]. Women are the majority of patients with this disease, and

Table 5 Association between Angle α and dry eye in different models

Presence of dry eye	Events(%)	Crude model		Model I		Model 2	
		β(95%CI)	*P*	β(95%CI)	*P*	β(95%CI)	*P*
Angle α							
≤0.3	43.81	0.062(0.016,0.108)	0.010	0.089(0.025,0.153)	0.008	0.149(0.025,0.272)	0.021
> 0.3	56.19	0.048(0.034,0.941)	0.035	0.068(0.006,0.129)	0.031	0.032(- 0.116,0.181)	0.653

Abbreviations: OR odds ratio, *CI* Confidence interval, *OSS* Oxford Staining Score, *CDEQ* Chinese dry eye questionnaire, *FNIBUT* first non-invasive tear break-up time, *MNIBUT* mean non-invasive tear break-up time, *Upper MGL* upper meibomian gland loss, *Lower MGL* Lower meibomian gland loss. Bold *p*-value represents < 0.05

the risk of the disease increases with age [24]. In addition, female patients tend to be diagnosed at a younger age and have more severe symptoms compared to men [25].

As an autoimmune disease that affects multiple organ systems [26], SS is also more predominant in females [27,28]. Studies have shown that SS causes chronic inflammation of the exocrine glands, which results in tissue destruction and dryness. Consequently, SS patients experience a decrease in aqueous tear production or secretion and are at a greater risk of developing DE.

SSDE can affect the tear film and ocular surface. Previously, researchers have compared dry eye performance between SS patients and healthy individuals. Numerous clinical studies have demonstrated ocular surface changes in SS patients in some classical clinical indicators, including decreased tear production, decreased tear break-up times (TBUT), and hyperosmolarity of tears [29,30]. A study by J. Shimazaki et al. [31] stated that the lower eyelids of SS patients exhibited more pronounced MGL than other patients. All of these findings are in accordance with our results. Previous studies have shown that an AUC of 0.7–0.8 indicates that the indicator has acceptable discriminatory power [32]. In this study, we have found that Schirmer I test, OSS, CDEQ, FNIBUT and MNIBUT all exhibited robust discriminatory capacity, which were beneficial to distinguish patients with SS.

Destruction of tear film and ocular surface can impair the corneal optical quality, which is the main cause of vision loss in patients with DE. In order to achieve clear vision, it is important to maintain the integrity and stability of the precorneal tear film [33,34]. In patients with DE, optical aberrations resulting from decreased tear stability and increased tear film breakup may negatively affect the observed image objectively and psychologically. Our study illustrated that, indicators related to optical quality, such as angle a, showed statistical differences in SSDE patients compared to healthy controls. Astigmatism is a common symptom of DE [35]. Furthermore, DE patients have higher tHOA as a consequence of the increased irregularities in their tear film [36]. In the current study, the iTrace is the only ophthalmic instrument capable of measuring both the angles a and ?, enabling the assessment of visual quality in patients with DE disease. Post-operative follow-up results of some ophthalmic surgeries have shown that excessively large angles a can lead to deviation of the visual axis center, reducing the patient's visual quality [37,38]. Our findings highlight the significant impact of SSDE on corneal optical quality and ocular surface health. The identified correlations between ocular surface parameters and corneal optical quality suggest potential biomarkers for early intervention. This study demonstrates that SSDE significantly impairs corneal optical quality and ocular surface health. Early detection and management of SSDE are crucial to preserving visual quality.

In the present study, some patients completed questionnaires. The ocular surface disease index questionnaire (OSDI) has been employed as a diagnostic and grading tool for DE in numerous studies [39,40,41]. However, this indicator was not statistically different between the two groups, this may be due to the small number of participants who completed the OSDI survey in this study. The Chinese Dry Eye Questionnaire (CDEQ) is designed for the characteristics of the living and working environments of Chinese, which makes it more suitable for Chinese patients with DE [42]. Combined with our findings, this questionnaire may be more accurate than the OSDI in assessing the ocular surface of Chinese patients. Goal of this paper is to examine corneal surface symptoms and measurements in a Chinese SSDE group compared to non-SS DE patients and normal controls, and then to hopefully identify specific corneal surface symptoms and indicators that are more helpful in predicting optical quality. The strengths of our study are the

inclusion of female patients with SSDE at a certain age and the wide variety of clinical indicators involved. These will greatly benefit patients with SS in terms of protecting their visual quality. This study identified significant correlations between ocular surface manifestations and corneal optical quality in Chinese female patients with SSDE. The findings highlight the importance of early detection and management of dry eye symptoms to preserve visual quality. Future research should explore the underlying mechanisms and potential therapeutic interventions to improve outcomes for patients with SSDE.

In spite of this, there are some limitations to this study. First, some participants provided incomplete or omitted information, which may have affected study results. In addition, the imbalance in the number of participants included in each group may cause some bias in the results. Second, although we have adjusted for the indicators, we have not completely eliminated the effects of unmeasured confounders. Another issue is that the number of cases in the groups of participants we included, as well as their ages, were not matched. Last but not least, this was a cross-sectional study. There is still a need for prospective and experimental studies to determine the causal relationship between visual performance and clinical ocular surface performance in patients with SS.

Conclusion

In conclusion, this study underscores the substantial impact of Sjogren's syndrome dry eye (SSDE) on corneal optical quality and ocular surface health. Our findings highlight the critical importance of early detection and proactive management of SSDE in order to effectively preserve visual quality and mitigate potential long-term complications.

Data availability

The datasets used and/or analyzed in this study are available upon request from the corresponding author.

References

1. Stapleton F, Alves M, Bunya VY, Jalbert I, Lekhanont K, Malet F, Na K, Schaumberg D, Uchino M, Vehof J, et al. TFOS DEWS II Epidemiology Report. Ocul Surf. 2017;15(3):334–65.
2. Sheppard J, Shen Lee B, Periman LM. Dry eye disease: identification and therapeutic strategies for primary care clinicians and clinical specialists. ANN MED. 2023;55(1):241–52.
3. Akpek EK, Wirta DL, Downing JE, Tauber J, Sheppard JD, Ciolino JB, Meides AS, Krösser S. Efficacy and Safety of a Water-Free Topical Cyclosporine, 0.1%, Solution for the Treatment of Moderate to Severe Dry Eye Disease: The ESSENCE-2 Randomized Clinical Trial. Jama Ophthalmol. 2023;141(5):459–66.
4. Nichols KK, Nichols JJ, Mitchell GL. The lack of association between signs and symptoms in patients with dry eye disease. Cornea. 2004;23(8):762–70.
5. Yang Y, Zhong J, Cui D, Jensen LD. Up-to-date molecular medicine strategies for management of ocular surface neovascularization. ADV DRUG DELIVER REV. 2023;201: 115084.
6. Tsubota K, Yokoi N, Shimazaki J, Watanabe H, Dogru M, Yamada M, Kinoshita S, Kim H, Tchah H, Hyon JY, et al. New Perspectives on Dry Eye Definition and Diagnosis: A Consensus Report by the Asia Dry Eye Society. Ocul Surf. 2017;15(1):65–76.
7. Yu K, Bunya V, Maguire M, Asbell P, Ying G. Systemic Conditions Associated with Severity of Dry Eye Signs and Symptoms in the Dry Eye Assessment and Management Study. Ophthalmology. 2021;128(10):1384–92.
8. He J, Chen J, Miao M, Zhang R, Cheng G, Wang Y, Feng R, Huang B, Luan H, Jia Y, et al. Efficacy and Safety of Low-Dose Interleukin 2 for Primary Sjögren Syndrome: A Randomized Clinical Trial. JAMA NETW OPEN. 2022;5(11): e2241451.
9. Baer AN, Gottenberg J, St Clair EW, Sumida T, Takeuchi T, Seror R, Foulks G, Nys M, Mukherjee S, Wong R, et al. Efficacy and safety of abatacept in active primary Sjögren's syndrome: results of a phase III, randomised, placebo-controlled trial. In. 2021;80: 339–48.
10. Brito-Zerón P, Theander E, Baldini C, Seror R, Retamozo S, Quartuccio L, Bootsma H, Bowman SJ, Dörner T, Gottenberg J, et al. Early diagnosis of primary Sjögren's syndrome: EULAR-SS task force clinical recommendations. EXPERT REV CLIN IMMU. 2016;12(2): 137–56.
11. Bjordal O, Norheim KB, Rødahl E, Jonsson R, Omdal R. Primary Sjögren's syndrome and the eye. SURV OPHTHALMOL. 2020;65(2):119–32.
12. Baudouin C, Aragona P, Messmer EM, Tomlinson A, Calonge M, Boboridis KG, Akova YA, Geerling G, Labetoulle M, Rolando M: Role of Hyperosmolarity in the Pathogenesis and Management of Dry Eye Disease: Proceedings of the OCEAN Group Meeting. The Ocular Surface. 2013;11(4):246–258.
13. Baudouin C, Irkeç M, Messmer EM, Benítez-Del-Castillo JM, Bonini S, Figueiredo FC, Geerling G, Labetoulle M, Lemp M, Rolando M, et al. Clinical impact of inflammation in dry eye disease: proceedings of the ODISSEY group meeting. ACTA OPHTHALMOL. 2018;96(2):111–9.
14. Akpek EK, Bunya VY, Saldanha IJ. Sjögren's Syndrome: More Than Just Dry Eye. Cornea. 2019;38(5):658–61.
15. Franceschini F, Cavazzana I, Andreoli L, Tincani A. The 2016 classification criteria for primary Sjogren's syndrome: what's new? BMC MED. 2017;15(1):69.
16. J. W: Ocular Surface Disease Index (OSDI) Administration and Scoring Manual. In.: Irvine, CA: Allergan, Inc; 2004.
17. Zhao H, Liu Z, Yang W, Xiao X, Chen J, Li Q, Zhong T: [Development and assessment of a dry eye questionnaire applicable to the Chinese population]. [Zhonghua yan ke za zhi] Chinese journal of ophthalmology. 2015;51 (9):647–654.
18. Wang MTM, Craig JP. Comparative Evaluation of Clinical Methods of Tear Film Stability Assessment: A Randomized Crossover Trial. JAMA OPHTHALMOL. 2018;136(3):291–4.
19. Begley C, Caffery B, Chalmers R, Situ P, Simpson T, Nelson JD. Review and analysis of grading scales for ocular surface staining. Ocul Surf. 2019;17 (2):208–20.
20. Tashbayev B, Yazdani M, Arita R, Fineide F, Utheim TP. Intense pulsed light treatment in meibomian gland dysfunction: A concise review. Ocul Surf. 2020;18(4):583–94.

21. Eom Y, Lee J, Keun Lee H, Myung Kim H, Suk Song J: Comparison of conjunctival staining between lissamine green and yellow filtered fluorescein sodium. Canadian journal of ophthalmology. Journal canadien d'ophtalmologie. 2015;50(4):273–277.
22. McKnight W: Chapter Ten - Operational Big Data: Key-Value, Document, and Column Stores: Hash Tables Reborn. In: Information Management. Edited by McKnight W. Boston: Morgan Kaufmann; 2014: 97–109.
23. Tsubota K, Pflugfelder SC, Liu Z, Baudouin C, Kim HM, Messmer EM, Kruse F, Liang L, Carreno-Galeano JT, Rolando M, et al. Defining Dry Eye from a Clinical Perspective. Int J Mol Sci. 2020;21(23):9271.
24. Messmer EM: The pathophysiology, diagnosis, and treatment of dry eye disease. DTSCH ARZTEBL INT 2015, 112(5):71–81, 82.
25. Matossian C, McDonald M, Donaldson KE, Nichols KK, MacIver S, Gupta PK: Dry Eye Disease: Consideration for Women's Health. Journal of women's health (2002) 2019, 28(4):502–514.
26. Chen W, Cao H, Lin J, Olsen N, Zheng SG. Biomarkers for Primary Sjögren's Syndrome. Genomics Proteomics Bioinformatics. 2015;13(4):219–23.
27. Manuel RSJ, Liang Y. Sexual dimorphism in immunometabolism and autoimmunity: Impact on personalized medicine. AUTOIMMUN REV. 2021; 20(4): 102775.
28. Brandt JE, Priori R, Valesini G, Fairweather D. Sex differences in Sjögren's syndrome: a comprehensive review of immune mechanisms. BIOL SEX DIFFER. 2015;6:19.
29. Stevenson W, Chauhan SK, Dana R: Dry eye disease: an immune-mediated ocular surface disorder. Archives of ophthalmology (Chicago, Ill.: 1960) 2012, 130(1):90–100.
30. Lemp MA. Advances in Understanding and Managing Dry Eye Disease. Am J Ophthalmol. 2008;146(3):350–6.
31. Shimazaki J, Goto E, Ono M, Shimmura S, Tsubota K. Meibomian gland dysfunction in patients with Sjögren syndrome. Ophthalmology. 1998;105 (8):1485–8.
32. Mandrekar JN. Receiver operating characteristic curve in diagnostic test assessment. Journal of thoracic oncology: official publication of the International Association for the Study of Lung Cancer. 2010;5(9):13 15–6.
33. Rieger G. The importance of the precorneal tear film for the quality of optical imaging. Br J Ophthalmol. 1992; 76(3):157–8.
34. Tutt R, Bradley A, Begley C, Thibos LN. Optical and visual impact of tear break-up in human eyes. Invest Ophth Vis Sci. 2000;41(13):4117–23.
35. Liu Z, Pflugfelder SC. Corneal surface regularity and the effect of artificial tears in aqueous tear deficiency. Ophthalmology. 1999;106(5):939–43.
36. Montés-Micó R, Cáliz A, Alió JL: Wavefront analysis of higher order aberrations in dry eye patients. Journal of refractive surgery (Thorofare, N.J.: 1995) 2004, 20(3):243–247.
37. Fu Y, Kou J, Chen D, Wang D, Zhao Y, Hu M, Lin X, Dai Q, Li J, Zhao Y. Influence of angle kappa and angle alpha on visual quality after implantation of multifocal intraocular lenses. J Cataract Refr Surg. 2019;45(9):1258–64.
38. Wang L. Guimaraes de Souza R, Weikert MP, Koch DD: Evaluation of crystalline lens and intraocular lens tilt using a swept-source optical coherence tomography biometer. J Cataract Refr Surg. 2019;45(1):35–40.
39. de Paiva CS, Trujillo-Vargas CM, Schaefer L, Yu Z, Britton RA, Pflugfelder SC. Differentially Expressed Gene Pathways in the Conjunctiva of Sjögren Syndrome Keratoconjunctivitis Sicca. Front Immunol. 2021;12: 702755.
40. Ren X, Chou Y, Wang Y, Jing D, Chen Y, Li X. The Utility of Oral Vitamin B1 and Mecobalamin to Improve Corneal Nerves in Dry Eye Disease: An In Vivo Confocal Microscopy Study. Nutrients. 2022;14(18):3750.
41. Tsai T, Alwees M, Rost A, Theile J, Dick HB, Joachim SC, Taneri S. Changes of Subjective Symptoms and Tear Film Biomarkers following Femto-LASIK. Int J Mol Sci. 2022;23(14):7512.
42. Zhao Hui LMAY. Development and evaluation of dry eye questionnaire in China. Chinese J Ophth. 2015;9: 647–54.

Acknowledgements

Support of this work were provided by Guangzhou Science and Technology Project, Natural Science Foundation Project of Guangdong Province, and Guangzhou Health Science and Technology Project.

Funding

This study was supported by Guangzhou Science and Technology Project (No. 2024A03J0207), Natural Science Foundation Project of Guangdong Province (No. 2019A1515011094), and Guangzhou Health Science and Technology Project (No. 205010606044).

Author information

Author notes

Jingyu Zhang, Qian Deng and Maierhaba Maitiyaer contributed equally and should be considered as co-first authors.

Authors and Affiliations

Ophthalmic Center, The Second Affiliated Hospital, Guangzhou Medical University, Guangzhou, Guangdong, China
Jingyu Zhang, Qian Deng, Li Wang, Yue Liang, Qiudan Huang & Zhiping Liu

Department of Rheumatology, The Second Affiliated Hospital, Guangzhou Medical University, Guangzhou, Guangdong, China
Maierhaba Maitiyaer & ShuiLian Yu

Guangdong Provincial Key Laboratory of Allergy & Clinical Immunology, The Second Affiliated Hospital, Guangzhou Medical University, Guangzhou, Guangdong, China
Jingyu Zhang, Maierhaba Maitiyaer, Li Wang, Yue Liang, ShuiLian Yu & Zhiping Liu

Department of Ophthalmology, Zhejiang Provincal People's Hospital Bijie Hospital, Bijie, Guizhou, China
Qian Deng

Department of Ophthalmology, University of Colorado, Aurora, CO, USA
Amy Michelle Huang

Contributions

Author Contributions: JZ and ZL designed the study; QD, MM, LW, YL QH, and SY participated in data collection, analysis and interpretation; JZ, AH, and ZL drafted the manuscript; All authors reviewed and approved the manuscript.

Corresponding authors

Correspondence to ShuiLian Yu or Zhiping Liu.

Credit: Zhang, J., Deng, Q., Maitiyaer, M. et al. The relation between corneal optical quality and clinical ocular surface manifestations in Chinese female with Sjogren's syndrome dry eye. BMC Ophthalmol 25, 399 (2025). https://doi.org/ 10.1186/s12886-025-04225-2

Astymin®-SN

Pure Crystalline Amino Acid I. V Infusion **200ml**

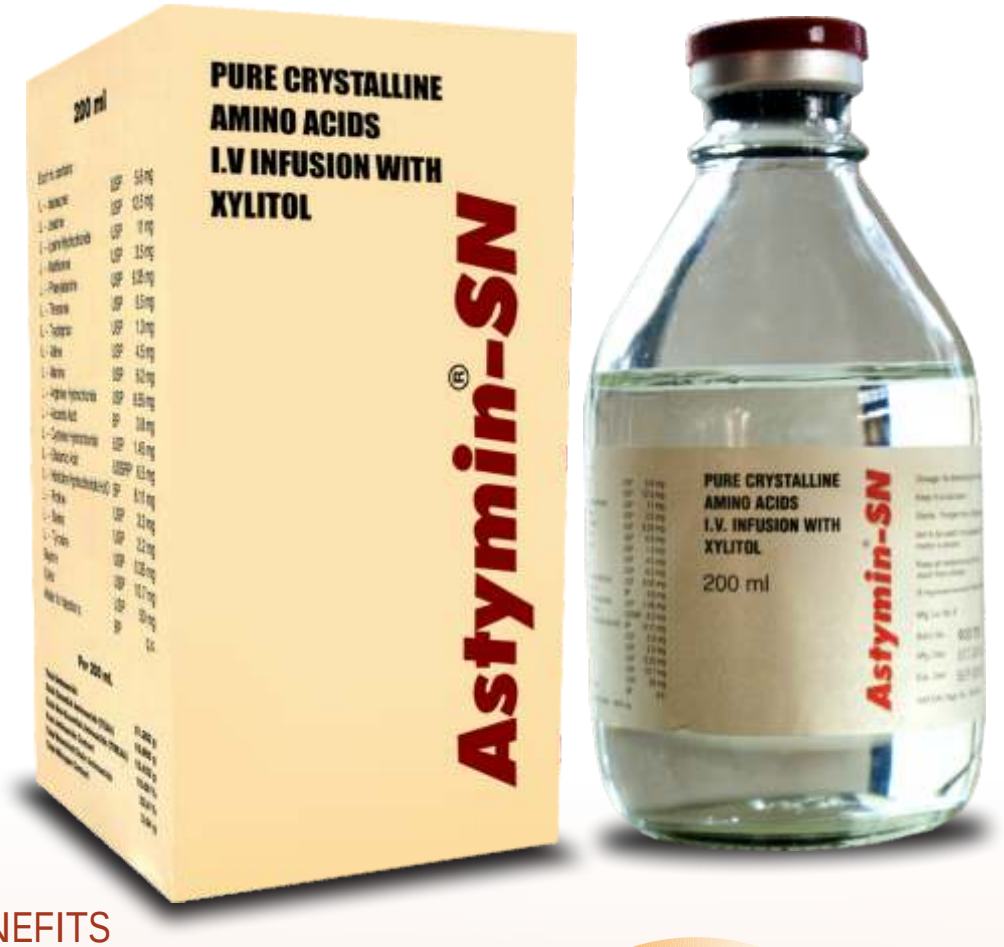

BENEFITS

- Reduced handling contamination
- Saves lives
- Reduce nursing time
- Reduce cost of hospitalisation
- Ratio of essential to non essential is 1:1
  - Meets the requirement set by WHO/FAO joint special committee on protein requirement[4].
  - Balanced proportion of branched chain amino acids[5]
- Useful in catabolic disease states and in conditions where rapid protein synthesis is desired.
  - High content of protein and nitrogen
- Reduce vulnerability to weight loss and muscle wasting
- Rapidly normalize negative nitrogen balance.

Specialized Nutritional Support

FIDSON

Fidson Healthcare Plc

...we value life

...the Amino Acid Infusion of choice.

Emzor Vaccines...

Protecting NIGERIANS

HEPATITIS B

...More Common Than You Think

Mother to child during child birth

Blood & blood materials / equipments

Tattoo

HEPATITIS B is 100x more contagious than HIV.

Hair and Nail Clipper

Unprotected Sexual contact

- With prevalence rate of **9.5%**, Nigeria is considered a high prevalence country*

THE SOLUTION:

It is as simple as 1, 2, 3.

✓ **Get Screened**
(positive result will require further investigation)

✓ **Get Vaccinated**

✓ **Get Protected for life!**

Emechebe, G.O, et al (2009). Hepatitis B Virus Infection in Nigeria-A review. Niger Med J 2009,50: 18-22.

Emzor Vaccines
(A member of the Emzor Group)

WE OFFER SIMPLE AFFORDABLE SOLUTIONS FOR PROTECTION AGAINST HEPATITIS B.

A MEMBER OF OUR PROFESSIONAL TEAM IS AVAILABLE TO DISCUSS TAILORED PROGRAMMES TO SUIT YOUR ORGANIZATION/INDIVIDUAL NEEDS.

CONTACT US ON:
07055368861, 07080606000, 08103483022 and 08025659116
Email: customerservice@emzorpharma.com

Professional Screening Services

*Ajuwon et al. BMC Infectious Diseases (2021) 21:1120

Emzor... Unlimited Wellness

Persistence of hepatitis C virus in peripheral blood mononuclear cells of patients who achieved sustained virological response following treatment with direct-acting antivirals is associated with a distinct pre-existing immune exhaustion status

Sylwia Osuch, Marta Kazek, Paulina Emmel, Hanna Berak, Marek Radkowski & Kamila Cortés-Fendorf

Abstract

Hepatitis C virus (HCV) is a primary hepatotropic pathogen responsible for acute and chronic hepatitis C, however, it can also cause "occult" infection (OCI), defined as the presence of the virus' genetic material in hepatocytes and/or peripheral blood cells, but not in plasma/serum. Assessment of the sustained virologic response (SVR) after treatment with direct-acting antivirals (DAA) is based exclusively on HCV-RNA testing in plasma/serum, which may preclude the diagnosis of post-treatment OCI. Possible clinical consequences of OCI were described previously, but its occurrence after DAA-based antiviral treatment programs and determinants of the virus persistence are not fully elucidated. The aim of this study was to assess the incidence of post-treatment OCI after successful DAA-based treatment and to identify clinical and immunological factors associated with this phenomenon. In 97 patients treated with DAA, HCV-RNA was tested by RT-PCR in peripheral blood mononuclear cells (PBMC) at baseline (i.e., before the onset of treatment) and at the time of SVR assessment. Before treatment, HCV-RNA was detectable in all patients' PBMC. All subjects responded to therapy according to the clinical criteria, but 9 (9.3%) patients revealed the HCV-RNA in PBMC at SVR. In most of these cases, post-DAA OCI was related to switch of the dominant infecting genotype. Post-treatment OCI was characterized by significantly lower pre-treatment HCV viral load and lower expression of Tim-3 (T-cell immunoglobulin and mucin domain-containing protein 3) on CD8+ T-cells. Our results imply that post-treatment OCI may be related to lower pretreatment viral load as well as distinct pre-existing immune exhaustion status.

Introduction

Hepatitis C virus (HCV) is a cause of chronic hepatitis C (CHC), which may lead to liver cirrhosis and hepatocellular carcinoma (HCC). Although hepatocytes are the primary site of HCV infection, CHC is increasingly recognized as a systemic disease, associated with a wide spectrum of accompanying symptoms[1,2]. Secondary tropism and extrahepatic replication have been demonstrated in PBMCs, macrophages, dendritic cells, bone marrow and central nervous system[3,4,5,6,7].

The "occult" HCV infection (OCI) is defined as the presence of the virus' genetic material in hepatocytes and/or peripheral blood cells, and not in plasma/serum[8,9]. Viral replication usually occurs at a low level[10], and the presence of anti-HCV antibodies can be either positive or negative[8,9].

OCI is prevalently observed in patients in whom the infection has resolved in the acute phase (up to 70% of cases) or who were treated with previous interferon-a-based therapies[8,11,12]. Studies conducted on the general population revealed OCI in 3% of apparently healthy subjects and in 2% of blood donors[13]. OCI has been described as transient, recurrent, or long-term and patients rarely manifest clinical symptoms and/or elevated liver enzymes[14]. Nevertheless, it may be also related to progressive inflammatory changes, liver fibrosis, and infection reactivation[15,16,17,18,19,20,21,22,23,24]. Although HCV from subjects with OCI was found to infect human lymphocytes from healthy donors[10], there is not enough evidence data to whether OCI is transmissible.

The best approach for OCI diagnosis is based on the use of sensitive molecular methods detecting HCV RNA in liver tissue[10]. However, because of its invasive character, PBMC testing has been also employed, because of a good concordance between detection of HCV-RNA in PBMC and liver tissue, reaching 70%[13,16,25].

Actual standard of CHC treatment is based on direct-acting antivirals (DAA) suppressing viral replication by inhibiting the activity of NS3

protease, NS5A protein or NS5B polymerase[21]. Treatment became shorter, less toxic and very effective, when compared to the previously used combination of interferon-a and ribavirin. Sustained virologic response (SVR), defined as a negative result of viral RNA testing in blood plasma/serum 12 or 24 weeks after the end of treatment, is achieved in > 90% of patients[26]. However, SVR is not always equal to the complete virus eradication and does not exclude the post-treatment OCI. Ongoing viral persistence following successful DAA treatment may lead to clinical progression of liver disease or relapse[22,27]. Thus, it is of importance to implement surveillance of patients who achieved SVR, as well as to investigate post-DAA OCI – including its possible determinants, which may lay both in the mechanisms of cell infection and the specific immune response of the host[16,28,29,30,31]. Similarly, since the risk of HCC development persists despite achieving SVR, OCI has been proposed as a potential risk factor. However, current evidence remains inconclusive and a larger, longitudinal studies are required to definitively assess whether persistent OCI may lead to hepatocarcino genesis[32,33,34,35,36,37,38].

Immune exhaustion is an immune cell dysfunction characteristic of chronic infections and cancer, originating from prolonged and high-level antigen exposure as well as inflammatory signals[39,40,41,42]. It was observed in chronic viral infections, such as HCV, HIV, HBV, adenovirus, polyomavirus, HTLV-1[43,44,45,46,47] and affects both CD8+ and CD4+ T-cells, but was also observed in NK or B-cells[48,49]. In particular, CD8+ T cells undergo a progressive loss of effector functions, encompassing impaired proliferation and ability to secrete effector cytokines, loss of cytotoxicity, upregulated expression of inhibitory receptors (iRs) as well as dysregulated transcriptional program, contributing to impaired viral control[39,40,50]. Some key iRs are PD-1, Tim-3 and LAG-3. Progression of exhaustion is characterized by excessive, constitutive, simultaneous expression of multiple iRs as well as upregulation of IL-1051,[52]. In addition to membrane-bound molecules, soluble iRs (eg., sPD-1, sTim-3, sLAG-3) are detectable in plasma, mainly as a result of enzymatic cleavage, cells breakdown or alternative splicing[53,54,55,56]. Understanding the immunological landscape of exhaustion in patients with post-DAA OCI is therefore of clinical relevance.

The aim of this study was to assess the incidence of post-treatment OCI after successful DAA treatment and to analyze possible clinical and immunological factors associated with this phenomenon.

Materials and methods

The research material

PBMC isolated from the whole blood by density gradient centrifugation using the Lymphoprep reagent (Stemcell Technologies) of 97 CHC patients from the Warsaw Hospital for Infectious Diseases were collected on the day of treatment initiation and 24 weeks after completion of treatment with DAA, corresponding to the SVR24 assessment time point.

All subjects qualified for the study achieved SVR by HCV RNA testing using a PCR method of a sensitivity of 12 IU/mL (Abbott RealTime HCV Viral Load Assay). The following data were collected: age, sex, BMI, bilirubin levels, ALT activity, liver elastography (FibroScan), HCV genotype (Inno-LIPA HCV II, Innogenetics) and viral load before treatment (Abbott RealTime HCV Viral Load Assay). The characteristics of the study group are presented in Table 1.

The study was conducted in compliance with the Declaration of Helsinki and was approved by the bioethics committee of the Medical University of Warsaw (approval number: AKBE/43/2022). Written informed consent was obtained from all patients prior to the study initiation.

Isolation of HCV RNA and degradation of contaminating DNA

RNA was isolated from PBMC samples containing 3 million cells by Chomczynski method using TRIzol reagent (Invitrogen) and resuspended in molecular biology grade water (Invitrogen). The DNA-free Kit (Ambion) was used in accordance with the manufacturer's recommendations to degrade any contaminating DNA.

Reverse transcription and amplification of the HCV 5' UTR fragment by polymerase chain reaction (PCR)

DNA-free RNA was reversely transcribed using a M-MLV reverse transcriptase (Invitrogen) according to the manufacturer's recommendations. A positive control template comprised synthetic 5' UTR (5' untranslated region) HCV RNA strands derived from a plasmid; negative control comprised a molecular biology grade water instead of a template.

A PCR reaction mixture was prepared using a forward (5'-TGRTGCACGGTCTACGAGACCTC-3') and reverse (5'-RAYCACTCCCCTG TGAGGAAC-3') reaction primers and FastStart Taq Polymerase Kit (Roche). One µl of cDNA was used as a reaction template. The PCR reaction comprised one cycle of initial denaturation at 94 °C for 5 min; 50 cycles, each consisting of denaturation for 1 min at 94 °C and primer annealing for 1 min at 58 °C, and one cycle of elongation for 7 min at 72 °C.

Table 1 Characteristics of the study participants.

Age [median (range)]		57 (25–88)
BMI [kg/m^2]		26.1 (15.0–46.7)
Sex [F/M]		61/36
Baseline bilirubin level [mg/dL] [median (range)]		13.1 (5.3–46.6)
ALT [IU/L] [median (range)]		61 (19–389)
Baseline viral load [IU/mL] [median (range)]		8.3×10^5 (6.2×10^3–1.1×10^7)
CD4 per CD3$^+$ cells [%]		65.9 (26.2–90.1)
CD8 per CD3$^+$ cells [%]		22.8 (6.9–57.1)
HCV genotype	1a	2
	1b	95
Liver fibrosis stage	F0/1	56
	F2	27
	F3	14
Treatment scheme and duration	Harvoni (Ledipasvir + Sofosbuvir) (8/12 weeks)	69
	Viekirax + Exviera (Ombitasvir + Paritaprevir + Ritonavir + Dasabuvir) (8/12 weeks)	21
	Zepatier (Elbasvir + Grazoprevir) (12 weeks)	7
Previous unsuccessful treatment history	DAA	1
	interferon-α + ribavirin	23

Nested PCR and electrophoresis

The nested PCR was performed using forward (5'-ACTGTCTTCA CGCAGAAAGCGTC-3') and reverse (5'-CAAGCACCCTATCAGGCAGTAC C-3') primers. One µl of the PCR product was used as a reaction template. The PCR steps included: one cycle of initial denaturation at 94 °C for 5 min; 30 cycles, each consisting of denaturation for 1 min at 94 °C and primer annealing for 1 min at 58 °C, and final extension for 7 min at 72 °C. The PCR product (273 bp) was visualized by 2% agarose gel electrophoresis using the SYBR Safe DNA Gel Stain reagent (Invitrogen).

Based on the previous amplification of serial dilutions of synthetic HCV RNA strands, derived from a plasmid with cloned HCV 5' UTR transcribed with T7 polymerase, the analytical sensitivity of the employed method was estimated to be ~ 10 genomic equivalents of the template[57,58].

5'UTR amplicon sequencing

5' UTR amplicons obtained from post-treatment PBMC samples along with their respective pre-treatment pairs were purified using Nucleospin PCR Clean-up and Gel Extraction Kit (Macherey– Nagel), quantified using the Qubit assay dsDNA HS kit (Thermo Fisher Scientific) and subjected to Sanger-based sequencing on ABI Prism Genetic Analyzer to detect dominant genotype strains.

Next-generation sequencing (NGS) analysis

In cases in which a switch in the

dominant genotype was detected in PBMC by Sanger-based sequencing, NGS of pre-treatment serum and PBMC samples was performed to search for minor variants of alternative genotype. In brief, 5'UTR amplicons were purified using the Nucleospin PCR Clean-up Kit (Macherey–Nagel) and quantified with the Qubit dsDNA HS Assay Kit (Thermo Fisher Scientific). Amplicon libraries were prepared according to Illumina standard protocols using indexing and sequenced on the Illumina MiSeq platform using 2× 300 bp sequencing kit (Illumina). The NGS data in FASTQ format were subjected to demultiplexing, adapter trimming and low-quality read removal using fastp (version 0.23.4). Sequence data quality control was then performed using FastQC (version 0.12.1). The summary quality control report was made using MultiQC (version 1.21). Read mapping to the reference (GenBank: AJ242654) was performed using BWA-MEM (version 0.7.17). SAM files were obtained, which were then converted to BAM files and sorted using samtools (version 1.15.1). Integrative Genomic Viewer version 2.19.1 was used to visualize the sequencing data.

Assessment of exhaustion markers expression on CD4+ and CD8+ T-cells by flow cytometry

Pre-treatment programmed death receptor-1 (PD-1) and T cell immunoglobulin and mucin domain-containing protein 3 (Tim-3) expression on CD4+ and CD8+ T-cells were assessed as described previously[59]. In brief, isolated PBMC, resuspended in PBS were stained with BD Horizon Fixable Viability Stain 780 (BD Biosciences) and mixed with FcR blocking reagent (Miltenyi Biotec) following the manufacturer's protocol. Next, one million cells were resuspended in Stain Buffer (BD Pharmingen), mixed with 5 µl of BV421 Mouse Anti-Human Tim-3 (CD366) Clone 7D3 (BD Horizon)), 5 µl of Alexa Fluor 647 Mouse Anti-Human PD-1 (CD279) Clone EH12.1, 5 µl of PerCP-Cy 5.5 Mouse Anti-Human CD3 Clone UCHT1, (both from BD Pharmingen), 5 µl of V500 Mouse Anti Human CD4 Clone RPA-TY (BD Horizon) and 1 µl of Mouse Anti-Human CD8 FITC Clone LT8 (ProImmune). Cells with added antibodies were incubated for 20 min at 4 °C, washed twice with PBS pH 7.2 (Life Technologies) and resuspended in 300 µL of Stain Buffer. The results were acquired immediately after staining by BD FACS Canto II Flow Cytometer (BD Biosciences), using BD FACS Diva version 6.0 program (BD Biosciences). Controls included unstained cells and isotype controls (Mouse Anti-Human IgG1 Alexa Fluor 647 and Mouse Anti-Human IgG1 BV421 instead of Alexa Fluor 647 Mouse Anti-Human PD-1 (CD279) and BV421 Mouse Anti-Human Tim-3 (CD366), respectively (both from BD Pharmingen).

For data analysis, the initial gate was set on lymphocytes on the forward scatter (FSC) vs side scatter (SSC) dot plot. Subsequently, singlet cells gate was set on FSC-H versus FSC-A dot plot. Next, based on SSC vs APC-Cy7 dot plot, only live cells were gated. Additionally, the following gates were employed: Cd3+, CD4+, CD8+, PD-1+, Tim-3+ and PD-1+Tim-3+. The analysis was performed using BD FACS Diva version 6.0 program (BD Biosciences).

Assessment of exhaustion markers plasma levels

IL-10, PD-1, Tim-3 and lymphocyte activation gene 3 (LAG-3) levels in plasma before and after treatment were assessed using Human IL-10 (High Sensitivity), PD-1, TIM-3, LAG-3 ELISA Kits (all from Thermo Fisher Scientific).

Data and statistical analysis

Web based Basic Local Alignment Search Tool (BLAST) available at https://blast.ncbi.nlm.nih.gov/doc/blast was used to search for nucleotide similarity of the sequenced 5'UTR reads against the core nucleotide database, choosing option of Hepacivirus hominis (taxid:3052230) to determine the viral genotype. Additionally, a maximum likelihood phylogenetic analysis based on Tamura-Nei model of the sequenced region was conducted using MEGA version 11 against 1b, 3a, 4a, and 4d reference sequences (GenBank accession numbers: AJ242654, MN231293.1, DQ418782.1 and KP888621.1, respectively) to confirm evolutionary relationship of genotypes[60].

Numerical data were graphically visualized using GraphPad program.

For the statistical analyses, Mann–Whitney, The Wilcoxon matched-pairs signed-ranks test and Fisher's exact tests were used. Statistical analysis was performed using the GraphPad Prism program. All P-values were two-tailed and considered significant when < 0.05.

Results

HCV RNA may persist in PBMC after successful DAA treatment

Before treatment, HCV RNA in PBMCs was detectable in all (97, 100%) patients, whereas after treatment, in 9 (9.3%) patients (i.e., # 5, 6, 14, 36, 38, 47, 48, 52 and 82). Two patients (i.e., # 5 and 6) were treated with ombitasvir + paritaprevir + ritonavir + dasabuvir, six patients (i.e., # 14, 36, 38, 47, 48, and 52) were treated with ledipasvir + sofosbuvir, and one patient (i.e., # 82) was treated with elbasvir + grazoprevir (Table

Table 2: Clinical and virological characteristics of patients in whom HCV RNA was detected in PBMC post-DAA treatment.

Patient number	DAA Treatment	History of previous CHC therapy (which)	Treatment duration [weeks]	Pre-treatment dominant HCV strain in serum	Pre-treatment dominant HCV genotype strain in PBMC	Age (years)	Sex [M/F]	BMI (kg/m^2)	Liver fibrosis stage	ALT [IU/L]	HCV RNA [IU/mL]	Post-treatment dominant HCV genotype strain in PBMC	Minor alternative genotype strain detection in PBMC/serum before treatment (frequency %)
005	Ombitasvir + Paritaprevir + Ritonavir + Dasabuvir	No	12	1b	1b	38	F	42.1	F2	53	$1{,}03 \times 10^6$	3a	PBMC:0.12–0.38%, serum: 0.11–0.26%
006	Ombitasvir + Paritaprevir + Ritonavir + Dasabuvir	No	12	1b	1b	40	M	37.7	F2	33	$7{,}12 \times 10^5$	1b	N/A
014	Ledipasvir + Sofosbuvir	Yes (IFN)	12	1b	1b	52	M	25.8	F2	115	$2{,}37 \times 10^5$	4d	PBMC: 0.12–0.75%, serum: 0.15–0.47%
036	Ledipasvir + Sofosbuvir	No	8	1b	N/A	81	F	25.0	F0/1	79	$1{,}94 \times 10^5$	N/A	N/A
038	Ledipasvir + Sofosbuvir	No	8	1b	N/A	73	F	29.6	F0/1	29	$1{,}57 \times 10^4$	N/A	N/A
047	Ledipasvir + Sofosbuvir	No	8	1b	1b	79	M	23.8	F0/1	34	$5{,}01 \times 10^5$	4a	PBMC: 0.01–0.18%, serum: 0.18–0.94%
048	Ledipasvir + Sofosbuvir	No	8	1b	1b	43	F	40.0	F0/1	53	$1{,}30 \times 10^5$	3a	PBMC: 0.11–0.17%, serum: 0.12–0.63%
052	Ledipasvir + Sofosbuvir	No	12	1b	1b	61	F	25.6	F0/1	255	$6{,}17 \times 10^3$	1b	N/A
082	Elbasvir + Grazoprevir	Yes (IFN)	12	1b	N/A	58	M	25.6	F0/1	63	$1{,}28 \times 10^4$	N/A	N/A

N/A, not available/not applicable

2). Two patients with detectable virus experienced previous non-effective IFN-based treatment (Table 2). All these patients were diagnosed as infected with HCV 1b by routine INNO-LiPA HCV II testing of serum samples before treatment. In six out of nine HCV RNA-positive patients (i.e., #5, 6, 14, 47, 48 and 52), the 5'UTR pre-and post-treatment nucleotide sequence pairs derived from PBMC were obtained by Sanger-based sequencing (Table 2). The analysis revealed that the dominant PBMC sequences were distinct in patients # 5, 14, 47, 48 (i.e., differing by 4–18 point mutations), while in patient # 6 these were nearly identical (i.e., 2 point mutations), and in patient # 52—identical (i.e., no point mutations). The BLASTn and phylogenetic analysis showed that all pre-treatment PBMC sequences were 1b, concordant with the routine analysis in serum, whereas post-treatment PBMC sequences switched to sequences 3a in patient 5 and 48, to 4d in patient 14 and to 4a in patient 47, and remained 1b in patients 6 and 52 (Table 2 and Supplementary Fig. 1). NGS analysis revealed that in all patients in whom a genotype switch was observed, the respective pre-treatment PBMC and serum samples contained also a minor alternative genotype variants of low frequency carrying polymorphisms specific to this genotype (i.e., 0.01–0.75% and 0.11–0.94%, respectively), Table 2

Sex, liver fibrosis and previous IFN treatment are not associated with post-treatment OCI

We did not find the significant difference in the distribution of sex, degree of liver fibrosis, the type and the fact of previous IFN treatment between patients with OCI and no OCI (Supplementary Table 1).

Patients with post-treatment OCI were characterized by a significantly lower pre-treatment viral load

Pre-treatment median age, BMI, bilirubin levels, ALT activity as well as percentage of CD4+ and CD8+ per CD3+ T-cells were not found to be significantly different in patients with OCI and no OCI (Fig. 1A–D,F,G, respectively and Supplementary Table 2). However, the median initial viral load was significantly lower in patients with OCI than in patients in whom no viral RNA was detected (1.9×10^5 (6.2×10^3–1.0×10^6) vs 9.3×10^5 (1.4×10^4–1.1×10^7) IU/mL, P = 0.002) (Fig. 1E)..

Patients with post-treatment OCI were characterized by a significantly lower pre-treatment Tim-3 expression on CD8+ T-cells

The median pre-treatment plasma IL-10, sPD-1, sTim-3 and sLAG-3 levels did not significantly differ between both groups of patients (Supplementary Table 2).

Although the median baseline percentages of PD-1 and PD-1 + Tim-3 expressing CD4+ and CD8+ T-cells did not significantly differ between the groups (Fig. 2A,C, respectively), we found that patients with OCI were characterized by significantly lower pre-treatment Tim-3 expression on CD8+ T-cells (7.8 (5.0–24.9) vs. 15.7 (4.3–46.7), P = 0.0164, Fig. 3B).

Patients with post-treatment OCI did not experience a decrease in exhaustion markers levels

A significant decrease in plasma IL-10 level was observed in patients who eradicated the virus from PBMC (from 0.68 (0.02–1.94) to 0.32 (0.00–5.09) pg/mL, P < 0.0001), unlike in patients in whom the virus persisted (from 0.65 (0.00–3.99 to 0.42 (0.00–1.56) pg/mL, NS) (Fig. 3A). A similar pattern was observed for sPD-1 (a significant decrease in a former group from 35.0 (8.4–162.6) to 27.3 (2.4–103.2) pg/mL, P < 0.0001, no significant decrease in the latter group—from 25.8 (17.6–47.9) to 17.4 (6.6–36.7) pg/mL, NS) (Fig. 2B). The same was observed for sTim-3 (reduction from 1985.3 (120.8–5746.8) to 1744.9 (235.7–6195.1) pg/mL, P < 0.0001 vs from 1860.0 (1064.1–2919.3) to 1526.2 (1117.2 – 3035.1) pg/mL, NS, respectively) (Fig. 2C) and sLAG-3 (reduction from 898.3 (276.9–9962.0) to (615.8 (163.8–11,156.0) pg/mL, P < 0.0001 vs from 510.5 (244.3–2503.0) to 425.2 (181.1–1300.0) pg/mL, NS, respectively (Fig. 2D).

There were no significant differences in post-treatment IL-10, sPD-1, sTim-3 and sLAG-3 between non-OCI and OCI groups.

Discussion

The primary aim of the presented study was to investigate the prevalence of OCI in patients after successful DAA treatment. We detected HCV-RNA in PBMC by ultrasensitive RT-PCR in all patients prior to treatment and in a relatively high percentage (i.e., 9.3%) of patients after the treatment. Other available DAA-based studies showed a similar scale of post-treatment OCI, ranging from 3.9 to 15%[16,31,61]. Interestingly, one of these studies reported the highest rate of OCI among patients after DAA treatment (15%) when compared to 10% after treatment with interferon and ribavirin, and 6.7% after spontaneous HCV clearance[16].

To disclose the putative mechanism behind HCV persistence in PBMC, we sequenced the 5'UTR HCV-RNA fragment in patients in whom the virus was detected after

Fig. 1

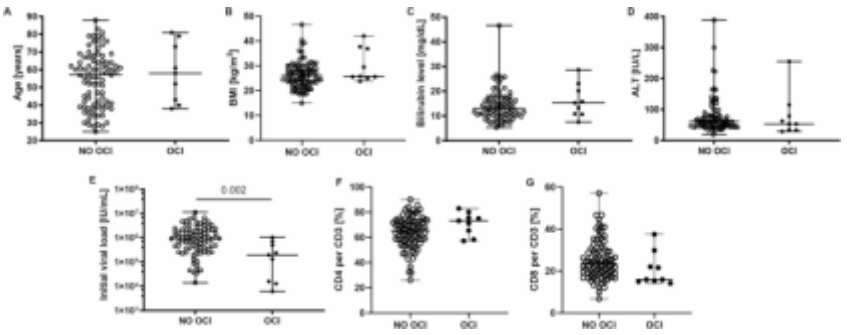

Baseline age (A), BMI (B), initial bilirubin levels (C), ALT activity (D), viral load (E), percentage of CD4+ (F) and CD8+ (G) T-cells in patients with undetectable (NO OCI) and detectable (OCI) HCV-RNA in PBMC after DAA treatment. Each point represents a single result, whiskers represent range, horizontal lines represent the median. P-value representing statistically significant difference in pairwise comparisons is indicated above the line.

Fig. 2

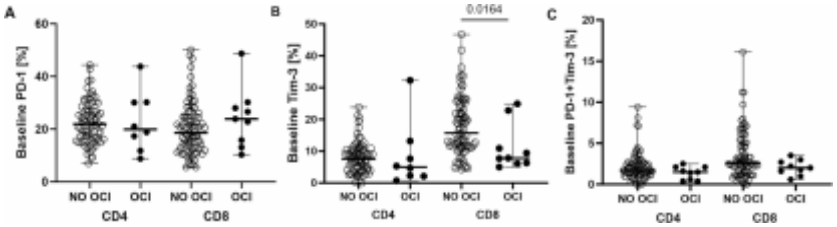

Flow cytometry analysis of percentages of CD4+ and CD8+ T-cells per total T-cells (i.e., CD3+) with membrane expression of PD-1 (A), Tim-3 (B) and PD-1 + Tim-3 (C) in patients with undetectable (NO OCI) and detectable (OCI) HCV-RNA in PBMC after DAA treatment. Each point represents a single result, whiskers represent range, horizontal lines represent the median. P-value representing statistically significant difference in pairwise comparisons is indicated above the line.

treatment along with the pre-treatment samples. The analysis revealed that the dominant PBMC post-treatment sequences were distinct in majority (66.7%) of patients and included a genotype change from 1b to 3a or 4a/d, with concomitant detection of minor alternative genotype strain, both in pre-treatment serum and PBMC. These findings suggest that post-DAA OCI in these patients was a result of pre-existing mixed genotype infection and not a re-infection with the alternative genotype. The treatment in these patients was oriented to genotype 1 with adjusted doses, scheme and duration according to the recommendations and routine serum genotyping. Thus, it has most likely resulted in elimination of the dominant and susceptible genotype 1 strain and selection of alternative genotype strain to which the treatment could have been suboptimal. Indeed, the mixed infecting genotype may be unequally responsive to the same DAA drugs combination[62].

Since the determinants of post-DAA OCI are poorly characterized, we analyzed the role of clinical parameters which could have predisposed to this condition, including age, sex, BMI, initial bilirubin concentration, ALT activity, viral load, liver fibrosis, the fact of previous HCV-oriented therapy and the therapeutic regimen. To reflect the possible immunological factors, we also investigated Cd4/CD8 T-cell percentage as well as the levels of some immunoregulatory molecules expression on T-cells (PD-1 and Tim-3 iRs) and in plasma (IL-10, sPD-1, sLAG-3 and sTim-3). We found that patients with post-treatment OCI presented significantly lower initial median viral titer than the remaining subjects, indicating the predictive potential of baseline viral load testing. Our previous studies showed that lymphotropic variants displayed structural and genomic differences within an internal ribosome entry site (IRES) present within the 5'UTR, essential for translation of the viral polyprotein [63,64]. Such specialization of the lymphotropic quasispecies was at cost of a lower translational efficiency, possibly reflecting adaptation to the alternative cell types as a virus strategy of immune evasion[65,66].

Interestingly, our study showed a distinct pre-treatment immuno-regulatory profile (i.e., lower percentages of CD8+ T-cells expressing Tim-3) related to the occurrence of post-DAA OCI. Given the fact that Tim-3 expression characterizes terminally exhausted cells, in contrast to PD-1, which is related to T-cell activation and initial stages of exhaustion[67], this suggests lower exhaustion. This could be due to observed in OCI patients lower viral load, and consequently, lower degree of antigenic stimulation known to be the driving force of exhaustion and Tim-3 expression[67]. Similar studies provided congruent findings on pre-existing immunoregulatory profile predisposing to HCV persistence after DAA, including the unfavorable (TT) IL28B genotype[19] as well as significant elevation of neutrocyte-to-lymphocyte ratio, indicative of systemic inflammation[30].

Importantly, patients who eradicated the virus from PBMC experienced a significant decrease

Fig. 3

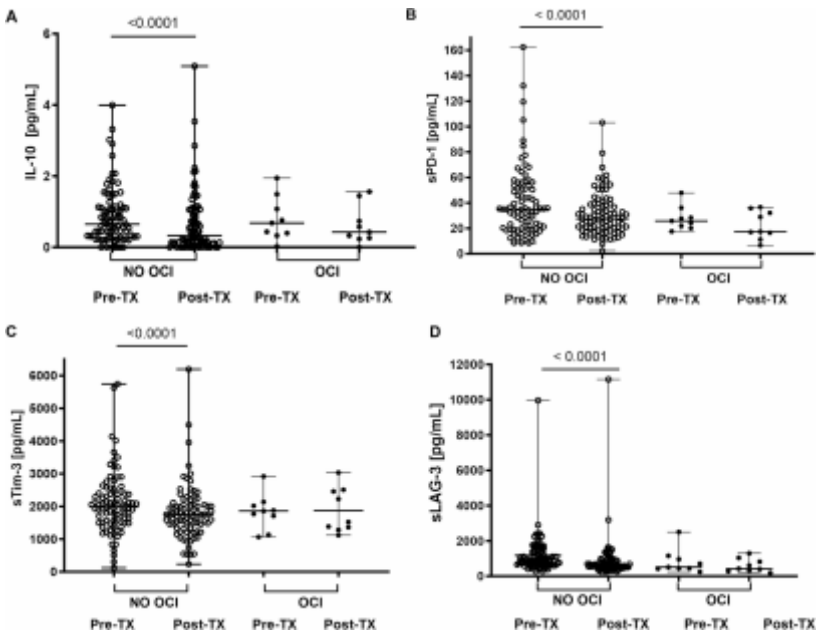

Baseline and post-treatment levels of IL-10 (A) sPD-1 (B), sTim-3 (C) and sLAG-3 (D) in plasma in patients with undetectable (NO OCI) and detectable (OCI) HCV-RNA in PBMC after DAA treatment. Each point represents a single result, whiskers represent range, horizontal lines represent the median. P-value representing statistically significant difference in pairwise comparisons is indicated above the line. Pre-TX, before treatment, Post-TX, post-treatment.

in levels of immunoregulatory IL-10, sPD-1, sLAG-3, sTim-3, not observed in patients in whom the virus persisted. However, there were no significant differences in pre- and post-treatment levels of these markers between non-OCI and OCI groups. Thus, the level of significance may be more attributable to sample size than to actual biological differences and these results should be interpreted with caution as exploratory and rather hypothesis-generating.

The presented study did not demonstrate the role of the type of therapeutic regimen on the occurrence of OCI, which is congruent with a previous study[61]. Similarly, we also did not find the effect of other factors such as sex, age, BMI, fibrosis stage, bilirubin, ALT levels, or previous IFN-based treatment on the occurrence of post-treatment OCI. This again points to the importance of immuno-virological characteristics predisposing to this condition.

This study has limitations, since it does not involve further sequential follow-up to verify the dynamics of OCI. Unfortunately, patients are lost to follow-up from the Outpatient Clinic after SVR verification. Thus, we could not study the potential risk of future viral reactivation from PBMC reservoirs. Nevertheless, a relapse in OCI patients have been previously documented[16,22]. The lack of simultaneous HCV-RNA assessment in liver tissue may be also considered as a shortcoming, however, performing liver biopsy is ethically unjustified in such a study design and, as stated above, there is overall a good concordance between detection of HCV RNA between these two compartments [25]. While we detected post-DAA HCV sequences in PBMC, we could not assess whether they represent a replication-competent virus. Thus, the clinical significance of such findings requires cautious interpretation. Despite best efforts, due to the low HCV RNA titers in PBMCs, full-genome sequencing was technically unfeasible, and we could not provide these data. Thus, the genotype determination was based on 5'UTR analysis of which detection is conducted with the highest sensitivity. While it fails to correctly identify HCV subtypes 1a and 1b, it is variable enough for discrimination of HCV genotypes 1 to 5, which was sufficient for the purpose of the study[68]. Furthermore, we acknowledge that PCR may preferentially amplify certain viral variants and thus might have generated bias in their proportions, which could have an impact on our interpretation of data.

Finally, our findings rely on small number of observations of patients with post-treatment OCI, which may not reflect the real biological effect in vivo.

To conclude, our study showed a high rate of OCI (9.3%) in successfully DAA-treated patients according to the clinical criteria, which should instigate not only serum but also routine PBMC testing when assessing treatment outcome, as well as suggests the need of longer surveillance of these patients. In most cases, post-DAA OCI was related to switch of the dominant infecting genotype. Patients with post-treatment OCI displayed significantly lower pretreatment viral load and distinct pre-existing immune exhaustion status—a lower expression of Tim-3 on CD8+ T-cells.

Data availability

Pre- and post- treatment nucleotide sequence pairs derived from PBMC obtained by Sanger-based sequencing

are available from Zenodo public repository (https://doi.org/10.5281/zenodo.15038917). Next-generation sequencing data of pre-treatment serum and PBMC samples performed on Illumina Mi-Seq are available from Zenodo repository (https://doi.org/10.5281/zenodo.15032240).

References

1. Webster, D. P., Klenerman, P. & Dusheiko, G. M. Hepatitis C. Lancet 385(9973), 1124–1135 (2015).
2. Gill, K. et al. Hepatitis C virus as a systemic disease: reaching beyond the liver. Hepatol Int 10(3), 415–423 (2016).
3. Pawelczyk, A. Consequences of extrahepatic manifestations of hepatitis C viral infection (HCV). Postepy Hig. Med. Dosw. (Online) 70, 349–359 (2016).
4. Radkowski, M. et al. Persistence of hepatitis C virus in patients successfully treated for chronic hepatitis C. Hepatology 41(1), 106–114 (2005).
5. Pawelczyk, A. et al. Detection of hepatitis C virus (HCV) negative strand RNA and NS3 protein in peripheral blood mononuclear cells (PBMC): CD3+, CD14+ and CD19+. Virol J 10, 346 (2013).
6. Radkowski, M. et al. Detection of active hepatitis C virus and hepatitis G virus/GB virus C replication in bone marrow in human subjects. Blood 95(12), 3986–3989 (2000).
7. Radkowski, M. et al. Search for hepatitis C virus negative-strand RNA sequences and analysis of viral sequences in the central nervous system: evidence of replication. J Virol 76(2), 600–608 (2002).
8. Wroblewska, A., Bielawski, K. P. & Sikorska, K. Occult infection with hepatitis C virus: Looking for clear-cut boundaries and methodological consensus. J. Clin. Med. 10(24), 5874 (2021).
9. Pham, T. N. & Michalak, T. I. Occult hepatitis C virus infection and its relevance in clinical practice. J. Clin. Exp. Hepatol. 1(3), 185–189 (2011).
10. MacParland, S. A. et al. Hepatitis C virus persisting after clinically apparent sustained virological response to antiviral therapy retains infectivity in vitro. Hepatology 49(5), 1431–1441 (2009).
11. Pham, T. N. et al. Hepatitis C virus persistence after sustained virological response to antiviral therapy in patients with or without past exposure to hepatitis B virus. J. Viral Hepat. 19(2), 103–111 (2012).
12. Chen, A. Y. et al. Persistence of hepatitis C virus traces after spontaneous resolution of hepatitis C. PLoS ONE 10(10), e0140312 (2015).
13. Austria, A. & Wu, G. Y. Occult hepatitis C virus infection: A review. J. Clin. Transl. Hepatol. 6(2), 155–160 (2018).
14. Attar, B. M. & Van Thiel, D. A new twist to a chronic HCV infection: Occult hepatitis C. Gastroenterol. Res. Pract. 2015, 579147 (2015).
15. Cortés-Mancera, F. M., J.C.R.M., Germán Osorio, Hoyos, S., Correa, G., Navas, M. C. Occult hepatitis C virus infection in a re-transplanted patient with liver failure of unknown etiology. Rev. Col. Gastroenterol. 25 (2010).
16. Wang, Y. et al. Detection of residual HCV-RNA in patients who have achieved sustained virological response is associated with persistent histological abnormality. EBioMedicine 46, 227–235 (2019).
17. Castillo, I. et al. Occult hepatitis C virus infection in patients in whom the etiology of persistently abnormal results of liver-function tests is unknown. J. Infect. Dis. 189(1), 7–14 (2004).
18. Berasain, C. et al. Pathological and virological findings in patients with persistent hyper transaminasaemia of unknown aetiology. Gut 47(3), 429–435 (2000).
19. Elmasry, S. et al. Detection of occult hepatitis C virus infection in patients who achieved a sustained virologic response to direct-acting antiviral agents for recurrent infection after liver transplantation. Gastroenterology 152(3), 550-553 e8 (2017).
20. Castillo, I. et al. Hepatitis C virus infection in the family setting of patients with occult hepatitis C. J. Med. Virol. 81(7), 1198–1203 (2009).
21. Kiser, J. J. & Flexner, C. Direct-acting antiviral agents for hepatitis C virus infection. Annu. Rev. Pharmacol. Toxicol. 53, 427–449 (2013).
22. Boschi, C. et al. Hepatitis C virus relapse 78 weeks after completion of successful direct-acting therapy. Clin. Infect. Dis. 65(6), 1051–1053 (2017).
23. Lawitz, E. et al. A phase 2a trial of 12-week interferon-free therapy with two direct-acting antivirals (ABT-450/r, ABT-072) and ribavirin in IL28B C/C patients with chronic hepatitis C genotype 1. J. Hepatol. 59 (1), 18–23 (2013).
24. Barreiro, P. et al. Very late HCV relapse following triple therapy for hepatitis C. Antivir. Ther. 19(7), 723–724 (2014).
25. Castillo, I. et al. Diagnosis of occult hepatitis C without the need for a liver biopsy. J. Med. Virol. 82(9), 1554–1559 (2010).
26. Gonzalez-Grande, R. et al. New approaches in the treatment of hepatitis C. World J. Gastroenterol. 22(4), 1421–1432 (2016).
27. Sarrazin, C. et al. Late relapse versus hepatitis C virus reinfection in patients with sustained virologic response after sofosbuvir-based therapies. Clin. Infect. Dis. 64(1), 44–52 (2017).
28. Meissner, E. G. et al. Endogenous intrahepatic IFNs and association with IFN-free HCV treatment outcome. J. Clin. Investig. 124(8), 3352–3363 (2014).
29. Alao, H. et al. Baseline intrahepatic and peripheral innate immunity

are associated with hepatitis C virus clearance during direct-acting antiviral therapy. Hepatology 68(6), 2078–2088 (2018).
30. Wroblewska, A. et al. Neutrocyte-to-lymphocyte ratio predicts the presence of a replicative hepatitis C virus strand after therapy with direct-acting antivirals. Clin. Exp. Med. 19(3), 401–406 (2019).
31. Mekky, M. A. et al. Prevalence and predictors of occult hepatitis C virus infection among Egyptian patients who achieved sustained virologic response to sofosbuvir/daclatasvir therapy: a multi-center study. Infect. Drug Resist. 12, 273–279 (2019).
32. Hanafy, A. S. et al. Residual hepatitis C virus in peripheral blood mononuclear cell as a risk factor for hepatocellular carcinoma after achieving a sustained virological response: A dogma or fiction. Eur. J. Gastroenterol. Hepatol. 31(10), 1275–1282 (2019).
33. Reig, M. et al. Unexpected high rate of early tumor recurrence in patients with HCV-related HCC undergoing interferon-free therapy. J. Hepatol. 65(4), 719–726 (2016).
34. Fujiwara, N. et al. Risk factors and prevention of hepatocellular carcinoma in the era of precision medicine. J. Hepatol. 68(3), 526–549 (2018).
35. Vranjkovic, A. et al. Direct-acting antiviral treatment of HCV infection does not resolve the dysfunction of circulating Cd8(+) T-cells in advanced liver disease. Front. Immunol. 10, 1926 (2019).
36. Kanwal, F. et al. Risk of hepatocellular cancer in HCV patients treated with direct-acting antiviral agents. Gastroenterology 153(4), 996-1005 e1 (2017).
37. Llorens-Revull, M. et al. Partial restoration of immune response in hepatitis C patients after viral clearance by direct-acting antiviral therapy. PLoS ONE 16(7), e0254243 (2021).
38. Finkelmeier, F. et al. Risk of de novo hepatocellular carcinoma after HCV treatment with direct-acting antivirals. Liver Cancer 7(2), 190–204 (2018).
39. Wherry, E. J. & Kurachi, M. Molecular and cellular insights into T cell exhaustion. Nat. Rev. Immunol. 15(8), 486–499 (2015).
40. Wherry, E. J. T cell exhaustion. Nat. Immunol. 12(6), 492–499 (2011).
41. Yi, J. S., Cox, M. A. & Zajac, A. J. T-cell exhaustion: Characteristics, causes and conversion. Immunology 129(4), 474–481 (2010).
42. McLane, L. M., Abdel-Hakeem, M. S. & Wherry, E. J. CD8 T cell exhaustion during chronic viral infection and cancer. Annu. Rev. Immunol. 37, 457–495 (2019).
43. Osuch, S., Metzner, K. J. & Caraballo Cortes, K. Reversal of T Cell exhaustion in chronic HCV infection. Viruses 12(8), 799 (2020).
44. Boni, C. et al. Characterization of hepatitis B virus (HBV)-specific T-cell dysfunction in chronic HBV infection. J. Virol. 81(8), 4215–4225 (2007).
45. McKinney, E. F. et al. T-cell exhaustion, co-stimulation and clinical outcome in autoimmunity and infection. Nature 523 (7562), 612–616 (2015).
46. Trautmann, L. et al. Upregulation of PD-1 expression on HIV-specific CD8+ T cells leads to reversible immune dysfunction. Nat. Med. 12(10), 1198–1202 (2006).
47. Urbani, S. et al. PD-1 expression in acute hepatitis C virus (HCV) infection is associated with HCV-specific CD8 exhaustion. J Virol 80(22), 11398–11403 (2006).
48. Bi, J. & Tian, Z. NK cell exhaustion. Front. Immunol. 8, 760 (2017).
49. Moir, S. & Fauci, A. S. B-cell exhaustion in HIV infection: The role of immune activation. Curr. Opin. HIV AIDS 9(5), 472–477 (2014).
50. Kemming, J., Thimme, R. & Neumann-Haefelin, C. Adaptive immune response against hepatitis C virus. Int. J. Mol. Sci. 21(16), 5644 (2020).
51. Jin, H. T. et al. Cooperation of Tim-3 and PD-1 in CD8 T-cell exhaustion during chronic viral infection. Proc. Natl. Acad. Sci. U. S. A. 107(33), 14733–14738 (2010).
52. Blackburn, S. D. & Wherry, E. J. IL-10, T cell exhaustion and viral persistence. Trends Microbiol. 15(4), 143–146 (2007).
53. Clayton, K. L. et al. Soluble T cell immunoglobulin mucin domain 3 is shed from CD8+ T cells by the sheddase ADAM10, is increased in plasma during untreated HIV infection, and correlates with HIV disease progression. J. Virol. 89(7), 3723–3736 (2015).
54. Zilber, E. et al. Soluble plasma programmed death 1 (PD-1) and Tim-3 in primary HIV infection. AIDS 33(7), 1253–1256 (2019).
55. Nielsen, C. et al. Alternative splice variants of the human PD-1 gene. Cell. Immunol. 235(2), 109–116 (2005).
56. Triebel, F. LAG-3: A regulator of T-cell and DC responses and its use in therapeutic vaccination. Trends Immunol. 24(12), 619–622 (2003).
57. Laskus, T. et al. The presence of active hepatitis C virus replication in lymphoid tissue in patients coinfected with human immunodeficiency virus type 1. J. Infect. Dis. 178(4), 1189–1192 (1998).
58. Laskus, T. et al. Hepatitis C virus negative strand RNA is not detected in peripheral blood mononuclear cells and viral sequences are identical to those in serum: A case against extrahepatic replication. J. Gen. Virol. 78(Pt 11), 2747–2750 (1997).
59. Osuch, S. et al. Decrease of T-

cells exhaustion markers programmed cell death-1 and T-cell immunoglobulin and mucin domain-containing protein 3 and plasma IL-10 levels after successful treatment of chronic hepatitis C. Sci. Rep. 10(1), 16060 (2020).
60. Tamura, K., Stecher, G. & Kumar, S. MEGA11: Molecular evolutionary genetics analysis version 11. Mol. Biol. Evol. 38(7), 3022–3027 (2021).
61. Yousif, M. M. et al. Prevalence of occult hepatitis C virus infection in patients who achieved sustained virologic response to direct-acting antiviral agents. Infez Med 26(3), 237–243 (2018).
62. Wada, N. et al. Mixed HCV infection of genotype 1B and other genotypes influences non-response during daclatasvir + asunaprevir combination therapy. Acta Med. Okayama 72(4), 401–406 (2018).
63. Jang, S. J. et al. Differences between hepatitis C virus 5' untranslated region quasispecies in serum and liver. J. Gen. Virol. 80(Pt 3), 711–716 (1999).
64. Bukowska-Osko, I. et al. Analysis of genotype 1b hepatitis C virus IRES in serum and peripheral blood mononuclear cells in patients treated with interferon and ribavirin. Biomed. Res. Int. 2014, 175405 (2014).
65. Raghwani, J. et al. Exceptional heterogeneity in viral evolutionary dynamics characterises chronic hepatitis C virus infection. PLoS Pathog. 12(9), e1005894 (2016).
66. Durand, T. et al. Occult infection of peripheral B cells by hepatitis C variants which have low translational efficiency in cultured hepatocytes. Gut 59(7), 934–942 (2010).
67. Jenkins, E. et al. The current state and future of T-cell exhaustion research. Oxf. Open Immunol. 4(1), iqad006 (2023).
68. Verbeeck, J. et al. Evaluation of versant hepatitis C virus genotype assay (LiPA) 2.0. J. Clin. Microbiol. 46(6), 1901–1906 (2008).

Acknowledgements

The study was supported from the National Science Center grants number 2015/19/D/NZ6/01303, 2024/54/E/NZ6/00334, and from the Medical University of Warsaw Young Investigators project number 1M24/1/M/ MBM/N/21/21.

Author information

Authors and Affiliations

Department of Immunopathology of Infectious and Parasitic Diseases, Medical University of Warsaw, 3C Pawinskiego Street, 02-106, Warsaw, Poland

Sylwia Osuch, Paulina Emmel, Marek Radkowski & Kamila Cortés-Fendorf

Laboratory of Genetics, University Clinical Center of the Medical University of Warsaw, Warsaw, Poland

Marta Kazek

Outpatient Clinic, Warsaw Hospital for Infectious Diseases, Warsaw, Poland

Hanna Berak

Contributions

Conceptualization: K.C.C.; Methodology, K.C.C., H.B. and S.O.; Software, S.O. and M.K.; Validation, K.C.C.; Formal Analysis, H.B.; Investigation, M.K., P.E. and S.O.; Resources, H.B.; Data Curation, S.O., H.B. and K.C.C.; Writing – Original Draft Preparation, S.O.; Writing – Review and Editing, M.K., H.B., M.R., K.C.C.; Visualization, M.K., P.E.; Supervision, K.C.C. and M.R.; Project Administration, K.C.C.; Funding Acquisition, K.C.C. and S.O. All authors have read and agreed to the published version of the manuscript.

Corresponding author

Correspondence to Kamila Cortés-Fendorf.

Ethics declarations

Competing interests

The authors declare no competing interests.

Keywords
Occult HCV infection, Sustained virologic response (SVR), Direct-acting antivirals (DAA), Immune exhaustion

Subjects
Genetics, Immunology, Microbiology, Molecular biology

Credit: Osuch, S., Kazek, M., Emmel, P. et al. Persistence of hepatitis C virus in peripheral blood mononuclear cells of patients who achieved sustained virological response following treatment with direct-acting antivirals is associated with a distinct pre-existing immune exhaustion status. Sci Rep 15, 19918 (2025). https://doi.org/10.1038/s41598-025-05084-z

CT texture features of lung adenocarcinoma with HER2 mutation

Wufei Chen, Pan Gao, Fang Lu, Ernuo Wang, Haiquan Liu & Ming Li

Abstract

Background

Mutations in human receptor tyrosine kinase epidermal growth factor receptor-2 (HER2) are rare. This study aimed to investigate the clinical characteristics and computed tomography (CT) texture features of lung adenocarcinoma (LUAD) patients with HER2 mutation.

Methods

This study included 933 LUAD patients from January 2018 to December 2023 and classified their CT textures accordingly.

Results

The data indicated that the incidence of HER2 mutation was higher in younger LUAD patients than in elder patients [7.5% (31/413) vs. 1.5% (8/520), $p < 0.0001$] and was associated with never-smokers [0% (0/78) vs. 4.6% (39/855), $p = 0.03$]. In this study, the tumors were categorized based on their diameter into T1a and ≥T1b. The data revealed that HER2 mutation was more frequent in T1a than in ≥T1b [11.0% (23/210) vs. 2.2% (16/723), $p < 0.0001$]. Furthermore, non-pSD was more common than pSD in LUAD with HER2 mutation than in LUAD with HER2 wild type [82.1% (31/39) vs.17.9% (7/39), $p = 0.01$]. Moreover, the size of pGGO (0.94 ± 0.29 cm vs. 1.24 ± 0.39 cm, $p = 0.0009$), mGGO (0.86 ± 0.39 cm vs. 1.5 ± 0.77 cm, $p < 0.0001$) and pSD (1.75 ± 0.81 cm vs. 2.5 ± 1.4 cm, $p < 0.05$) in LUAD patients with HER2 mutation was smaller than those with HER2 wild type patients. In addition, when LUADs with HER2 wild type transformed from pGGO to mGGO, their sizes increased significantly (1.50 ± 0.77 cm vs. 1.24 ± 0.39 cm). It was also observed that the incidence of LUAD with HER2 mutation of ≤1 cm was significantly more than that of > 1 cm comparing to that in LUAD with HER2 wild type [14.8% (12/81) vs. 1.7% (3/173), $p < 0.0001$].

Conclusion

This study indicated that the incidence of HER2 mutation was higher in younger and never-smoking LUAD patients. Furthermore, the growth of LUAD with HER2 mutation was slower than that of those with HER2 wild type. Moreover, most LUAD with HER2 mutation changed into pSD after > 1 cm.

Introduction

Lung cancer is a leading cause of cancer-related death globally. World Health Organization estimated that in 2020, lung cancer caused 1.76 million deaths, accounting for approximately 19% of the total cancer-related deaths [1,2]. Non-small cell lung cancer (NSCLC) comprises 80 to 85% of all lung cancers, and 40% of these are adenocarcinoma histologically [3].In 2004, it was identified that epidermal growth factor receptor gene (EGFR) mutation was associated with lung adenocarcinomas (LUAD) patients [4,5], and advancements in genomic sequencing and targeted therapy have further sub-classified LUAD based on the driver oncogenes.

Human epidermal growth factor 2 (HER2, also known as ERBB2, NEU, or EGFR2) is a member of the ERBB family of receptor tyrosine kinases. It is encoded by the ERBB2 gene, which is an important driver oncogene for lung cancer. ERBB2 gene is located on the long arm of chromosome 17 (17 q21) and has been observed to activate the downstream signaling pathways, such as PI3K-AKT and MEK-EPK, which causes cell proliferation and migration [6,7]. Several studies have indicated that HER2 mutations in exon 20 cause constitutive activation of downstream signaling and promote the development of lung tumors in mouse models [8]. Moreover, proteins encoded by the HER2 gene are a tyrosine kinase receptor of the ErbB family. In addition, it has been observed that HER2 has no direct activating ligand and serves as the preferred and most stable hetero-dimerization partner for all the other family receptors, especially EGFR [9]. The most economical and effective non-invasive technique to diagnose lung cancer is Computed tomography (CT) scan [10]. Furthermore, it is significant and interesting to understand the imaging features of some special lung cancers and is potentially useful for guiding lung cancer therapy.

Radiogenomics is a field that investigates the radiological appearance of tumors as well as the genomic alterations, such as driver oncogenes [11]. However, studies on the imaging features of LUAD with

HER2 mutation are limited. Therefore, this study aimed to assess the clinical characteristics and CT texture features of LUAD patients with HER2 mutation.

Methods

Patients

This study followed the Declaration of Helsinki and was authorized by the Ethics Review Board of Huadong Hospital, affiliated with Fudan University (approval number 2023 0108). Because of its retrospective nature, the requirement of patient informed consent was waived for this study. A total of 933 histologically confirmed LUAD patients with primary lung cancer from January 2018 to December 2023 were included in this study. All tissue specimens were obtained surgically and no pre-operative treatments were given. Patients were selected consecutively. The inclusion criteria included patients who (a) were pathologically diagnosed with LUAD, (b) had HER2 mutation test reports, and (c) had clinical data, including age, sex, and smoking history. All 933 patients met the inclusion criteria, and of these, only 818 patients had preoperative CT scans, which were used to evaluate the CT features of the lesion.

Computed tomographic assessment

For preoperative chest CT scans three scanners including GE Discovery CT750 HD, 64-slice Light Speed VCT (GE Medical Systems), and Somatom Definition Flash were employed. The scanning parameters were: 120 kVp, 100–200 mAs, 0.75–1.5 pitch range, and 1–1.25 mm collimation widths. Furthermore, for all the imaging data, a medium sharp reconstruction algorithm was used, which provided 1–1.25 mm thick images.

Interpretation of computed tomographic images

The CT images were reviewed by 2 radiologists with 10 to 12 years of experience in chest CT diagnosis independently. The radiologists were not blinded to surgical resection of LUAD patients; however, they were blinded to clinical data as well as gene expression and mutational status. For CT image analysis, both mediastinal (width = 350 HU; level = 40 HU) and lung (width = 1500 HU; level = -650 HU) window settings were employed. Moreover, lesion location, size, and texture were retrospectively analyzed. In addition, the lesions' long-axis diameter at its largest section was also measured. Furthermore, lesions with ground-glass opacities were categorized as pure GGO (pGGO), those with 1% < GGO < 100% were classified as mixed GGO (mGGO), while those lacking any GGO were deemed pure solid LUADs (pSD). For statistical analysis, pGGO and mGGO categories were combined as non-pSD. In the case of multiple lesions on images, the largest lesion was selected for the observation.

Statistical analysis

SAS version 9.4 (SAS Institute Inc., Cary, NC) was employed for all the statistical analyses. The distribution differences in categorical variables were assessed via the chi-square ($?^2$) test, whereas an independent t-test was performed to assess differences in continuous variables. The p-value < 0.05 was deemed statistically significant.

Results

Patient demographics characteristics

This study included a total of 933 LUAD patients aged between 18 and 86 years (average age = 61.8 years) including 393 females and 540 males. Of these 933 patients, 39 (4.2%) had HER2 mutation and 78 patients had a history of smoking.

Correlation of HER2 status and clinical factors

Statistical analysis (Table 1) indicated that the incidence of HER2 mutation was higher in younger LUAD patients than in elder patients [7.5% (31/413) vs. 1.5% (8/520), p < 0.0001]. Furthermore, correlation analysis between HER2 and smoking revealed that HER2 mutation was negatively associated with smoking in the whole cohort [0% (0/78) vs. 4.6% (39/855), p = 0.03].

Based on their diameter, the tumors were categorized into ≤1 cm and > 1 cm. The results indicated that HER2 mutation was more frequent in small tumors than in larger ones [11.0% (23/210) vs. 2.2% (16/723), p < 0.0001]. Lymph node metastasis and HER2 mutations were correlated. The tumor was also categorized into histopathological subtypes with or without some components and there was statistically no correlation between HER2 mutation and histopathological subtypes.

Computed tomographic texture of HER2 mutation and wild-type LUAD patients

Of the 933 patients, 818 patients had CT scan data, and 38 were positive for HER2 mutation. Of these 818 patients with CT scans, 754 had single lesions, while 64 had multiple lesions. The data showed that non-pSD was more common than pSD in LUAD with HER2 mutation than in LUAD with HER2 wild type [82.1% (31/39) vs.17.9% (7/39), p = 0.01] (Table 2).

Comparison between LUADs of pGGO and mGGO in HER2 mutation

Table 1 Correlation between clinical features and HER2 status

	HER2 mutation	HER2 wild	*P* value
Sex			0.5
Male	13	380	
Female	26	514	
Age			< 0.0001
≤60	31	382	
> 60	8	512	
Smoking			0.03*
Yes	0	78	
No	39	816	
Tumor stage			< 0.0001
T1a	23**	187	
≥T1b	16	707	
N status			
N (-)	39	870	0.24*
N (+)	0	24	
Pathological subtypes			
With lepidic	5	131	0.75
Without lepidic	34	763	
With acinar	6	251	0.08
Without acinar	33	643	
With papillary	4	93	0.98
Without papillary	35	801	
With micropapillary	2	126	0.11#
Without micropapillary	37	768	
With solid	1	55	0.56#
Without solid	38	839	

Note...*Fisher's exact test of probabilities, #continuity adjustment.** The number of pSD LUAD was 1.

Table 2 Comparison of the frequency of HER2 mutation and wild type in LUAD of pSD and non-pSD

CT texture	HER2 mutation	HER2 wild type	*P* value
Non-pSD	32 (82.1%)	476 (61.0%)	
pSD	7 (17.9%)	304 (59.0%)	0.01

Note: Non-pSD = pGGO (pure ground glass opacity LUADs) + mGGO (mixed ground glass opacity LUADs), pSD = pure solid LUAD,

and wild-type LUAD patients

The CT data from three textures indicated that the size of pGGO (0.94 ± 0.29 cm vs. 1.24 ± 0.39 cm, p = 0.0009), mGGO (0.86 ± 0.39 cm vs. 1.5 ± 0.77 cm, p < 0.0001) and pSD (1.75 ± 0.81 cm vs. 2.5 ± 1.4 cm, p < 0.05) in LUAD patients with HER2 mutation was smaller than those with HER2 wild type patients. There was no size difference for HER2 mutation lesions between pGGO and mGGO. However, in LUAD with HER2 wild-type patients, mGGO lesions were significantly larger than pGGO (1.50 ± 0.77 cm vs. 1.24 ± 0.39 cm) (Table 3).

Furthermore, LUAD lesions were categorized into ≤1 cm and > 1 cm, and the frequency of ≤1 cm LUAD lesions with HER2 mutation was significantly more than that of > 1 cm compared to HER2 wild type [14.8% (12/81) vs. 1.7% (3/173), p < 0.0001] (Table 4).

Discussion

The literature has estimated that the incidence of HER2 mutations is 2–6.7% in NSCLC adenocarcinomas [12,13,14,15,16,17,] which is consistent with this study (4.2%). The association of HER2 mutation with smoking remains controversial. Some studies have suggested that HER2 mutation does not correlate with smoking [15,18,19]. However, most studies have

Table 3 Comparison between LUADs of different CT textures for HER2 mutation and wild-type

	HER2 mutation		HER2 wild type		*p*-value
	Number	Average ± SD (min, max), cm	Number	Average ± SD (min, max), cm	
pGGO	17	0.94 ± 0.29 (0.55, 1.54)	237	1.24 ± 0.39 (0.40, 3.0)	0.0009
mGGO	15	0.86 ± 0.39 (0.50, 1.91)	239	1.5 ± 0.77 (0.5, 4.4)	< 0.0001
pSD	7	1.75 ± 0.81 (0.56, 3.05)		2.5 ± 1.4 (0.45, 9.8)	< 0.05
p-value		0.5*		*< 0.0001	

Note: pGGO = LUADs of pure ground-glass opacity, mGGO = LUADs of mixed ground-glass opacity, pSD = LUAD of pure solid. SD = standard deviation. *pGGO vs. mGGO

Table 4 The frequency of mGGO LUADs and pSD LUAND in different sizes correlating HER2 mutation and wild-type

	HER2 mutation	HER2 wild type	*P* value
mGGO			
≤1 cm	12 (14.8%)	69 (85.2%)	
> 1 cm	3 (1.7%)	170 (98.3%)	< 0.0001

Note: pGGO = pure ground glass opacity LUADs, mGGO = mixed ground glass opacity LUADs, pSD = pure solid LUADs.

indicated that HER2 mutation is more common in non-smokers [16, 20,21,22], such as a study of 666 HER2 mutations in 13,920 patients [18]. In this study, the incidence of smokers was 8.4%, which was significantly lower than 55.8% of that reported by H. Shigematsu et al. [16] in the Asian group. This discriment might be because in their study the HER2 mutation was only 2.4%. Our study revealed that HER2 mutation was associated with non-smokers and was statistically significant, which was consistent with most studies.

Several studies correlate HER2 mutation with younger age patients [19–21]. However, this is still controversial as some studies suggest that HER2 mutations are not correlated with age [14,22]. Furthermore, some literature suggests that HER2 mutations are associated with the female gender [16,23–26], while some deny it [15,19,22, 27]. This study showed that HER2 mutation was more common in younger patients and women than in older individuals and men; however, there was no statistical difference, which might be because of the small sample size and warrants further research with a large sample si

This study indicated that LUAD with HER2 mutation was more frequent in tumors with T1a cm than that ≥T1b, this was consistent with the data from the previous study. R. Zhao et al. [18] found LUAD with HER2 mutation more common in early LUAD and inversely proportional to the degree of invasion. However, they found LUAD with HER2 mutation frequently correlated lepidic components, which is inconsistent with the present study. Here, correlation was observed between HER2 mutation and histopathological subtypes. However, further experimental studies are required to validate these findings.

Previous studies on CT imaging features in LUAD with HER2 mutation were scarce because HER2 mutations are rare in lung cancer. Here, a larger sample of LUAD CT characteristics was analyzed, which indicated that non-PSD was more common than pSD in HER2 mutation LUAD patients.

The genomic landscape analysis of 37 patients with ground glass opacities (GGOs) revealed that ERB2 had a higher mutation frequently, accounting for 8% [28]. Another study showed that LUAD GGO tumors had higher HER2 mutation incidence [24], partially consistent with this study. X. Liu et al. [30] showed that LUAD with HER2 mutation was more frequently classified as cluster 4 lesion (small GGO lesions with a maximum diameter of 1.0 ± 0.9 cm). Here, the average sizes of HER2 mutation carrying LUAD pGGO and mGGO were 0.94 ± 0.29 cm and 0 0.86 ± 0.39 cm, respectively, which are in line with the results of X. Liu et al. [29].

The theory of progressive radiologic evolution from non-solid LUADs to part-solid and forming most solid LUADs is well known [30, 31]. Studies have shown that a GGO LUAD initially increases in size, followed by the appearance and subsequent enlargement of a solid portion within the lesion [32]. Furthermore, it has been observed that lesions that transition from pGGO to mGGO or from mGGO to solid have a rapid increase in size [33,34,35]. Here, it was observed that the size of pGGO or mGGO in the HER2 wild-type LUAD was significantly larger than those with HER2 mutation LUAD. Moreover, when the LUADs transformed from pGGO into mGGO, the sizes of LUADs with HER2 wild type increased significantly, but that with HER2 mutation did not change significantly. In addition, for mGGO lesions with HER2 mutation, the frequency of ≤1 cm was more than that of > 1 cm compared to HER2 wild type. This suggested that most LUADs with HER2 mutation changed into pSD after 1 cm.

Overall, this study indicated that LUAD with HER2 mutation was smaller in size than LUAD with HER2 wild type for GGO-LUAD, mGGO-LUAD, or pSD-LUAD, respectively. Therefore, it can be inferred that LUAD with HER2 mutation had a slower growth speed than their counterpart. Furthermore, as LUAD with HER2 mutation transformed into mGGO, the size did not increase as observed in LUADs with HER2 wild type. This study will provide a reference for future research on this question.

Limitations

This study has certain limitations. First, the study sample was small; therefore, I, the details of HER mutation tumor stratification could not be analyzed. Second, the analysis was limited to adenocarcinoma, and other histologic subtypes were not addressed. However, the majority of HER2 mutations are found in adenocarcinoma. Third, no survival data were collected in this

study; therefore, the relationship between tumors of different textures and survival was not assessed.

Conclusion

In summary, this study revealed that HER2 mutation was more common in younger and never smokers LUAD patients. Furthermore, most LUADs manifested as non-pSD in CT scans. Moreover, the size of LUAD with HER2 mutation was smaller than that with HER2 wild type and most LUAD with HER2 mutation transformed into pSD after their size increased > 1 cm.

Data availability

All data generated or analysed during this study are included in this published article.

Abbreviations

HER2: Human epidermal growth factor 2
EGFR: Epidermal growth factor receptor gene
CT: Computed tomography
LUAD: Lung adenocarcinoma
pGGO: Pure ground glass opacity
mGGO: Mixed ground glass opacity
pSD: Pure solid
NSCLC: Non-small cell lung cancer

References

1. Thai AA, Solomon BJ, Sequist LV, Gainor JF, Heist RS. Lung cancer. Lancet (London England). 2021; 398(10299): 535–54.
2. Zhang Y, Elgizouli M, Schöttker B, Holleczek B, Nieters A, Brenner H. Smoking-associated DNA methylation markers predict lung cancer incidence. Clin Epigenetics. 2016; 8:127.
3. Ladanyi M. W. P. Pao Lung adenocarcinoma: guiding EGFR-targeted therapy and beyond. Mod Pathology: Official J United States Can Acad Pathol Inc 21: 2008;2:S16–22.
4. Lynch TJ, Bell DW, Sordella R, Gurubhagavatula S, Okimoto RA, Brannigan BW, Harris PL, Haserlat SM, Supko JG, Haluska FG, Louis DN, Christiani DC, Settleman J, Haber DA. Activating mutations in the epidermal growth factor receptor underlying responsiveness of non-small-cell lung cancer to gefitinib. N Engl J Med. 2004;350(21):2129–39.
5. Paez JG, Jänne PA, Lee JC, Tracy S, Greulich H, Gabriel S, Herman P, Kaye FJ, Lindeman N, Boggon TJ, Naoki K, Sasaki H, Fujii Y, Eck MJ, Sellers WR, Johnson BE, Meyerson M. EGFR mutations in lung cancer: correlation with clinical response to gefitinib therapy. Sci (New York N Y). 2004;304(5676):1497–500.
6. Xu H, Liang Q, Xu X, Tan S, Wang S, Liu Y, Liu L. Afatinib combined with anlotinib in the treatment of lung adenocarcinoma patient with novel HER2 mutation: a case report and review of the literature. World J Surg Oncol. 2021;19 (1):330.
7. Peters S, Zimmermann S. Targeted therapy in NSCLC driven by HER2 insertions. Translational lung cancer Res 3(2)2014;84– 8.
8. Pillai RN, Behera M, Berry LD, Rossi MR, Kris MG, Johnson BE, Bunn PA, Ramalingam SS, Khuri FR. HER2 mutations in lung adenocarcinomas: a report from the Lung Cancer Mutation Consortium. Cancer. 2017;123(21): 4099–105.
9. Sawan P, Plodkowski AJ, Li AE, Li BT, Drilon A, Capanu M, Ginsberg MS. CT features of HER2-mutant lung adenocarcinomas. Clin Imaging. 2018; 51:279–83.
10. Yue JY, Chen J, Zhou FM, Hu Y, Li MX, Wu QW, Han DM. CT-pathologic correlation in lung adenocarcinoma and squamous cell carcinoma. Medicine. 2018;97 (50):e13362.
11. Mazurowski MA. Radiogenomics: what it is and why it is important. J Am Coll Radiology: JACR. 2015;12(8):862–6.
12. Garrido-Castro AC, Felip E. HER2 driven non-small cell lung cancer (NSCLC): potential therapeutic approaches. Translational lung cancer Res. 2013;2 (2):122–7.
13. Kim EK, Kim KA, Lee CY, Shim HS. The frequency and clinical impact of HER2 alterations in lung adenocarcinoma. PLoS ONE. 2017;12(2):e0171280.
14. Li C, Fang R, Sun Y, Han X, Li F, Gao B, Iafrate AJ, Liu XY, Pao W, Chen H, Ji H. Spectrum of oncogenic driver mutations in lung adenocarcinomas from east Asian never smokers. PLoS ONE. 2011;6(11):e28204.
15. Li X, Zhao C, Su C, Ren S, Chen X, Zhou C. Epidemiological study of HER-2 mutations among EGFR wild-type lung adenocarcinoma patients in China. BMC Cancer. 2016;16(1):828.
16. Shigematsu H, Takahashi T, Nomura M, Majmudar K, Suzuki M, Lee H, Wistuba II, Fong KM, Toyooka S, Shimizu N, Fujisawa T, Minna JD, Gazdar AF. Somatic mutations of the HER2 kinase domain in lung adenocarcinomas. Cancer Res. 2005;65 (5):1642–6.
17. Tan AC, Saw SPL, Chen J, Lai GGY, Oo HN, Takano A, Lau DPX, Yeong JPS, Tan GS, Lim KH, Skanderup AJ, Chan JWK, Teh YL, Rajasekaran T, Jain A, Tan WL, Ng QS, Kanesvaran R, Lim WT, Ang MK, Tan DSW. Clinical and genomic features of HER2 exon 20 insertion mutations and characterization of HER2 expression by immunohistochemistry in East Asian Non-small-cell Lung Cancer. JCO Precision Oncol. 2022; 6:e2200278.
18. Zhao R, Li J, Guo L, Xiang C, Chen S, Zhao J, Shao J, Zhu L, Ye M, Qin G, Chu T, Han Y. EGFR and ERBB2 exon 20 insertion mutations in Chinese non-small cell Lung Cancer patients: pathological and molecular characterization, and first-line systemic treatment evaluation. Target Oncol. 2024;19(2):277–88.
19. Arcila ME, Chaft JE, Nafa K, Roy-Chowdhuri S, Lau C, Zaidinski M, Paik PK, Zakowski MF, Kris MG, Ladanyi M. Prevalence, clinicopathologic associations, and molecular spectrum of ERBB2 (HER2) tyrosine kinase mutations in lung adenocarcinomas. Clin cancer Research: Official J Am Association Cancer Res. 2012;18(18):4910–8.
20. Zhao M, Zhan C, Li M, Yang X, Yang X, Zhang Y, Lin M, Xia Y, Feng M, Wang Q. Aberrant status and clinicopathologic characteristic associations of 11 target genes in 1,321 Chinese patients with lung adenocarcinoma. J Thorac Disease. 2018;10(1):398–407.
21. Wu X, Zhao J, Yang L, Nie X, Wang Z, Zhang P, Li C, Hu X, Tang M, Yi Y, Du X, Xia X, Guan Y, Yu Z, Gu W, Quan X, Li L, Shi H. Next-generation sequencing reveals Age-dependent genetic underpinnings in lung adenocarcinoma. J Cancer. 2022;13(5):1565–72.
22. Hsu KH, Ho CC, Hsia TC, Tseng JS, Su KY, Wu MF, Chiu KL, Yang TY, Chen KC, Ooi H, Wu TC, Chen HJ, Chen HY, Chang CS, Hsu CP, Hsia JY, Chuang CY, Lin CH, Chen JJ, Chen KY, Liao WY, Shih JY, Yu SL, Yu CJ, Yang PC, Chang GC. Identification of five driver gene mutations in patients with treatment-naïve lung adenocarcinoma in Taiwan. PLoS ONE. 2015;10(3):e01 20852.

23. Mazières J, Peters S, Lepage B, Cortot AB, Barlesi F, Beau-Faller M, Besse B, Blons H, Mansuet-Lupo A, Urban T, Moro-Sibilot D, Dansin E, Chouaid C, Wislez M, Diebold J, Felip E, Rouquette I, Milia JD, Gautschi O. Lung cancer that harbors an HER2 mutation: epidemiologic characteristics and therapeutic perspectives. J Clin Oncology: Official J Am Soc Clin Oncol. 2013;31(16):1997–2003.
24. Eng J, Hsu M, Chaft JE, Kris MG, Arcila ME, Li BT. Outcomes of chemotherapies and HER2 directed therapies in advanced HER2-mutant lung cancers, lung cancer (Amsterdam. Netherlands). 2016;99:53–6.
25. Pao W, Girard N. New driver mutations in non-small-cell lung cancer, the Lancet. Oncology. 2011;12(2):175–80.
26. Li C., Sun Y., Fang R., Han X., Luo X., Wang R., Pan Y., Hu H., Zhang Y., Pao W., Shen L., Ji H., Chen H. Lung adenocarcinomas with HER2-activating mutations are associated with distinct clinical features and HER2/EGFR copy number gains. J Thorac Oncology: Official Publication Int Association Study Lung Cancer. 2012;7(1): 85–9.
27. Wu D, Xie Y, Jin C, Qiu J, Hou T, Du H, Chen S, Xiang J, Shi X, Liu J. The landscape of kinase domain duplication in Chinese lung cancer patients. Annals Translational Med. 2020;8(24):1642.
28. Cao P, Hu S, Kong K, Han P, Yue J, Deng Y, Zhao B, Li F. Genomic landscape of ground glass opacities (GGOs) in East asians. J Thorac Disease. 2021;13(4): 2393–403.
29. Liu X, Xu T, Wang S, Chen Y, Jiang C, Xu W, Gong J. CT-based radiomic phenotypes of lung adenocarcinoma: a preliminary comparative analysis with targeted next-generation sequencing. Front Med. 2023;10: 1191019.
30. Jung W, Cho S, Yum S, Chung JH, Lee KW, Kim K, Lee CT, Jheon S. Stepwise Disease Progression Model of Subsolid Lung Adenocarcinoma with cystic airspaces. Ann Surg Oncol. 2020;27 (11):4394–403.
31. Kakinuma R, Noguchi M, Ashizawa K, Kuriyama K, Maeshima AM, Koizumi N, Kondo T, Matsuguma H, Nitta N, Ohmatsu H, Okami J, Suehisa H, Yamaji T, Kodama K, Mori K, Yamada K, Matsuno Y, Murayama S, Murata K. Natural history of Pulmonary Subsolid nodules: a prospective Multicenter Study. J Thorac Oncology: Official Publication Int Association Study Lung Cancer. 2016;11(7):1012–28.
32. Takashima S, Maruyama Y, Hasegawa M, Yamanda T, Honda T, Kadoya M, Sone S. CT findings and progression of small peripheral lung neoplasms having a replacement growth pattern, AJR. Am J Roentgenol. 2003;180(3):817–26.
33. Lee SW, Leem CS, Kim TJ, Lee KW, Chung JH, Jheon S, Lee JH, Lee CT. The long-term course of ground-glass opacities detected on thin-section computed tomography. Respir Med. 2013;107(6):904–10.
34. Zhang Z, Zhou L, Min X, Li H, Qi Q, Sun C, Sun K, Yang F, Li X. Long-term follow-up of persistent pulmonary subsolid nodules: natural course of pure, heterogeneous, and real part-solid ground-glass nodules. Thorac cancer. 2023;14(12):1059–70.
35. Chang B, Hwang JH, Choi YH, Chung MP, Kim H, Kwon OJ, Lee HY, Lee KS, Shim YM, Han J, Um SW. Natural history of pure ground-glass opacity lung nodules detected by low-dose CT scan. Chest. 2013;143(1):172–8.

Acknowledgements

The authors would like to thank all the reviewers who participated in the review and MJEditor (www.mjeditor.com) for their linguistic assistance during the preparation of this manuscript.

Funding

This study was supported by The Ministry of Science and Technology of the People's Republic of China (CN): 2022YFF1203301 and Research Project Plan of Shanghai Municipal Health Commission(20214Y0309).

Author information

Author notes

Wufei Chen and Ernuo Wang contributed equally to this work.

Authors and Affiliations

Department of Radiology, Huadong Hospital, Fudan University Shanghai China, Shanghai, China

Wufei Chen, Pan Gao, Fang Lu, Ernuo Wang, Haiquan Liu & Ming Li

Contributions

Haiquan Liu: Conceptualization; investigation; validation; writing – original draft. Wufei Chen and Pan Gao: Data curation and Formal analysis. Fang Lu and Ernuo Wang: reference review and Investigation.

Corresponding authors

Correspondence to Haiquan Liu or Ming Li.

Ethics declarations

Ethics approval and consent to participate

The Ethics Review Board of Huadong Hospital, Affiliated with Fudan University approved this retrospective study (No.20230108) and it was performed following the Declaration of Helsinki. The requirement for informed consent was waived.

Consent for publication

Not applicable.

Conmpeting interests

There are no conficting interests that the authors declare.

Credits: Chen, W., Gao, P., Lu, F. et al. CT texture features of lung adenocarcinoma with HER2 mutation. BMC Cancer 25, 287 (2025). https://doi.org/10.1186/s12885-025-13686-z

Artificial intelligence in in-vitro fertilization (IVF): A new era of precision and personalization in fertility treatments

David B. Olawade [a b c], Jennifer Teke [b d], Khadijat K. Adeleye [e], Kusal Weerasinghe [b], Momudat Maidoki [f], Aanuoluwapo Clement David-Olawade [g]

[a] Department of Allied and Public Health, School of Health, Sport and Bioscience, University of East London, London, United Kingdom
[b] Department of Research and Innovation, Medway NHS Foundation Trust, Gillingham ME7 5NY, United Kingdom
[c] Department of Public Health, York St John University, London, United Kingdom
[d] Faculty of Medicine, Health and Social Care, Canterbury Christ Church University, United Kingdom
[e] Elaine Marieb College of Nursing, University of Massachusetts, Amherst MA, USA
[f] Department of General Surgery, Medway NHS Foundation Trust, Gillingham ME7 5NY, United Kingdom
[g] Endoscopy Unit, Glenfield Hospital, NHS Trust, University Hospitals of Leicester, Leicester, United Kingdom

Abstract

In-vitro fertilization (IVF) has been a transformative advancement in assisted reproductive technology. However, success rates remain suboptimal, with only about one-third of cycles resulting in pregnancy and fewer leading to live births. This narrative review explores the potential of artificial intelligence (AI), machine learning (ML), and deep learning (DL) to enhance various stages of the IVF process. Personalization of ovarian stimulation protocols, gamete selection, and embryo annotation and selection are critical areas where AI may benefit significantly. AI-driven tools can analyze vast datasets to predict optimal stimulation protocols, potentially improving oocyte quality and fertilization rates. In sperm and oocyte quality assessment, AI can offer precise, objective analyses, reducing subjectivity and standardizing evaluations. In embryo selection, AI can analyze time-lapse imaging and morphological data to support the prediction of embryo viability, potentially aiding implantation outcomes. However, the role of AI in improving clinical outcomes remains to be confirmed by large-scale, well-designed clinical trials. Additionally, AI has the potential to enhance quality control and workflow optimization within IVF laboratories by continuously monitoring key performance indicators (KPIs) and facilitating efficient resource utilization. Ethical considerations, including data privacy, algorithmic bias, and fairness, are paramount for the responsible implementation of AI in IVF. Future research should prioritize validating AI tools in diverse clinical settings, ensuring their applicability and reliability. Collaboration among AI experts, clinicians, and embryologists is essential to drive innovation and improve outcomes in assisted reproduction. AI's integration into IVF holds promise for advancing patient care, but its clinical potential requires careful evaluation and ongoing refinement.

Keywords
In-vitro fertilization; Artificial intelligence; Machine learning; Deep learning (DL); Gamete selection; Embryo annotation

1. Introduction

In-vitro fertilization (IVF) has been a groundbreaking advancement in assisted reproductive technology since the birth of the first "test-tube baby" in 1978 [1]. This technique has offered hope to millions of couples struggling with infertility, providing an alternative pathway to parenthood. IVF has evolved significantly over the past four decades, incorporating various technological advancements to enhance its efficacy [2]. However, despite these innovations, the success rates of IVF remain suboptimal, with only approximately one-third of cycles resulting in pregnancy and an even smaller proportion leading to the birth of a healthy baby. It is important to note that while artificial intelligence (AI) offers the potential to optimize certain aspects of IVF, clinical validation of AI's impact on improving live birth rates remains limited.

The challenges faced in IVF involve complex biological, medical, and technical factors [3,4]. One of the

primary hurdles is the variability in patient response to ovarian stimulation protocols [5,6]. Personalizing these protocols to suit individual patient profiles is crucial for optimizing the quantity and quality of oocytes retrieved [7,8,9]. However, AI is not capable of directly enhancing oocyte quality; instead, it can help in tailoring stimulation protocols by identifying predictive factors for optimal responses [10,11]. Even with personalized approaches, predicting patient response remains challenging, leading to inconsistent outcomes. Furthermore, the selection of high-quality gametes and embryos is essential for improving fertilization rates and embryo viability [12,13], yet current methods heavily rely on subjective assessments by embryologists.

To address these complexities, AI encompasses various computational techniques that enable machines to mimic human intelligence [14]. Machine learning (ML), a subset of AI, involves the development of algorithms that can learn from and make predictions based on data [15]. Deep learning (DL), a more advanced subset of ML, utilizes neural networks with multiple layers to analyze complex patterns in large datasets [16]. These technologies have already demonstrated potential in various medical fields, including radiology [17], oncology, and genomics by providing precise, data-driven insights that enhance clinical decision-making [16].However, the application of AI in IVF remains in its early stages, and while early results are promising, comprehensive clinical validation is still required before AI can be routinely integrated into IVF practices [18].

Recent studies have shown that AI, ML, and DL present opportunities to transform IVF practices [18,19, 20,21]. Integrating AI into IVF can potentially address several critical areas that influence the procedure's success. For instance, AI-driven tools can analyze vast amounts of patient data to identify patterns and correlations that may not be apparent to human practitioners. This capability can enhance the personalization of ovarian stimulation protocols, ensuring that each patient receives the most suitable treatment plan [11]. Additionally, AI can improve gamete and embryo selection by providing objective assessments based on detailed morphological and genetic data [22,23], reducing the subjectivity and variability associated with manual evaluations. However, it is crucial to acknowledge that while AI can standardize and streamline certain procedures, its direct effect on improving IVF success rates requires further large-scale clinical trials [24].

Moreover, AI can play a significant role in the quality control of IVF laboratories [24,25]. By continuously monitoring key performance indicators and laboratory conditions, AI systems can ensure that the highest standards are maintained, thus increasing the consistency and reliability of IVF outcomes. The scheduling and workflow optimization capabilities of AI can also enhance the efficiency of IVF procedures, minimizing delays and ensuring the timely handling of gametes and embryos [26]. Yet, the impact of these efficiencies on clinical outcomes like pregnancy and live birth rates remains to be fully validated in a broader clinical context [25].

Despite significant advancements in assisted reproductive technology, the success rates of in-vitro fertilization (IVF) remain disappointingly low, with only about one-third of cycles resulting in pregnancy and even fewer leading to live births. This highlights a pressing need for more effective and reliable methods to enhance IVF outcomes. The rationale for this review is rooted in the potential of artificial intelligence (AI), machine learning (ML), and deep learning (DL) to address these challenges by providing objective, data-driven tools that can optimize various stages of the IVF process. The novelty of this review lies in its comprehensive examination of how these advanced technologies can be integrated into IVF practices to improve patient-specific stimulation protocols, gamete and embryo selection, and overall laboratory efficiency. The primary objectives of this narrative review are to explore current evidence supporting the use of AI, ML, and DL in IVF, to identify the potential benefits and limitations of these technologies, and to outline future directions for research and clinical implementation. This review aims to contribute to ongoing efforts to enhance IVF success rates and reduce patient emotional and financial burdens by synthesizing the latest findings and proposing new avenues for innovation. Fig. 1 below highlights different applications of AI integrated into IVF practices.

2. Methods

2.1. Literature search

A comprehensive literature search was conducted to gather relevant studies and articles on the application of artificial intelligence (AI), machine learning (ML), and deep learning (DL) in in-vitro fertilization (IVF). The literature databases searched included PubMed, Scopus, Web of Science, and Google Scholar. The search was performed using a combination of keywords and MeSH terms, such as "artificial intelligence," "machine learning," "deep learning," "in-vitro fertilization," "IVF," "ovarian stimulation," "oocyte quality," "embryo selection," "sperm selection," and "IVF outcomes." The search was limited to articles published in English from January 2000 to July

2024 to capture the most recent and relevant advancements in the field.

While this review adhered to a structured methodology, it is important to clarify that it is a narrative review, not a systematic one. The goal was to explore and synthesize emerging themes and advancements in the application of AI in IVF, rather than to evaluate the efficacy of interventions systematically. Thus, the approach prioritized conceptual synthesis and thematic organization over strict quantitative analysis.

2.2. Inclusion and exclusion criteria

The review included peer-reviewed articles and reviews that addressed the use of AI, ML, and DL in various aspects of IVF. Relevant studies discussed AI's impact on ovarian stimulation protocols, gamete selection, embryo assessment, and IVF laboratory quality control. Articles providing data on AI-driven IVF outcomes, such as pregnancy rates, live birth rates, and embryo viability, were considered. The search initially yielded 315 articles. After reviewing titles and abstracts, 118 articles were deemed potentially relevant. Following a detailed full-text review, 53 studies were included based on inclusion criteria, as summarized in Fig. 2. Articles not directly related to IVF, those focusing on other reproductive technologies, non-English publications, and studies without a clear focus on applying AI, ML, or DL in IVF were excluded.

2.3. Risk of bias evaluation

As this review is a narrative synthesis, it does not systematically evaluate the risk of bias for included studies. However, efforts were made to ensure reliability by selecting studies published in peer-reviewed journals

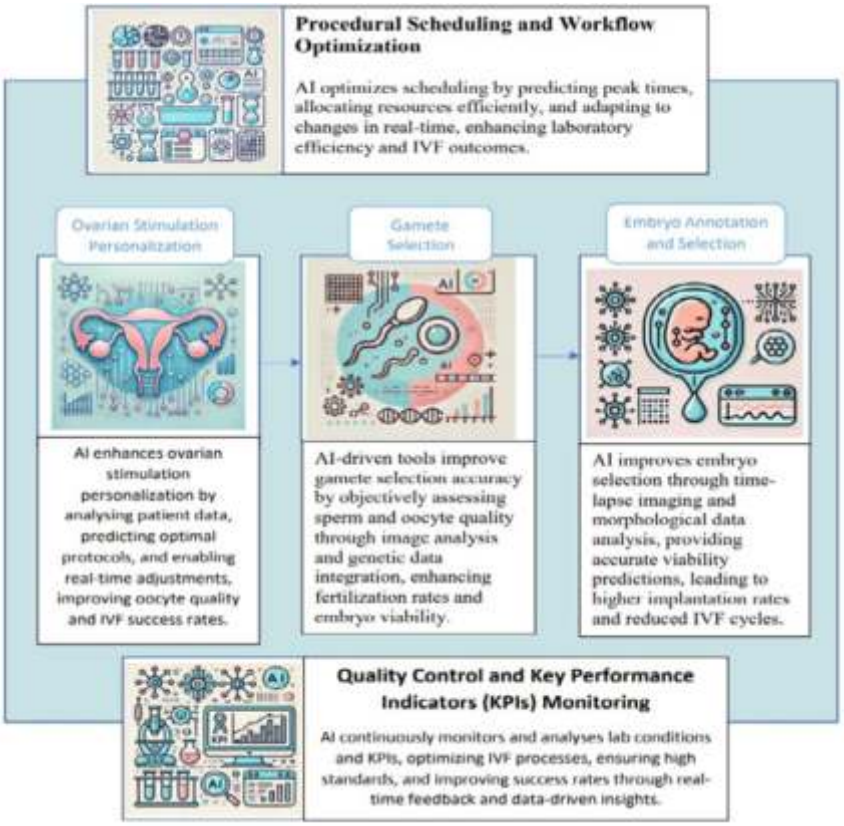

Fig. 1. Different applications of AI integrated into IVF practices.

Fig. 2. PRISMA flow diagram of the article selection process.

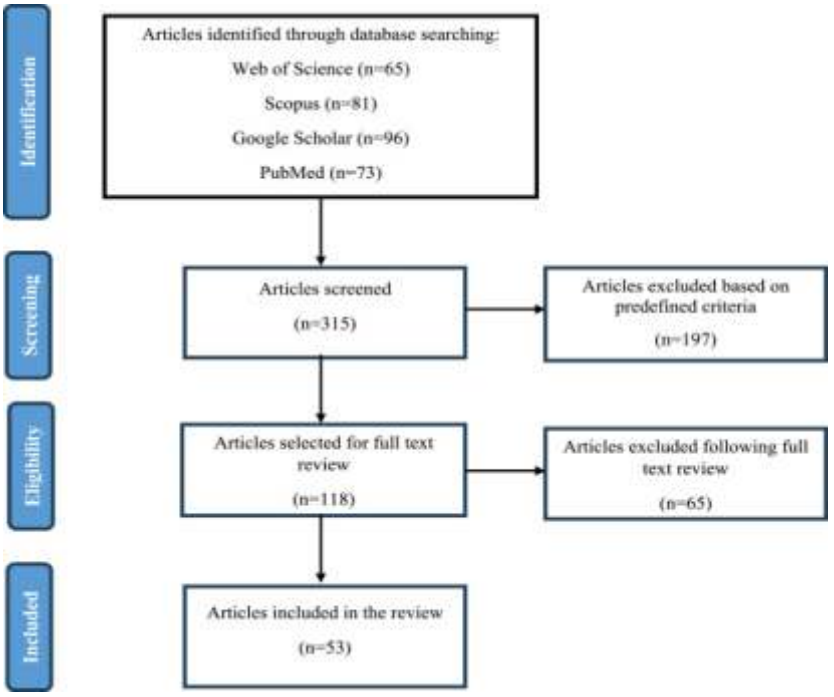

and critically appraising their methodological rigor during data extraction.

2.4. Synthesis of results

Findings from the selected studies were synthesized narratively, focusing on conceptual and thematic insights into AI applications across the IVF process. The studies were grouped based on key aspects of IVF, including ovarian stimulation, gamete selection, embryo selection, and laboratory management. The themes identified during data extraction were structured to reflect critical areas of AI integration in IVF including personalization of ovarian stimulation protocols, gamete and embryo selection, quality control in IVF laboratories, and workflow optimization. The narrative synthesis critically analyzed AI applications' potential benefits and limitations, aiming to provide a comprehensive overview of current evidence and highlight areas for future research.

3. Personalization of ovarian stimulation protocols

Ovarian stimulation protocols are critical to in-vitro fertilization (IVF) success as they optimize the number and quality of oocytes retrieved [5,27]. These protocols typically involve the administration of gonadotrophins to stimulate the ovaries to produce multiple follicles and to retrieve a sufficient number of mature oocytes that can be fertilized to create viable embryos [28]. Personalization of ovarian stimulation has become increasingly important due to the variability in patient characteristics such as age, ovarian reserve, and hormonal profile [29,30]. For instance, younger patients with a higher ovarian reserve may require different stimulation protocols compared to older patients or those with diminished ovarian reserve. Despite personalized approaches, predicting individual patient responses to stimulation remains challenging. Suboptimal stimulation can lead to various issues, including ovarian hyperstimulation syndrome (OHSS), poor oocyte quality, and, ultimately, lower IVF success rates [31].

Artificial intelligence (AI) can potentially revolutionize the personalization of ovarian stimulation protocols by leveraging vast datasets and advanced analytical techniques [21,32]. Recent advances in AI, particularly in machine learning (ML) and deep learning (DL), have shown promise in improving the accuracy and efficacy of these protocols. AI can analyze extensive datasets comprising patient characteristics, historical responses to stimulation protocols, and IVF outcomes [33,34]. AI can provide insights that may elude traditional analysis by identifying patterns and correlations within these datasets [35]. For instance, AI can identify subtle correlations between specific patient profiles and their responses to different stimulation protocols, enabling more precise treatment tailoring.

Machine learning algorithms can develop predictive models to estimate each patient's optimal type and dose of gonadotropins [36]. These models consider various factors, including age, body mass index (BMI), antral follicle count (AFC), and anti-Müllerian hormone (AMH) levels. AI models can predict the best day for monitoring a patient, trigger day options, and the number of oocytes [11]. AI systems can integrate data from previous IVF cycles to refine predictions for future treatments. This iterative learning process allows the AI to improve its recommendations continuously. By incorporating historical patient data, AI can enhance the personalization of stimulation protocols, resulting in improved clinical outcomes. Moreover, AI can also facilitate real-time adjustments to stimulation protocols [37]. By monitoring patients' responses during the stimulation phase, AI algorithms can recommend modifications to the dosage or type of gonadotropins. This dynamic approach ensures that the protocols are constantly optimized to achieve the best possible outcomes, reducing the incidence of complications like OHSS and enhancing overall treatment efficacy [21].

4. Gamete selection

Gamete selection is a pivotal step in the in-vitro fertilization (IVF) process, significantly impacting fertilization success rates and subsequent embryo development [38]. Accurately selecting high-quality sperm and oocytes can enhance the likelihood of successful fertilization, implantation, and a successful pregnancy [39]. While effective to some extent, traditional methods of gamete selection are often subjective and reliant on embryologists' expertise [40]. Advances in artificial intelligence (AI) and deep learning (DL) offer the potential to revolutionize gamete selection by providing objective, data-driven tools that can improve the accuracy and consistency of these assessments [41].

4.1. Sperm classification and selection

Traditional sperm selection methods rely heavily on manual assessment and basic laboratory techniques such as visual evaluation of motility and morphology using microscopy [42,43]. These methods are inherently subjective and can vary significantly between practitioners. Manual assessment is also time-consuming and may not always accurately predict the fertilization potential of sperm [42]. AI and DL technologies can significantly enhance sperm

selection by analyzing motility, morphology, and other relevant parameters with high precision [24,44]. While some studies indicate comparable outcomes between AI-based and traditional methods, DL models, trained on large datasets of sperm images and associated outcomes, can classify sperm quality more accurately than traditional methods [45,46]. These models can identify subtle morphological features and motility patterns that correlate with successful fertilization. For instance, DL algorithms can analyze high-resolution video footage of sperm movement to assess motility parameters such as velocity, linearity, and amplitude of lateral head displacement [47]. By providing a more objective and precise assessment of sperm quality, AI and DL can improve the chances of selecting the best sperm for fertilization. This not only increases the likelihood of successful fertilization but also enhances the overall quality of the resulting embryos. AI-driven sperm selection can be particularly beneficial in cases of male factor infertility, where the selection of the highest-quality sperm is critical for achieving positive outcomes.

4.2. Oocyte quality assessment

Oocyte quality is a crucial determinant of successful fertilization and subsequent embryo development [48,49]. Traditional assessment methods for oocyte quality primarily rely on morphological criteria observed under a microscope, such as the appearance of the zona pellucida, cytoplasm, and polar body [50]. However, these assessments are subjective and can vary between embryologists, leading to inconsistencies in oocyte quality assessment. AI offers a transformative approach to oocyte quality assessment by providing objective analyses based on high-resolution images of oocytes [11,51].

Table 1. AI applications in gamete selection.

Aspect of Gamete Selection	Traditional Methods	AI Applications/Models Used	Benefits of AI Applications
Sperm Classification and Selection [44]	Manual assessment using microscopy for motility and morphology	DL models (e.g., Convolutional Neural Networks) analyzing high-resolution images and video footage	- Increased precision and objectivity in motility and morphology assessment - Identification of subtle features correlating with fertilization potential - Improved consistency and reliability in sperm selection
Motility Analysis [55]	Visual inspection of sperm movement under a microscope	Computer Vision and DL models analyzing motility patterns	- Detailed quantification of motility parameters - Enhanced detection of optimal motile sperm - Reduced subjectivity in motility assessment
Morphology Assessment [56]	Kruger's strict criteria assessed visually by embryologists	Machine Learning models (e.g., Support Vector Machines) trained on large datasets of sperm images	- Objective classification of sperm morphology - Higher accuracy in identifying sperm with optimal morphology - Consistency across different observers and laboratories
Oocyte Quality Assessment [51,57]	Morphological evaluation of zona pellucida, cytoplasm, and polar body	AI-based image analysis (e.g., Convolutional Neural Networks) on high-resolution oocyte images	- Objective analysis of subtle morphological features - Integration of multiple imaging modalities - Improved selection of high-quality oocytes

continued on page 47

continued from page 46

Table 1. AI applications in gamete selection.

Aspect of Gamete Selection	Traditional Methods	AI Applications/Models Used	Benefits of AI Applications
Real-time Adjustments [58,59]	Adjustments based on manual observation and clinical judgment	AI-driven real-time recommendations for sperm and oocyte quality assessment	- Dynamic optimization of selection criteria - Immediate feedback for embryologists - Enhanced decision-making during the selection process
Data Integration from Previous Cycles [51]	Manual review of patient history and past IVF outcomes	AI models integrating historical patient data for personalized predictions	- Improved personalization of gamete selection - Continuous refinement of selection criteria based on past outcomes - Enhanced IVF success rates through tailored approaches

Advanced image analysis techniques powered by AI can identify subtle features that correlate with oocyte quality, which may not be discernible through manual evaluation. For example, AI algorithms can assess the ooplasm's homogeneity, the zona pellucida's integrity, and the presence of cytoplasmic inclusions or vacuoles, all of which are important indicators of oocyte health.

Furthermore, AI can integrate data from multiple imaging modalities, such as time-lapse microscopy and confocal imaging, to comprehensively assess oocyte quality. Time-lapse imaging allows continuous monitoring of oocyte development, providing dynamic information that AI can analyze to predict developmental potential [52]. By combining morphological data with dynamic developmental patterns, AI can enhance the accuracy of oocyte quality assessment, leading to better fertilization rates and higher-quality embryos.

4.3. Integration of genetic data

In addition to morphological assessments, the integration of genetic data into AI-driven gamete selection processes holds significant promise. Preimplantation genetic testing (PGT) can identify chromosomal abnormalities and genetic disorders in oocytes and embryos [53]. AI algorithms can analyze genetic data alongside morphological and developmental information to provide a more holistic assessment of gamete quality [54]. This integrated approach can improve the selection of genetically normal gametes, thereby increasing the chances of a successful pregnancy and reducing the risk of genetic disorders.

Table 1 provides an overview of how AI applications and models can enhance the various aspects of gamete selection in IVF, improving precision, objectivity, and overall outcomes.

5. Embryo annotation and selection

Embryo annotation and selection are critical steps in the in-vitro fertilization (IVF) process, significantly influencing the likelihood of successful implantation and pregnancy [60,61]. Traditional methods for selecting embryos primarily rely on morphological assessment, where embryologists visually evaluate the embryos under a microscope. This assessment typically considers cell number, symmetry, and fragmentation factors. Some clinics also incorporate genetic testing, such as preimplantation genetic testing (PGT), to identify chromosomal abnormalities [62,63]. However, these methods are inherently subjective and can vary between embryologists, leading to inconsistent and sometimes inaccurate predictions of embryo viability [64].

5.1. Traditional methods

Morphological assessment of embryos involves examining their appearance at various stages of development [64]. On Day 3, embryos are usually evaluated based on the number and regularity of blastomeres and the degree of fragmentation. On Day 5, the focus shifts to the formation and quality of the blastocyst, including the appearance of the inner cell mass and the trophectoderm [65]. While these assessments provide valuable

Table 2. AI applications in embryo annotation and selection.

Aspect of Embryo Selection	Traditional Methods	AI Models/Tools Used	Benefits of AI Applications
Morphological Assessment [68]	Visual assessment of cell number, symmetry, and fragmentation	Convolutional Neural Networks (CNNs) analyzing static images of embryos	- Objective and consistent assessment - Reduced inter-embryologist variability - Enhanced identification of viable embryos
Time-Lapse Imaging Analysis [61]	Manual observation of developmental stages	Time-lapse imaging systems with AI (e.g., EmbryoScope, Eeva)	- Continuous monitoring of embryo development - Detection of subtle morphological changes and dynamic behaviors - Improved prediction of implantation potential
Dynamic Monitoring [23]	Periodic manual checks of embryo development	AI algorithms analyzing time-lapse videos	- Identification of key developmental milestones - More accurate assessment of embryo quality - Better selection of embryos for transfer
Genetic Data Integration [53].	Preimplantation Genetic Testing (PGT) for aneuploidies	AI models integrating genetic, morphological, and developmental data	- Comprehensive assessment of embryo quality - Increased selection accuracy for genetically normal embryos - Reduced risk of genetic disorders
Predictive Modeling [69]	Predictions based on clinical judgment and experience	Machine Learning models (e.g., Random Forest, Support Vector Machines)	- Data-driven predictions of embryo viability - Integration of diverse data sources (e.g., patient history, stimulation protocols) - Improved decision-making for embryo transfer

continued on page 49

information, they do not always correlate with the embryo's ability to implant and develop into a healthy pregnancy. These evaluations are subjective, with significant variability between embryologists' assessments. Genetic testing, such as PGT, can provide additional insights into the chromosomal status of embryos [53]. By identifying aneuploidies, genetic testing can help select embryos with the highest potential for successful implantation [66]. However, PGT is invasive, expensive, and not universally available. Moreover, it cannot assess an embryo's functional potential beyond its chromosomal makeup, leaving gaps in predicting overall viability.

5.2. AI in embryo selection

Artificial intelligence (AI) and deep learning (DL) technologies have the potential to revolutionize embryo selection by providing more objective, accurate, and comprehensive assessments [14,15]. AI can analyze large datasets of time-lapse imaging and morphological data to predict embryo viability more precisely than traditional methods. Time-lapse imaging systems capture continuous images of embryos as they develop, providing a detailed record of their morphological changes. AI algorithms can analyze these time-lapse videos to identify patterns and developmental milestones associated with successful implantation and development [67]. AI can provide a more dynamic and nuanced assessment of embryo quality by examining parameters such as cleavage patterns, blastocyst formation, and the timing of key developmental events. Recent studies have demonstrated that AI models analyzing timelapse imaging can significantly improve the accuracy of embryo viability predictions [23].

continued from page 48

Table 2. AI applications in embryo annotation and selection.

Aspect of Embryo Selection	Traditional Methods	AI Models/Tools Used	Benefits of AI Applications
Real-time Adjustments [70,71]	Adjustments based on manual observation and clinical judgment	AI-driven real-time recommendations	- Dynamic optimization of selection criteria - Immediate feedback for embryologists - Enhanced decision-making during the selection process
Scoring Systems [72,73]	Embryo grading based on visual criteria	AI-generated scoring systems (e.g., Life Whisperer, iDAScore)	- Objective and reproducible scoring - Better prediction of implantation and pregnancy outcomes - Streamlined workflow in the embryology lab
Outcome Prediction [74]	Predictions based on historical success rates	AI models analyzing historical IVF data (e.g., IVF outcome prediction models)	- Personalized predictions of success rates - Tailored treatment recommendations - Higher chances of successful pregnancy with fewer cycles
Dynamic Monitoring (Time-lapse Imaging) [52]	Periodic manual observation of oocyte development stages	AI models analyzing time-lapse video to assess developmental potential	- Continuous monitoring of oocyte development - Identification of optimal developmental patterns - Prediction of fertilization and embryo development potential
Genetic Assessment Integration [53]	Preimplantation Genetic Testing (PGT) based on chromosomal analysis	AI models combining genetic data with morphological and developmental information	- Comprehensive assessment of genetic and morphological quality - Increased selection accuracy for genetically normal gametes - Reduced risk of genetic disorders in resulting embryos

For instance, AI can detect subtle morphological changes and dynamic behaviors difficult for human observers to discern. These models can predict implantation potential with higher accuracy, leading to better embryo selection for transfer and increased implantation rates.

In addition to time-lapse imaging, AI can enhance the traditional morphological assessment of embryos. Deep learning models, particularly convolutional neural networks (CNNs), can be trained on large datasets of embryo images to recognize features that correlate with high viability [68]. These models can analyze static images of embryos at various stages of development, providing an objective assessment that reduces inter-embryologist variability. AI-driven morphological assessments can identify features such as blastomere symmetry, cell junction quality, and the degree of fragmentation with greater precision than manual evaluations. By combining these assessments with time-lapse imaging data, AI provides a comprehensive analysis encompassing static and dynamic aspects of embryo development.

AI's ability to integrate and analyze diverse datasets allows for the development of predictive models that can forecast embryo viability [69]. These models can incorporate morphological data, time-lapse imaging, and genetic information to provide a holistic assessment. By identifying embryos with the highest potential for successful implantation and development, AI can increase implantation rates and reduce the number of cycles required to achieve a successful pregnancy [22]. For example, machine learning algorithms can be trained on historical IVF data, including patient demographics, stimulation protocols, and outcomes. These models can then predict the likelihood of success for new

Table 3. Quality control and key performance indicators monitoring in IVF.

Component	Traditional Methods	AI Models/Tools Used	Key Performance Indicators (KPIs)	Advantages of AI
Environmental Monitoring [76]	Manual recording and periodic checks of temperature, humidity, air quality	AI-driven environmental sensors and IoT devices	Temperature stability, humidity levels, air quality	Continuous real-time monitoring, immediate deviation alerts, consistent optimal conditions
Fertilization Rates [82]	Manual calculation and periodic analysis based on fertilization success	Machine Learning algorithms analyzing fertilization data	Number of fertilized oocytes, fertilization rate per cycle	Real-time analysis, early identification of issues, data-driven recommendations for improvement
Blastocyst Formation [83]	Visual assessment and manual recording of blastocyst development stages	Time-lapse imaging systems with AI analysis (e.g., EmbryoScope	Blastocyst formation rate, time to blastocyst stage	Continuous monitoring, precise tracking of developmental stages, better prediction of blastocyst viability
Clinical Pregnancy Rates [76]	Retrospective analysis of clinical pregnancy outcomes	Predictive analytics models integrating multiple data sources)	Clinical pregnancy rate, implantation rate	Real-time tracking, predictive insights for improving protocols, enhanced understanding of success factors
Procedural Adherence [84]	Manual checks and audits of adherence to protocol	Workflow management systems with AI (e.g., electronic lab notebooks with AI analytics)	Adherence to protocols, the incidence of deviations	Automated adherence tracking, immediate feedback on deviations, improved protocol consistency
Embryo Culture Conditions [79,85]	Manual observation and recording of cultural conditions	AI-driven monitoring systems analyzing cultural conditions	Culture media pH levels, oxygen concentration	Continuous monitoring, optimal condition maintenance, reduced variability in embryo development
Gamete and Embryo Handling [76]	Manual assessment and periodic reviews	AI algorithms analyzing handling data and procedural videos	Handling error rate, gamete/embryo viability post-handling	Identification of best practices, reduction of handling errors, consistent high-quality gamete and embryo handling

continued on page 51

patients, helping clinicians make more informed decisions about embryo selection and transfer.

Table 2 provides a comprehensive overview of how AI models and tools are being used to enhance various aspects of embryo annotation and selection, improving precision, objectivity, and overall IVF outcomes.

6. Quality control and key performance indicators monitoring

Consistent quality control in IVF laboratories is crucial for maintaining high standards and ensuring the success of assisted reproductive technologies [75]. Quality control encompasses a range of practices to monitor and optimize laboratory conditions and procedures to achieve the best possible patient outcomes. Key performance indicators (KPIs) such as fertilization rates, blastocyst formation rates, and clinical pregnancy rates are essential metrics that reflect the laboratory's performance and overall effectiveness [76]. Monitoring these KPIs allows laboratories to identify improvement areas, ensuring that all IVF processes function optimally. High standards in quality control are not only critical for achieving successful pregnancies but also for maintaining patient trust and adhering to regulatory requirements [75].

Artificial intelligence (AI) offers significant advancements in the realm of quality control by enabling continuous monitoring and analysis of laboratory conditions and procedural outcomes [77]. Machine learning (ML) algorithms can process vast amounts of data from various sources within the laboratory, including environmental sensors, procedural logs, and patient records [78]. By analyzing this data, AI systems can identify patterns and deviations from established KPIs that may indicate potential issues or areas for improvement. For instance, AI can

continued from page 50

Table 3. Quality control and key performance indicators monitoring in IVF.

Component	Traditional Methods	AI Models/Tools Used	Key Performance Indicators (KPIs)	Advantages of AI
KPI Tracking and Reporting [86]	Manual compilation and analysis of KPI data	AI-based dashboards and reporting tools (e.g., Tableau with Integrated AI)	Fertilization rates, blastocyst formation rates, clinical pregnancy rates	Real-time KPI tracking, automated reporting, easy identification of trends and issues
Root Cause Analysis of Failures [87]	Retrospective manual analysis of procedural failures	AI-driven root cause analysis tools (e.g., anomaly detection algorithms)	Failure rates, time to identify and correct issues	Faster identification of failure causes, data-driven insights, preventive measures implementation
Continuous Improvement [82,88]	Periodic reviews and manual updates of protocols	Continuous learning AI systems updating protocols based on new data	Improvement rate, protocol update frequency	Dynamic protocol optimization, incorporation of the latest evidence, ongoing performance enhancement

monitor environmental conditions such as temperature, humidity, and air quality within the laboratory to ensure they remain within optimal ranges for gamete and embryo culture. Any deviations from these parameters can be immediately flagged, allowing laboratory staff to take corrective actions before these conditions negatively impact the IVF outcomes. Additionally, AI can track procedural adherence, ensuring that protocols are followed consistently, which is crucial for maintaining the quality and viability of gametes and embryos.

AI-driven quality control systems can also provide real-time feedback and recommendations based on the analysis of KPI data [79]. For example, if fertilization rates are observed to be below expected levels, AI algorithms can analyze procedural data to identify potential causes, such as variations in sperm or oocyte handling techniques, and suggest modifications to improve outcomes [32]. Similarly, if blastocyst formation rates are suboptimal, AI can recommend adjustments in culture conditions or protocols based on historical data and current trends [20]. By continuously monitoring and optimizing laboratory conditions and procedures, AI helps ensure that each IVF process is performed to the highest standards [9,80]. This enhances the likelihood of successful pregnancies and reduces errors and variability, ultimately contributing to better patient outcomes and increased confidence in IVF treatments. Furthermore, AI's ability to analyze complex datasets and provide actionable insights can support ongoing improvements in laboratory practices. Continuous learning and adaptation of AI algorithms based on new data can drive innovations and refine IVF protocols, ensuring that laboratories remain at the forefront of assisted reproductive technologies [81]. This dynamic approach to quality control, underpinned by AI, represents a significant advancement in pursuing excellence in IVF outcomes as highlighted in Table 3.

7. Procedural scheduling and workflow optimization

Efficient scheduling and workflow management are critical in busy IVF laboratories, where timely execution of procedures is paramount for maintaining the quality of gametes and embryos [89]. Delays or inefficiencies in the workflow can lead to suboptimal conditions, which may negatively impact fertilization rates, embryo development, and overall IVF success rates. Common challenges include coordinating multiple procedures that need to occur within specific time windows, managing the availability of laboratory staff and equipment, and responding to unexpected changes, such as equipment failures or variations in patient needs. Inefficient scheduling can result in extended waiting times, increased stress for patients and staff, and potentially lower clinical outcomes [90].

Artificial intelligence (AI) offers transformative potential for optimizing scheduling and workflow management in IVF laboratories [11]. By analyzing historical data and real-time workflow patterns, AI can predict the optimal timing for various procedures, ensuring that each step is carried out at the most appropriate moment. This optimization can significantly reduce waiting times and enhance the timely handling of gametes and embryos, ultimately improving laboratory efficiency and success rates. AI can analyze extensive

datasets from past cycles to identify patterns and bottlenecks in the workflow. By understanding these patterns, AI algorithms can forecast busy periods and allocate resources accordingly [91]. This ensures that critical procedures, such as oocyte retrieval, fertilization, and embryo transfer, are performed without unnecessary delays [92]. For example, AI can predict peak times for laboratory activities and suggest optimal staff scheduling to meet these demands.

Machine learning (ML) algorithms can predict the best timing for each procedure based on various factors, including patient-specific data, laboratory conditions, and historical outcomes. This predictive capability ensures that procedures are scheduled when conditions are most favorable, enhancing the quality of gametes and embryos [41]. For instance, AI can determine the optimal time for oocyte retrieval based on the maturation status of the follicles, ensuring that oocytes are collected at their peak quality [21]. AI-driven scheduling tools can adapt to unexpected changes, such as equipment malfunctions or sudden shifts in patient conditions. By continuously monitoring the workflow and available resources, AI can make real-time adjustments to the schedule, ensuring that disruptions are minimized. This adaptability is crucial in maintaining smooth operations and avoiding delays that could compromise the quality of the IVF process [57].

AI can also optimize allocating laboratory resources, including staff, equipment, and lab space. By predicting the needs for each procedure and ensuring that resources are available when needed, AI helps avoid overbooking and underutilization. This efficient allocation not only improves workflow but also enhances the working environment for laboratory staff, reducing stress and potential errors. Several AI-driven scheduling tools are being developed and implemented in IVF laboratories [93]. These tools utilize advanced algorithms to create dynamic schedules that can be adjusted in real-time based on changing conditions. For example, AI platforms can integrate data from patient management systems, laboratory information systems, and real-time monitoring devices to provide comprehensive scheduling solutions. These platforms offer features such as automatic rescheduling in response to delays, predictive analytics for resource planning, and real-time alerts for staff and patients.

AI-driven scheduling reduces waiting times by optimizing the schedule and ensuring the timely execution of procedures. This improves the overall patient experience and reduces the stress associated with the IVF process [94]. Timely handling of gametes and embryos ensures they are maintained optimally, enhancing their quality and viability. This can lead to higher fertilization rates, better embryo development, and increased success rates for IVF cycles [25]. Enhanced laboratory efficiency is another significant benefit of AI-driven scheduling. By streamlining the workflow, reducing bottlenecks, and improving overall efficiency, laboratories can handle a higher volume of cycles without compromising quality. AI's ability to adapt to unexpected changes ensures that the laboratory can respond quickly to disruptions, maintaining smooth operations and minimizing delays. Additionally, AI optimizes the allocation of resources, ensuring that staff, equipment, and lab space are used efficiently, reducing waste, and enhancing productivity.

8. Challenges of AI application in IVF

The application of artificial intelligence (AI) in in-vitro fertilization (IVF) presents significant challenges that must be addressed before widespread clinical adoption [93]. One major issue is the lack of large-scale clinical validation. Many AI models in IVF are developed and tested on small, single-center datasets, which limits their generalizability. These studies are often conducted in highly controlled environments with relatively homogeneous patient populations, lacking diversity in real-world clinical settings. Without robust, multi-center, randomized controlled trials that validate these models across various patient demographics and clinical contexts, the efficacy and safety of AI-driven tools remain uncertain. For instance, while some studies suggest AI improves embryo selection accuracy, few provide long-term outcome data, such as live birth rates or the health of children born through AI-guided IVF.

One reason for inconsistent findings across different centers is the lack of standardized recording and reporting practices. Variations in how data is collected, interpreted and reported can lead to discrepancies in AI performance and make it difficult to compare results across studies. For example, centers may use different criteria for evaluating embryo quality or success rates, which can influence AI model training and results. Establishing a consensus on standardized data collection, detailed recording of IVF outcomes, and uniform reporting protocols for AI applications in IVF would help ensure consistency and allow for more reliable cross-center comparisons. Such standardization would enable a more precise evaluation of AI's effectiveness across different clinical environments.

Another significant challenge is bias in the datasets used to train AI models. AI relies heavily on historical data to identify patterns and make predictions [95]. If the data used to train these algorithms does not represent the broader population, it can introduce significant bias, resulting in inequitable treatment outcomes. For example, most AI models in IVF have been developed using data from predominantly Western populations, which may not accurately reflect the diversity of reproductive health issues across different ethnicities, age groups, or socio-economic backgrounds. This bias could lead to unequal success rates, where certain patient groups benefit more from AI-guided treatment than others. Addressing this requires the development of more diverse and representative datasets encompassing a more comprehensive range of patient demographics and regular auditing of AI systems to identify and correct bias. The failure to mitigate these biases risks perpetuating health disparities in reproductive medicine.

Data privacy and security are also critical concerns in the application of AI in IVF. Given that AI systems require access to large datasets, including sensitive personal and genetic information, the potential for data breaches or misuse is a significant ethical concern [96]. Patients undergoing IVF are already in a vulnerable position, and the improper handling of their data could lead to privacy violations, discrimination, or other harm. Current regulatory frameworks such as the General Data Protection Regulation (GDPR) in Europe and the Health Insurance Portability and Account- ability Act (HIPAA) in the United States offer guidance on protecting patient information, but the use of AI necessitates even stricter protocols [97,98,99]. The integration of AI into clinical practice demands robust encryption methods, secure storage solutions, and strict access controls to safeguard patient data at every stage of the process.

In addition to privacy concerns, ethical transparency remains a crucial challenge in AI-driven IVF. Many AI algorithms function as "black boxes," meaning that their decision-making processes are not easily interpretable by clinicians or patients [100,101]. This lack of transparency can lead to challenges in clinical practice, where healthcare providers may struggle to explain or justify AI-driven recommendations to patients. For example, suppose an AI model suggests the selection of one embryo over another without a clear rationale. In that case, it may be difficult for clinicians to gain patient trust or confidence. Moreover, AI algorithms typically base their recommendations on statistical patterns rather than considering individual patient preferences, lifestyle factors, or other clinical nuances that human judgment might factor into decision-making. This can result in over-reliance on AI systems, where clinicians follow AI recommendations without thoroughly evaluating their relevance or applicability to the patient's case [96,102]. Developing more interpretable AI models and ensuring clinicians are trained to critically assess AI-generated outputs in the context of their professional expertise are essential.

9. Conclusion

Artificial intelligence (AI), machine learning (ML), and deep learning (DL) have the potential to significantly transform in-vitro fertilization (IVF) practices by providing objective, data-driven tools that enhance various stages of the IVF process. These technologies can personalize ovarian stimulation protocols, ensuring that each patient receives the most effective treatment based on their unique characteristics. By optimizing gamete selection through precise assessments of sperm and oocyte quality, AI can improve fertilization rates and embryo viability. Additionally, AI-driven embryo selection can lead to higher implantation success rates, reducing the number of cycles required to achieve pregnancy and thus lowering the emotional and financial burdens on patients [39]. Integrating AI into quality control and workflow optimization further enhances the efficiency and effectiveness of IVF laboratories. AI's ability to continuously monitor and analyze key performance indicators (KPIs) helps maintain high standards and consistent outcomes. Moreover, AI-driven scheduling and resource management can streamline laboratory operations, minimizing delays and ensuring the timely handling of gametes and embryos.

Despite the promising benefits, the application of AI in IVF must be approached with careful consideration of ethical implications. Ensuring data privacy and security is paramount to protect sensitive patient information. AI algorithms must be trained on diverse datasets to avoid biases and ensure fairness and inclusivity in care. Regular audits and updates of AI models are necessary to maintain their accuracy and mitigate any emerging biases. Continued research and development are crucial to refine AI technologies further and validate their efficacy in clinical settings. Collaborative efforts between AI experts, reproductive endocrinologists, embryologists, and ethicists will be essential to address the challenges and maximize the potential of AI in IVF. By adhering to ethical standards and continuously improving AI applications, the IVF field can offer more effective, equitable, and efficient treatments, ultimately enhancing the overall success rates

and patient experiences in assisted reproductive technology.

Declaration of competing interest

The authors declare that they have no known competing financial interests or personal relationships that could have appeared to influence the work reported in this paper.

References

1. S. Fishel. First in vitro fertilization baby— This is how it happened Fertil Steril, 110 (1) (2018), pp. 5-11
2. M.E. Graham, A. Jelin, A.H. Hoon Jr, A.M. Wilms Floet, E. Levey, E.M Graham Assisted reproductive technology: short-and long-term outcomes Dev Med Child Neurol, 65 (1) (2023), pp. 38-49
3. R. Klitzman. Unconventional combinations of prospective parents: ethical challenges faced by IVF providers BMC Med Ethics, 18 (2017), pp. 1-13
4. S. Ferber, N.J. Marks, V. Mackie IVF and assisted reproduction Springer (2020)
5. M.M. Alper, B.C. Fauser. Ovarian stimulation protocols for IVF: is more better than less? Reprod Biomed Online, 34 (4) (2017), pp. 345-353
6. M. Razafintsalama-Bourdet, M. Bah, G. Amand, L. Vienet-Lègue, C. Pietin-Vialle, H. Bry-Gauillard, et al. Random antral follicle count performed on any day of the menstrual cycle has the same predictive value as AMH for good ovarian response in IVF cycles J Gynecol Obstet Hum Reprod, 51 (1) (2022), Article 102233
7. P.R. Jirge, M.M. Patil, R. Gutgutia, J. Shah, M. Govindarajan, V.S. Roy, et al. Ovarian stimulation in assisted reproductive technology cycles for varied patient profiles: an Indian perspective J Hum Reprod Sci, 15 (2) (2022), pp. 112-125
8. K. Palinska-Rudzka, R. Mathur. Principles of controlled ovarian stimulation for assisted reproduction. Obstet Gynaecol Reprod Med, 33 (4) (2023), pp. 91-96
9. C. Canon, L. Leibner, M. Fanton, Z. Chang, V. Suraj, J.A. Lee, et al. Optimizing oocyte yield utilizing a machine learning model for dose and trigger decisions, a multi-center, prospective study Sci Rep, 14 (1) (2024 20), p. 18721. https://www.nature.com/articles/ s41598-024-69165-1
10. M. Fanton, V. Nutting, F. Solano, P. Maeder-York, E. Hariton, O. Barash, et al. An interpretable machine learning model for predicting the optimal day of trigger during ovarian stimulation Fertil Steril, 118 (1) (2024), pp. 101-108. https://www.sciencedirect.com/science/article/pii/ S0015028222002448
11. G. Letterie, A. MacDonald, Z. Shi An artificial intelligence platform to optimize workflow during ovarian stimulation and IVF: process improvement and outcome-based predictions Reprod Biomed Online, 44 (2) (2022), pp. 254-260
12. I. Oseguera-López, S. Ruiz-Díaz, P. Ramos-Ibeas, S. Pérez-Cerezales. Novel techniques of sperm selection for improving IVF and ICSI outcomes. Front Cell Dev Biol, 7 (2019), p. 298
13. J.B. Chorya, T.V. Sutaria, R.K. Chaudhari, C.F. Chaudhari. Impact of gamete health on fertilization and embryo development: an overview Asian Pac J Reprod, 11 (5) (2022), pp. 201-207
14. A. Konar. Artificial intelligence and soft computing: behavioral and cognitive modeling of the human brain CRC press (2018)
15. J. Alzubi, A. Nayyar, A. Kumar. Machine learning from theory to algorithms: an overview. J Phys Conf Ser (2018), Article 012012
16. I.H. Sarker. Deep learning: a comprehensive overview on techniques, taxonomy, applications and research directions. SN Comput Sci, 2 (6) (2021), p. 420
17. R. Najjar. Redefining radiology: a review of artificial intelligence integration in medical imaging Diagnostics, 13 (17) (2023), p. 2760
18. J.M. Raimundo, P. Cabrita. Artificial intelligence at assisted reproductive technology Procedia Comput Sci, 181 (2021), pp. 442-447
19. A. Goyal, M. Kuchana, K.P.R. Ayyagari. Machine learning predicts live-birth occurrence before in-vitro fertilization treatment. Sci Rep, 10 (1) (2020), p. 20925
20. D. Cimadomo, V. Chiappetta, F. Innocenti, G. Saturno, M. Taggi, A. Marconetto, et al. Towards automation in IVF: pre-clinical validation of a deep learning-based embryo grading system during PGT-A cycles. J Clin Med, 12 (5) (2023), p. 1806
21. E. Hariton, Z. Pavlovic, M. Fanton, V.S. Jiang. Applications of artificial intelligence in ovarian stimulation: a tool for improving efficiency and outcomes. Fertil Steril, 120 (1) (2023), pp. 8-16
22. V.W. Fitz, M.K. Kanakasabapathy, P. Thirumalaraju, H. Kandula, L.B. Ramirez, L. Boehnlein, et al. Should there be an "AI" in TEAM? Embryologists selection of high implantation potential embryos improves with the aid of an artificial intelligence algorithm J Assist Reprod Genet, 38 (2021), pp. 2663-2670
23. M.F. Kragh, H. Karstoft. Embryo selection with artificial intelligence: how to evaluate and compare methods? J Assist Reprod Genet, 38 (7) (2021), pp. 1675-1689
24. P. Cherouveim, C. Velmahos, C.L. Bormann. Artificial intelligence for sperm selection— A systematic review. Fertil Steril, 120 (1) (2023), pp. 24-31
25. H.L. Khan, S. Khan, S. Bhatti, S. Abbas. Role of artificial intelligence in quality assurance in ART: a review. Fertil Reprod, 5 (01) (2023), pp. 1-7
26. D.K. Gardner. The way to improve ART outcomes is to introduce more technologies in the laboratory. Reprod Biomed Online, 44 (3) (2022), pp. 389-392
27. G.N. Allahbadia, Y. Morimoto. Ovarian stimulation protocols Springer (2016)
28. D. Glujovsky, R. Pesce, M. Miguens, C.E. Sueldo, K. Lattes, A Ciapponi. How effective are the non-conventional ovarian stimulation protocols in ART? A systematic review and meta-analysis. J Assist Reprod Genet, 37 (12) (2020), pp. 2913-2928
29. B.W. Mol, P.M. Bossuyt, S.K. Sunkara, J.A.G. Velasco, C. Venetis, D. Sakkas, et al. Personalized ovarian stimulation for assisted reproductive technology: study design considerations to move from hype to added value for patients. Fertil Steril, 109 (6)

(2018), pp. 968-979
30. B. Doroftei, O.D. Ilie, N. Anton, O.A. Marcu. Scripcariu IS, Ilea C. A narrative review discussing the efficiency of personalized dosing algorithm of follitropin delta for ovarian stimulation and the reproductive and clinical outcomes. Diagnostics, 13 (2) (2023), p. 177
31. T. Haahr, S.C. Esteves, P. Humaidan. Individualized controlled ovarian stimulation in expected poor-responders: an update. Reprod Biol Endocrinol, 16 (2018), pp. 1-9
32. R. AlSaad, A. Abd-Alrazaq, F. Choucair, A. Ahmed, S. Aziz, J. Sheikh. Harnessing artificial intelligence to predict ovarian stimulation outcomes in in vitro fertilization: scoping review J Med
33. C.L. Curchoe, C.L. Bormann. Artificial intelligence and machine learning for human reproduction and embryology presented at ASRM and ESHRE 2018. J Assist Reprod Genet, 36 (2019), pp. 591-600
34. C. Siristatidis, S. Stavros, A. Drakeley, S. Bettocchi, A. Pouliakis, P. Drakakis, et al. Omics and artificial intelligence to improve in vitro fertilization (IVF) success: a proposed protocol Diagnostics, 11 (5) (2021), p. 743
35. M. Mann, C. Kumar, W.F. Zeng, M.T. Strauss Artificial intelligence for proteomics and biomarker discovery Cell Syst, 12 (8) (2021), pp. 759-770.
36. K. Zielinski, S. Pukszta, M. Mickiewicz, M. Kotlarz, P. Wygocki, M. Zielen, et al. Personalized prediction of the secondary oocytes number after ovarian stimulation: a machine learning model based on clinical and genetic data PLoS Comput Biol, 19 (4) (2023), Article e1011020
37. A. Cesario, M. D'Oria, F. Bove, G. Privitera, I. Boškoski, D. Pedicino, et al. Personalized clinical phenotyping through systems medicine and artificial intelligence. J Pers Med, 11 (4) (2021), p. 265
38. R.D. Rezaeiye, A. Mehrara, A.M.A. Pour, J. Fallahi, S. Forouhari. Impact of various parameters as predictors of the success rate of in vitro fertilization. Int J Fertil Steril, 16 (2) (2022), p. 76
39. L.C. Martínez, L. Murria, M.Á. Valera, A. Cobo, M. Meseguer. Testing the ability of an artificial in? ligence (AI) algorithm in predicting implantation and ongoing pregnancy potential of vitrified-warmed blastocysts from a single image. Fertil Steril, 120 (4) (2023). https://www.fertstert.org/article/S0015-0282(23)00909-3/abstract
40. S. Ozturk. Selection of competent oocytes by morphological criteria for assisted reproductive technologies. Mol Reprod Dev, 87 (10) (2020), pp. 1021-1036
41. S. Hanassab, A. Abbara, A.C. Yeung, M. Voliotis, K. Tsaneva-Atanasova, T.W. Kelsey, et al. The prospect of artificial intelligence to personalize assisted reproductive technology. npj Digit Med, 7 (1) (2024), p. 55
42. Dias T.R., Cho C.L., Agarwal A. Sperm assessment: traditional approaches and their indicative value. In vitro fertilization: a textbook of current and emerging methods and devices. 2019;249–63.
43. G. Marzano, M.S. Chiriacò, E. Primiceri, M.E. Dell'Aquila, J. Ramalho-Santos, V. Zara, et al. Sperm selection in assisted reproduction: a review of established methods and cutting-edge possibilities. Biotechnol Adv, 40 (2020), Article 107498
44. J.B. You, C. McCallum, Y. Wang, J. Riordon, R. Nosrati, D. Sinton. Machine learning for sperm selection Nat Rev Urol, 18 (7) (2021), pp. 387-403
45. S.A. Hicks, J.M. Andersen, O. Witczak, V. Thambawita, P. Halvorsen, H.L. Hammer, et al. Machine learning-based analysis of sperm videos and participant data for male fertility prediction Sci Rep, 9 (1) (2019), p. 16770
46. L. Spencer, J. Fernando, F. Akbaridoust, K. Ackermann, R Nosrati Ensembled deep learning for the classification of human sperm head morphology Adv Intell Syst, 4 (10) (2022), Article 2200111
47. S. Shahali, M. Murshed, L. Spencer, O. Tunc, L. Pisarevski, J. Conceicao, et al. Morphology classification of live unstained human sperm using ensemble deep learning Adv Intell Syst (2024), Article 2400141
48. M. Conti, F. Franciosi. Acquisition of oocyte competence to develop as an embryo: integrated nuclear and cytoplasmic events. Hum Reprod Update, 24 (3) (2018), pp. 245-266
49. Y. Lemseffer, M.E. Terret, C. Campillo, E. Labrune. Methods for assessing oocyte quality: a review of literature Biomedicines, 10 (9) (2022), p. 2184
50. B. Balaban, I. Keles, T. Ebner. Morphological assessment of oocyte quality. Man Oocyte Retr Prep Hum Assist Reprod (2022), p. 85
51. K. Si, B. Huang, L. Jin. Application of artificial intelligence in gametes and embryos selection. Hum Fertil, 26 (4) (2023), pp. 757-777
52. P. Bhide, D.Y. Chan, D. Lanz, O. Alqawasmeh, E. Barry, D. Baxter, et al. Clinical effectiveness and safety of time-lapse imaging systems for embryo incubation and selection in in-vitro fertilisation treatment (TILT): a multicentre, three-parallel-group, double-blind, randomised controlled trial Lancet, 404 (10449) (2024), pp. 256-265
53. J. Buldo-Licciardi, M.J. Large, D.H. McCulloh, C. McCaffrey, J.A. Grifo. Utilization of standardized preimplantation genetic testing for aneuploidy (PGT-A) via artificial intelligence (AI) technology is correlated with improved pregnancy outcomes in single thawed euploid embryo transfer (STEET) cycles. J Assist Reprod Genet, 40 (2) (2023), pp. 289-299
54. B. Aydin, D. Hudkova, C. Halicigil. Maximizing donor egg efficiency: artificial intelligence and genetically certified oocytes Cryopreservation. Z.P. Nagy, A.C. Varghese, A Agarwal (Eds.), Assisted reproduction: a practitioner's guide to methods, management and organization [Internet], Springer International Publishing, Cham (2024), pp. 471-490, 10.1007/978-3-031-58214-1_48
55. D. Celebi, A.D. Omur, S.A. Akarsu. Celbis SC, Baser S. Artificial intelligence in gamete cell selection and semen microbiologic analysis. J Clin Vet Res, 2 (2) (2022)
56. A.F.S. Farías, D. Sakkas, A. Chavez-Badiola, O. Ocali, G. Mendizabal, R. Valencia, et al. Single-sperm motility analysis during ICSI using an artificial intelligence sperm identification software (SID) and correlation with morphology. Fertil Steril, 118 (4) (2022), pp. e56-e57
57. G. Letterie. Artificial intelligence and assisted reproductive technologies: 2023. Ready for prime time? Or not.

Fertil Steril, 120 (1) (2023), pp. 32-37
58. S.T. Young, W.L. Tzeng, Y.L. Kuo, M.L. Hsiao, S.R. Chiang. Real-time tracing of spermatozoa IEEE Eng Med Biol Mag, 15 (6) (1996), pp. 117-120. https://ieeexplore.ieee.org/abstract/document/544519/?casa_token=GpP9AUPYZ_IAAAAA:86t9dMCGNa5M003wdfi5aUrK28h06yIMzH2bqZ3J0z3jOcaP-bzEKv23-sMqpvYn1 TznvcmW
59. F. Itoi, T. Miyamoto, T. Himaki, H. Honnma, M. Sano, J. Ueda. Importance of real-time measurement of sperm head morphology in intracytoplasmic sperm injection. Zygote, 30 (1) (2022), pp. 9-16 https://www.cambridge.org/core/journals/zygote/article/importance-of-realtime-measurement-of-sperm-head-morphology-in-intracytoplasmic-sperm-injection/7C10CF2237C9970EFC132D38EC AAC11E
60. M. Feyeux, A. Reignier, M. Mocaer, J. Lammers, D. Meistermann, P. Barrière, et al. Development of automated annotation software for human embryo morphokinetics. Hum Reprod, 35 (3) (2020), pp. 557-564
61. J. Berntsen, J. Rimestad, J.T. Lassen, D. Tran, M.F Kragh. Robust and generalizable embryo selection based on artificial intelligence and time-lapse image sequences. PLoS One, 17 (2) (2022), Article e0262661
62. B.S. Harris, K.C. Bishop, J.A. Kuller, S. Alkilany, T.M. Price. Preimplantation genetic testing: a review of current modalities. F S Rev, 2 (1) (2021), pp. 43-56
63. T. Stankewicz. Optimizing ivf by controlling for both embryonic aneuploidy and endometrial receptivity using genetic testing. University of Kent (United Kingdom (2021)
64. Kort J., Behr B. Traditional embryo morphology evaluation: from the zygote to the blastocyst stage. In vitro fertilization: a textbook of current and emerging methods and devices. 2019; 493–504.
65. R. Sciorio, M. Meseguer. Focus on time-lapse analysis: blastocyst collapse and morphometric assessment as new features of embryo viability Reprod Biomed Online, 43 (5) (2021), pp. 821-832
66. Z. Rosenwaks, A.H. Handyside. Is preimplantation genetic testing for aneuploidy an essential tool for embryo selection or a costly 'add-on'of no clinical benefit? Fertil Steril, 110 (3) (2018), pp. 351-352.
67. J. Berntsen, J. Rimestad, J.T. Lassen, D. Tran, M.F. Kragh. Robust and generalizable embryo selection based on artificial intelligence and time-lapse image sequences. PLoS One, 17 (2) (2022), Article e0262661. https://journals.plos.org/plosone/article?id=10.1371/journal.pone.0262661
68. e Z ul. M. Ishaq, S. Raza, H. Rehar, S. Abadeen, D. Hussain, R.A. Naqvi, et al. Assisting the human embryo viability assessment by deep learning for in vitro fertilization. Mathematics, 11 (9) (2023), p. 2023
69. I. Dimitriadis, N. Zaninovic, A.C. Badiola, C.L. Bormann. Artificial intelligence in the embryology laboratory: a review Reprod Biomed Online, 44 (3) (2022), pp. 435-448.
70. J. Stegmaier, F. Amat, W.C. Lemon, K. McDole, Y. Wan, G. Teodoro, et al. Real-time three-dimensional cell segmentation in large-scale microscopy data of developing embryos. Dev Cell, 36 (2) (2016), pp. 225-240. https://www.cell.com/developmental-cell/fulltext/S1534-5807(15)00837-0
71. K. Lundin, H. Park. Time-lapse technology for embryo culture and selection Ups J Med Sci, 125 (2) (2020), pp. 77-84. https://ujms.net/index.php/ujms/article/view/5629.
72. A. Chavez-Badiola, A. Flores-Saiffe-Farías, G. Mendizabal-Ruiz, A.J. Drakeley, J. Cohen Embryo ranking intelligent classification algorithm (ERICA): artificial intelligence clinical assistant predicting embryo ploidy and implantation. Reprod Biomed Online, 41 (4) (2020), pp. 585-593. https://www.sciencedirect.com/science/article/pii/S1472648320303734?casa_token=jM2SA9P-Ji8AAAAA: C8UFa-LeFSxiUz37Ly1owL_ZAjDoQ5Jih_ goblqsJq_NKiOe7MH5BSbWgMObLU6mYdhMNWaf
73. S. Ueno, J. Berntsen, M. Ito, T. Okimura, K. Kato. Correlation between an annotation-free embryo scoring system based on deep learning and live birth/neonatal outcomes after single vitrified-warmed blastocyst transfer: a single-centre, large-cohort retrospective study. J Assist Reprod Genet, 39 (9) (2022), pp. 2089-2099. https://link.springer.com/10.1007/s10815-022-02562-5
74. S. De Gheselle, C. Jacques, J. Chambost, C. Blank, K. Declerck, I. De Croo, et al. Machine learning for prediction of euploidy in human embryos: in search of the best-performing model and predictive features. Fertil Steril,117(4) (2022), pp.738-746. https://www.sciencedirect. com/science/article/pii/S001502822102238X
75. P. Durai. Quality control in the assisted reproductive technology laboratory. CRC Press (2024)
76. G. Fabozzi, D. Cimadomo, R. Maggiulli, A. Vaiarelli, F.M. Ubaldi, L. Rienzi. Which key performance indicators are most effective in evaluating and managing an in vitro fertilization laboratory? Fertil Steril, 114 (1) (2020), pp. 9-15.
77. Q.U. Ain, R. Nazir, A. Nawaz, H. Shahbaz, A. Dilshad, I.U. Mufti, et al. Machine Learning Approach towards Quality Assurance, Challenges and Possible Strategies in Laboratory Medicine. J Clin Transl Pathol, 4 (2) (2024), pp. 76-87.
78. A.M. Rahmani, E. Yousefpoor, M.S. Yousefpoor, Z. Mehmood, A. Haider, M. Hosseinzadeh, et al. Machine learning (ML) in medicine: review, applications, and challenges Mathematics, 9 (22) (2021), p. 2970
79. C.L. Bormann, C.L. Curchoe, P. Thirumalaraju, M.K. Kanakasabapathy, R. Gupta, R. Pooniwala, et al. Deep learning early warning system for embryo culture conditions and embryologist performance in the ART laboratory. J Assist Reprod Genet, 38 (7) (2021), pp. 1641-1646
80. S. Tamir. Artificial intelligence in human reproduction: charting the ethical debate over AI in IVF AI Ethics, 3 (3) (2023), pp. 947-961
81. S. Medenica, D. Zivanovic, L. Batkoska, S. Marinelli, G. Basile, A. Perino, et al. The future is coming: artificial intelligence in the treatment of infertility could improve assisted reproduction outcomes—The value of regulatory frameworks. Diagnostics, 12 (12) (2022), p. 2979

82. E.R. Hammond, D.E. Morbeck. Tracking quality: can embryology key performance indicators be used to identify clinically relevant shifts in pregnancy rate? Hum Reprod, 34 (1) (2019), pp. 37-43
83. Wang H tian, Hong P ping, Li H yang, W. Zhou, T Li. Use of a new set of key performance indicators for evaluating the performance of an in vitro fertilization laboratory in which blastocyst culture and the freeze-all strategy are the primary treatment in patients with in vitro fertilization. J Int Med Res, 49 (9) (2021), Article 03000605211044364
84. R. Di Paola, A. Cuccarollo, S. Garzon. Risk, safety, and outcome monitoring in the IVF clinic Management of infertility, Elsevier (2023), pp. 397-404. https://www.sciencedirect.com/science/article/pii/B9780323899079000089
85. Zaca C., Borini A., Coticchio G. Laboratory monitoring for embryo culture. Manual of embryo culture in human assisted reproduction. https://books.google.com/books?hl=en&lr=&id=a3IqEAAAQBAJ&oi=fnd&pg=PA84&dq=Quality+Control+and+Key+Performance+Indicators+Monitoring+in+IVF+Embryo+Culture+Conditions&ots=ShuiWM_MtI&sig=BhuV6RgiQBuLNmAjs5bheNbBDKA.
86. J.G. Franco Jr, C.G. Petersen, A.L. Mauri, L.D. Vagnini, A. Renzi, B. Petersen, et al. Key performance indicators score (KPIs-score) based on clinical and laboratorial parameters can establish benchmarks for internal quality control in an ART program. JBRA Assist Reprod, 21 (2) (2017), p. 61. https://www.ncbi.nlm.nih.gov/pmc/articles/PMC5473694/
87. D. Li, Y. Gao. Introduction of quality control and risk management in IVF laboratory. Qual Manag Assist Reprod Lab (2024), pp. 1-17
88. Doody K., Calhaz-Jorge C., Smeenk J. Quality data to assurance improve clinical of ART care practice: using. Assisted reproductive technology surveillance: https://books.google.com/books?hl=en&lr=&id=dIOWDwAAQBAJ&oi=fnd&pg=PA69&dq=Quality+Control+and+Key+Performance+Indicators+Monitoring+in+IVF+Continuous+Improvement&ots=8ocSTxGw2H&sig=gw71OQflBBkJw16WtFg6V82Vqqs.
89. J. Cohen, M. Alikani, A Gilligan. Updated guidelines for setting up an assisted reproductive technology laboratory. Textbook of assisted reproductive techniques, CRC Press (2023), pp. 1-8
90. J. Passet-Wittig, M. Bujard. Medically assisted reproduction in developed countries: overview and societal challenges. Res Handb Sociol Fam (2021), pp. 417-438
91. Z.J. Pavlovic, V.S. Jiang, E. Hariton. Current applications of artificial intelligence in assisted reproductive technologies through the perspective of a patient's journey. Curr Opin Obstet Gynecol, 36 (4) (2024), pp. 211-217.
92. N. Zaninovic, O. Elemento, Z. Rosenwaks. Artificial intelligence: its applications in reproductive medicine and the assisted reproductive technologies. Fertil Steril, 112 (1) (2019), pp. 28-30
93. D.J.X. Chow, P. Wijesinghe, K. Dholakia, K.R. Dunning.Does artificial intelligence have a role in the IVF clinic? Reprod Fertil, 2 (3) (2021), pp. C29-C34
94. T.L.D. Health. Enhancing the success of IVF with artificial intelligence Lancet, 5 (2023). Digital health
95. W. Liang, G.A. Tadesse, D. Ho, L. Fei-Fei, M. Zaharia, C. Zhang, et al. Advances, challenges and opportunities in creating data for trustworthy AI Nat Mach Intell, 4 (8) (2022), pp. 669-677. https://www.nature.com/articles/s42256-022-00516-1
96. M.A.M. Afnan, C. Rudin, V. Conitzer, J. Savulescu, A. Mishra, Y. Liu, et al. Ethical implementation of artificial intelligence to select embryos in in vitro fertilization. Proceedings of the 2021 AAAI/ACM conference on AI, ethics, and society, ACM (2021), pp. 316-326. https://dl.acm.org/doi/10.1145/3461702.3462589
97. I. Silva, M. Soto. Privacy-preserving data sharing in healthcare: an in-depth analysis of big data solutions and regulatory compliance. Int J Appl Health Care Anal, 7 (1) (2022), pp. 14-23. http://norislab.com/index.php/IJAHA/article/ view/39
98. A. Panesar. Precision health and artificial intelligence: with privacy, ethics, bias, health equity, best practices, and case studies. Apress, Berkeley, CA (2023). https://link.springer.com/10.1007/978-1-4842-9162-7
99. Frank E., Olaoye G. Privacy and data protection in AI-enabled healthcare systems.2024 https://www.researchgate.net/profile/Edwin-Frank/publication/378287462_Privacy_and_data_protection_in_AI-enabled_healthcare _systems/links/65d0dc54476dd15fb343ff84/Privacy-and-data-protection-in-AI-enabled-healthcare-systems. pdf.
100. D. GhoshRoy, P.A. Alvi, K.C. Santosh. AI tools for assessing human fertility using risk factors: a state-of-the-art review. J Med Syst, 47 (1) (2023), p. 91. https://idp.springer.com/authorize/casa?redirect_uri=https://link.springer.com/article/10.1007/s10916-023-01983-8&casa_token=NrqwKnfxLzkAAAAA:2cONbCFL6tXtn8EpGZ6GT37AIJEowqtRvKaynQJQ–MQPaQjiWaf29XmGJ37xoYViYZIXPI_TK4OHHo
101. A. De, S. Saraf, T.K. Mishra, B.K. Tripathy. Interpretation and visualization techniques in AI systems and applications. Explainable, interpretable, and transparent ai systems, CRC Press (2024), pp. 279-301. https://w.w.w.taylorfrancis.com/chapters/edit/10.1201/9781003442509-16/interpretation-visualization-techniques-ai-systems-applications-arka-de-sameeksha-saraf-tusar-kanti-mishra-tripathy
102. H. Alolabi, C.C.J. Aarthy. Ethical challenges presented by advanced artificial intelligence in diagnostics and treatment recommendations. J Empir Soc Sci Stud, 5 (1) (2021), pp. 30-47. https://publications.dlpress.org/index.php/jesss/article/view/31

Credit: Olawade DB, Teke J, Adeleye KK, Weerasinghe K, Maidoki M, Clement David-Olawade A. Artificial intelligence in in-vitro fertilization (IVF): A new era of precision and personalization in fertility treatments. J Gynecol Obstet Hum Reprod. 2025 Mar;54(3):102903. doi: 10.1016/j.jogoh.2024.102903. Epub 2024 Dec 27. PMID: 39733809.

zolon
Healthcare Limited
(A member of the Emzor Group)

INTELLIGENT zolon Healthcare Limited (A member of the Emzor Group) SOLUTIONS

ZERO MALARIA

with **ZOMAL®**

Dihydroartemisinin 40mg + Piperaquine Phosphate 320mg

Curative Antimalarial

just **1 DOSE per day for 3 DAYS**

If symptoms persist after 3 days, consult your Doctor

#LongerProtectionfromMalaria

Edic Building, 13, Town Planning Way, Ilupeju, Lagos, Nigeria. Tel: +234 (0) 700 225 5965, 0700 CALL ZOLON

Zolon Healthcare Limited | Zolon Healthcare Limited | Zolon Healthcare Limited | Zolon Healthcare

DE-DEON'S

SYRUP OF HAEMOGLOBIN
VITAMIN B12

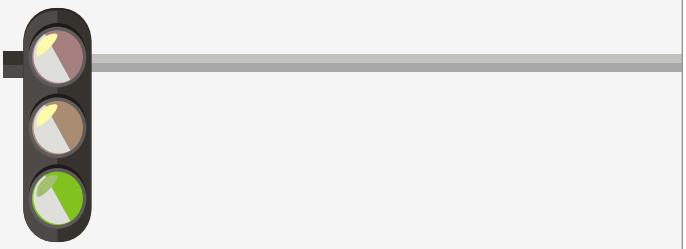

Iron formulations are a means to an "end" - Hemoglobin.
De-Deon's Syrup of Hemoglobin, the "end" in itself.

Have you had your De-Deon's today?

YOU'RE GOOD TO GO...

Manufactured & Marketed by:

Daily-Need Industries Ltd

Quality | Integrity | Transparency

Email: info@dailyneedgroup.com | www.dailyneedgroup.com

Shalina MEDSPACE

Revolutionizing Medical Learning in Africa

Step into a new realm of medical learning with **Shalina MedSpace.** Designed exclusively for Africa's medical community, it offers **Free, Unlimited Access** to premium medical literature and resources across multiple therapy areas – accessible anytime, anywhere on your mobile.

Explore an exclusive collection of:

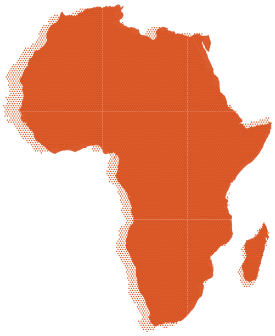

- Premium full-text Journals & Ebooks
- Latest Clinical Guidelines & Medical Magazines
- Ready-to-stream Medical Videos
- LIVE Webinars & Courses
- Medical Calculators
- Curated global and local Medical News
- Communities for peer learning, and much more…

To get full access to all medical resources, download Shalina Medspace app and register now.

1. Scan the QR code to download the app OR visit the website at www.shalinamedspace.com
2. Register with your Mobile Number and Email